University of Venda

GREEN SYNTHESIS OF GEOPOLYMERIC MATERIALS USING MUSINA COPPER MINE TAILINGS: A CASE OF BENEFICIAL MANAGEMENT OF MINE TAILINGS

A Master's research project submitted to the University of Venda, School of Environmental Sciences, Department of Ecology and Resource Management

By

MATIDZA MURENDENI
STUDENT NO.: 11606389

Signature…… Date……..

Supervisor: Prof. W.M Gitari (University of Venda)

Signature…… Date……

Co-supervisor: Mr. Muzerengi C (University of Venda)

Signature…… Date……..

DECLARATION

I, Murendeni Matidza hereby declare that "**Green synthesis of geopolymeric materials using Musina copper mine tailings: A case of beneficial management of mine tailings"** is my own work in design and execution. It has never been submitted for any degree or examination in any other university and that all the sources of information herein have been duly, appropriately and acknowledged by means of comprehensive list of references.

Signature: ……. Date: ……

ACKNOWLEDGEMENTS

First and foremost I would like to thank the Almighty God for giving me life, wisdom, good health and the strength to make this possible to execute. I thank Him for his sufficient grace that covers me daily in everything that I do and His blessings and love.

I would like to express my heartfelt gratitude and appreciation to my son Tshivhenga T.M, my mother, Matidza T.P and my siblings for their love, encouragement and moral support. Not forgetting a dear friend Tshikororo T.M for his moral support, encouragement and assistance during the course of the project.

I would like to express my sincere and humble appreciation to **Prof Gitari W.M** for the endless dedicated assistance, invaluable comments, suggestions, constructive criticisms and encouraging me throughout this project. Your contribution went the extra mile in making the project become a success.

My gratitude goes out to my co-supervisor **Mr. Muzerengi C** for his contribution to this project.

I would like to express my heartfelt gratitude to **Dr. Mudzielwana R** for his endless contribution in assistance, suggestions and comments made to construct this project.

My profound gratitude also goes to the Environmental Remediation and Nano science Research Group members for their invaluable comments, assistance when necessary and suggestions.

I would also like to acknowledge the financial support from NRF Project No. SFH160621173063, Grant No. 106097, Research and Innovation Directorate, University of Venda, Project No. SES/17/MEG/16 and Sasol-Inzalo Foundation.

DEDICATION

This work is dedicated to my son, Tshivhenga T.M who is always encouraging me to finish so he can attend my graduation. He is the reason I preserver and achieve things that are beyond my expectation. I love you my baby and are dear to my heart. To my mother Matidza T.P, I thank you for always encouraging me to excel and finish this project. Furthermore, I am highly appreciative of the support you give me may God bless you abundantly for your selflessness. Lastly to the late Mr. Munzhedzi N.A thank you for the love and support you gave me, may your soul rest in peace. You will forever be cherished and be in my heart.

ABSTRACT

Mine tailings (MT) have been a global problem due to the environmental impacts the waste generates such as air, soil and water pollution. The detrimental impacts include a global problem such as acid mine drainage (AMD) which has been difficult to clean-up. Several studies have been conducted to find alternative measures in reducing or mitigating impacts such as AMD and air pollution. Several studies have revealed how alumino-silicate mineral waste can be used as raw material to produce construction materials. This study aimed at evaluating the potential of synthesizing a geopolymer material from Musina copper mine tailings. Tailings were characterized for their physicochemical and mineralogical compositions using standard laboratory techniques in order to evaluate suitability in geopolymerization.

First section of the results presented physicochemical and mineralogical characterization of the Musina copper tailings together with the bioavailability of the chemical species. It was observed that the tailings are mainly composed of SiO_2 and Al_2O_3 as the major oxides indicating that they are aluminosilicate material. Mineralogical analysis revealed dominance of quartz, epidote and chlorite as the major minerals. The bioavailability assessment showed that largely Cu and Ca are bioavailable and highly soluble in an aqueous solution while Al, Mg, Ni, Co, Cr and Fe have a high proportion in non-labile phase.

Second section presented the preliminary results wherein the potential application of Musina copper tailings in geopolymerization was evaluated. The results showed that Musina copper tailings can be used to synthesize a geopolymer material. However, it was recommended that several parameters influencing geopolymerization need to be evaluated. The third section presented the evaluation of optimum parameters that influence the geopolymerization process, which include type of alkali activators, alkali activator concentration, curing temperature, liquid-solid (L/S) ratio and curing regime. It was observed that a mixture of NaOH:$Na_2SiO_3.5H_{20}$ at a ratio of 70:30 yields a better geopolymer material. The concentration of 10 M NaOH:$Na_2SiO_3.5H_{20}$ at a ratio of 70:30 was observed to be the best that yielded the UCS that is acceptable according to SANS-1215 standards. When evaluating curing regime, it was found that the material cured using greenhouse has lower UCS as compared to the material cured using oven. The

effect of temperature showed that the UCS decreases with increasing curing temperature. An admixture of river sand and cement was introduced which resulted in a high UCS of 21.16 MPa when using an admixture of cement. The mineralogical composition of the geopolymer bricks showed formation of secondary minerals such as phlogopite, fluorapatite, diopside and actinolite. Batch leaching conducted on the geopolymer bricks detected high leaching of Na from the bricks.

Based on the findings of the study of the raw MT potential to produce geopolymer bricks, it was concluded that the material can be used to produce bricks that are within the SANS 1215 requirements. The study further recommended that the study a focus on using cylindrical moulds, other alkali activators and a mechanical mixer. It was also recommended that the greenhouse be restructured to contain heat within the greenhouse during the evening so as to allow constant temperature within.

ACADEMIC OUTPUT

Published articles

Gitari, M.W., Akinyemi, S.A., Thobakgale, R., Ngoejane P.C., Ramugondo, L., Matidza, M., Mhlongo, S.E., Dacosta, F.A and Nemapate, N., 2017. **Physicochemical and Mineralogical Characterization of Musina Mine Copper and New Union Gold Mine Tailings: Implications for Fabrication of Beneficial Geopolymeric Construction Materials**. Journal of African Earth Science, 137(2018), pp.218-228.

TABLE OF CONTENTS

LIST OF FIGURES

LIST OF TABLES

LIST OF EQUATIONS

ACRONYMS

AAM	Alkali-activated Materials
AMD	Acid Mine Drainage
ASTM	American Society for Testing and Materials
BET	Brunauer Emmet Teller
CPB	Cemented Paste Backfill
DMR	Department of Mineral Resources
DWAF	Department of Water Affairs
EC	Electrical Conductivity
FTIR	Fourier Transform Infrared Spectroscopy
GH	Greenhouse
GHG	Greenhouse gas
GPa	GigaPascal
IARC	International Agency for Research on Cancer
ICP-MS	Inductively Coupled Plasma-Mass Spectrometer
LCT	Leachable Concentration Threshold
LOI	Loss On Ignition
MPa	MegaPascal
MT	Mine Tailings
PSD	Particle Size Distribution SABS- South African Bureau of Standards
OPC	Ordinary Portland Cement
SADC	Southern African Development Community
SANS	South African National Standards
SEM-EDS	Scanning Electron Microscopy- Energy Dispersive Spectroscopy
TEM	Transmission Electron Microscopy
TDS	Total Dissolved Solids
UCS	Unconfined Compressive Strength
USCS	Unified Soil Classification System
US EPA	United States Environmental Protection Agency
UV	Ultra-Violet
WHO	World Health Organisation
XRD	X-Ray Diffraction
XRF	X-Ray Fluorescence

Chapter 1: Introduction

1.1 Background

Copper is a minor, high thermal and electrical conductive element in the earth's crust. Statistics indicate that it is the third most widely used metal after aluminium (Al) and iron (Fe) because of its high durability (Babu et.al., 2002). It is characterised by being a soft, ductile and malleable metal which is one of the few metals that are usable in its metallic form as opposed to metals that need to undergo purification prior to use. Copper origin is within the ground in the form of ore bodies that are extracted through mining practices using either; open cast mining or underground mining. Copper ore bodies have a slight variation from each other because of difference in mineralisation, mode of formation and their local geology (Wilson et.al., 1998).

During mining the above mentioned copper bodies are extracted and undergo processing where the copper is separated from the ore residues. The residues may contain remnants of copper, quartz, sulphides and iron and other toxic chemical species, which are dumped into a pile called a mine tailing. The major environmental impacts from waste disposal at mine sites can be divided into two categories:

(i) The loss of productive land following its conversion to a waste storage area and;

(ii) Surrounding surface and groundwater may have an increase of acidity and an introduction of sediment and other contaminants (Malatse and Ndlovu, 2015 and Mining Facts, 2014). The second category can be caused by certain minerals, including gold, copper, and nickel, associated with acid drainage problems that can cause long-term impairment to waterways and biodiversity.

The aforementioned impacts are mainly determined by the type of mine tailing present within the area, these tailings are namely carbonate silicate and acidic tailing. The major problem with metal species is that they are able to survive harsh environmental conditions on exposure. For example, copper on exposure to the soil for a long period of time can accumulate to toxic levels, which may find its way into the human body through the food chain. Copper within the human body is essential because it is a constituent for many enzymes such as cytochrome c oxidase, superoxide dismutase, ceruloplasmin, dopamine B-hydroxylase, lysyl oxidase and monoamine oxidase (Watts, 1989). According to Watts (1989) the human body requires 80 mg of copper

content with high levels distributed within the brain and liver. Excess or insufficient levels of copper (copper deficiency) within the body in comparison to other nutrients may result in the disruption that the enzymes prior mentioned provides (Watts, 1989 and Klevay, 2000). In the United States of America copper toxicity is a common problem due to high copper or low zinc levels in the soils and hard or soft water regions, the intake of copper ranges from 3-5 mg per day (Watts, 1989). Whilst in India the intake of copper is much higher than the USA with an average of 6 mg per day and an intake of 13 mg in other regions (Watts, 1989).

In the Witwatersrand's region situated within Gauteng province several studies have indicated severe AMD occurring due to the surrounding mine tailings that were extracted from gold ores that started in the 18th century (Tutu et.al, 2008 and Marsden, 1986). Naicker et.al., (2003) conducted a study within the Witwatersrand region which indicated that the groundwater that was seeping out from disused tailing dumps contained low pH and the water emerged into the surface area with elevated metal concentrations being introduced into Central Rand streams. Investigations on surrounding wetlands indicated that the wetlands were serving as a sink for metal pollutants by trapping the pollutants into sediments and peatlands (McCarthy and Venter, 2006). The problem has been ongoing and affecting most mining areas within the country. Researchers have focused on the physicochemical behaviour of different mines on a global scale in order to acquire the proper remediation strategies to similar tailings.

According to population statistics (2016), South Africa has a human population of about 55.91 million (Stats SA, 2016). This population is growing and consequently leads to an increase in demand for housing which puts enormous pressure on the natural materials used for constructions of building bricks such as gravel and clay soils. Conventional bricks are produced from clay fired in high-temperature kilns (900°C- 1 000°C) or from ordinary Portland cement (OPC) concrete (Zang, 2013). In the production of 1 ton of OPC, about 1.5 tons of raw materials is needed which in turn produces 1 ton (80%) of CO_2 which is released to the atmosphere. The depletion of these clay materials has created a need for an alternative source of construction materials.

Geopolymerization is an innovative technology that transforms alumino-silicate materials into useful products called geopolymers or inorganic polymers. Geopolymers are alumino-silicate materials with a three dimensional (3D) amorphous micro-structure, they are an alternative for OPC which also reduces the emission of CO_2 gases during kilning by 80%. The process of

geopolymerization can be described as a series of heterogeneous chemical reactions that interacts solid alumino-silicate oxides with alkali metal silicate solutions at highly alkaline conditions. The process undergoes a number of reactions;

- Dissolution occurs when mixing an alkali solution (hydroxide ions) with an amorphous alumina-silicate material at mild temperatures to yield amorphous to semi-crystalline polymeric structures (Fig. 1.1), consisting of Si–O–Al and Si–O–Si bonds (Dimas et.al., 2009 and Bakri et.al., 2011). The amorphous to semi-crystalline structures serve as nuclei for particle growth.
- Dissolution results in the formation of Si and/or Si-Al oligomers. Oligomers are a molecular complex that consists of a few unlimited monomer units, in contrast to a polymer.
- Finally, the process undergoes the poly-condensation of these oligomers to form a three-dimensional alumina-silicate framework.

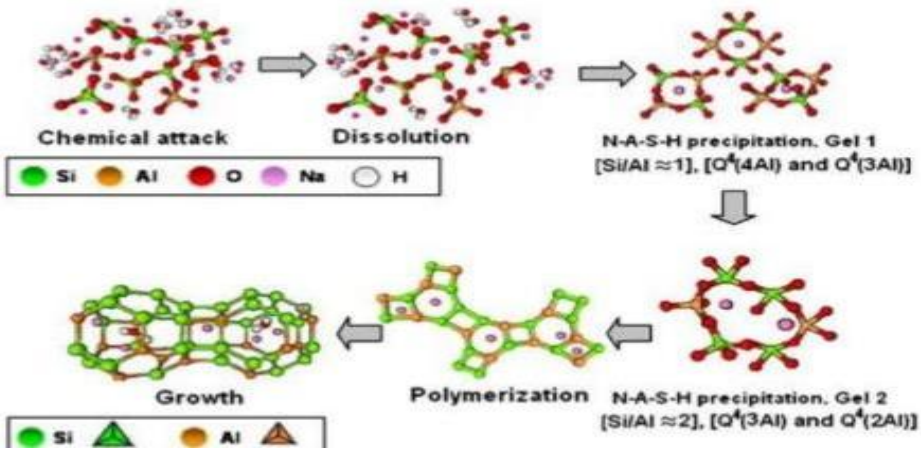

Figure 1. 1: Schematic diagram of the geopolymerization process (Fernandaz et.al., 2005).

The function of the alkaline solution is to break and dissolve the silica and alumina bonds in the initial material. The cation (K^+ or Na^+) available in the alkali solution acts as a charge balancing agent for aluminium and initiates the gelling phase where hardening of particles form a continuous structure. However, even though Al plays a major role in regulating the setting time of geopolymer formation, the amount of Si present is responsible for higher later strength development of these systems. The tailings material is the overall ingredient which determines the degree of geopolymerization as compared to the by-products that are used throughout the process. Most importantly the atomic ratio Si:Al in the polysialate structure determines the application of the geopolymer. For instance a low ratio initiates a very rigid 3D- network whilst

a high ratio (>15) provides a polymeric character to the geopolymer. More shall be discussed in chapter 2.

The molecular expression of geopolymer gel can be represented by the following formula:

$$Mn\ [-(SiO_2)\ z\text{-}AlO_2]\ n \qquad \text{Equation 1. 1}$$

Where M is the cation (sodium or potassium), n is the degree of polymerization, z the Si/Al molar ratio that is normally in the range of 1-15 / up to 300 (Davidovits, 1982 and 1994). The geopolymerization process can be applied on a wide variety of solid alumino-silicate raw materials for the synthesis of geopolymers. Among the potential solid alumino-silicate raw materials, industrial solid wastes such as coal fly ash, alumina, red mud, metallurgical slag, building demolition materials, mine tailings etc., are the most important raw materials (Cheng and Chiu 2003; Malatse and Ndlovu, 2015).

1.2 Problem Statement

Tailings is a finely ground rock that is left over after the ore has been treated in the concentrator, it's a combination of fine grained (typically silt sized, in the range from (0.01 mm to 0.60 mm), solid material remaining after the recoverable metals and minerals have been extracted from mined ore and the remaining process water. Tailings tend to accumulate considerable amounts of metal species (mainly pyritic residues) derived from uneconomic minerals and may leach for many years after the mining has ceased. Through time the tailings (gold, platinum, copper and other commodities) geochemical reaction results in acid mine drainage (AMD) and the release of metal species into humans and the environment (Davies and Rice, 2001). Such environmental impacts are due to the absence of minerals such as alumino-silicates and carbonates in the tailing which act as a neutralizer from the generated sulphide oxides (Rice and Herman, 2012). Tailings such as gold and platinum produce acidic leachates such as AMD due to the presence of pyritic residues, but there are other mine tailings that do not contain pyritic residues such as Musina copper mine tailings that are rich in aluminosilicate residues. Studies of the area detected a concentration that increased as follows within the mine tailings: Pb<Cu<As<Cu<Zn<As however, within the ground water sources high presence of Ni was detected at a level of 6.49 µg/g (Singo, 2012). Concentrations were established to be of low to medium within the abandoned copper tailings, thereby, it is concluded that Musina defunct mine and its surroundings is relatively pristine and is a less contaminated area although through time and continuous accumulation the outcomes may be different. Besides tailings producing

leachates based on their mineralogy and surrounding environment, tailings also lead to land loss and salinity into rivers to mention a few. Godfrey et.al. (2007) indicated that the land lost to gold mine tailings within the Witwatersrand basin in Johannesburg is an estimated surface area of 200 km^2 and the abandoned copper mine tailing dump located in Musina occupies an estimated 4.99 km^2. South Africa is at present faced with the challenges resulting from acid mine drainage; and the government and mining companies are under pressure to find viable solutions to this problem. This, coupled with the increasing landfill costs, and stricter implementation and enforcement of environmental legislation, has caused the scientific community to focus on finding innovative methods of utilizing mine tailings (Malatse and Ndlovu, 2015). There is consequently a momentous need to developing other long-term, commercially viable uses for mine tailings in order to minimize the disposal costs and the impact on the environment. The study seeks to develop a cost effective geopolymerization technology that will provide land for development, agricultural practices and influence the socio-economic development of the area.

1.3 Objectives

Main objective of this work is to evaluate the feasibility of utilising Musina copper mine tailings in synthesis of construction materials based on geopolymerization technology and incorporating a solar dryer for curing the geopolymer moulds.

Specific Objectives

1. Evaluate the physicochemical and mineralogical characterisation of Musina copper mine tailings and the synthesized geopolymeric products.
2. Evaluate the geochemical partitioning of major and trace elements in the tailings and the potential mobility/bioavailability of the major and trace elements within the tailing deposit.
3. To evaluate the optimum conditions for synthesizing a geopolymer material from Musina mine tailings.
4. Assess the level of encapsulation of synthesized mine tailing or geopolymer through the potential mobility/bioavailability of major and trace elements.

1.4 Research questions

- What are the physicochemical properties and bioavailability and/or mobility of toxic

metals and metalloid species of the tailings prior and after synthesis?

- Is the metal species bioavailable fraction in the tailings of concern to the environment with respect to the tailing being a construction material?
- Which alkali activator concentration and tailings and/or admixture will attribute better mechanical properties?
- Is there a difference in the physicochemical and mechanical properties of the brick produced within a solar dryer versus hot air oven dryer, and which curing method displays early mechanical properties?

1.5 Hypothesis

Copper mine tailings can be successfully synthesised into geopolymer bricks that meet the SANS 1215 requirements for concrete bricks.

1.6 Assumption

It is assumed that the geopolymer synthesis method developed in this study will be applied to all silica and alumina rich tailings in the country to produce bricks.

1.7 Significance of the study

According to the Department of Mineral Resources (DMR) (2014) database there are 4 378 derelict and verified ownerless mines which is increasing on a daily basis due to mines being uneconomic to mine and the nation economic constrains. The mines become unmanaged after shutting down and become a problem of the DMR to manage. At the moment the DMR can rehabilitate 10 mines per years (Olalde, 2015), while the country continues to face a growing environmental, health and social challenges due to the mining industry. These challenges include AMD which is dominant within the Witswatersrand region, dust containing metal species from tailings and erosion into surrounding areas. The study seeks to assist the DMR in reducing such challenges. Most importantly the technology will be beneficial to the country in two-fold namely:

(1) The recycling of highly problematic copper tailings to useful and valuable commercial-grade products; and

(2) The prevention of siltation and tailing erosion.

In addition to the obvious economic benefits that would arise from this approach, the practice has a significant opportunity to reduce global carbon dioxide emissions, reduce consumption of raw materials for cement production and reduction of energy consumption by using a solar drier as opposed to an oven for producing a brick. The potential for industrial start-ups and cheap construction materials is also a benefit but most importantly the reclamation of the land for other uses such as agriculture, property development, forestry, etc depending on the suitability of the soil.

1.8 Thesis structure

Chapter 1: Introduction

Chapter 2: Literature Review

Chapter 3- Part A: Physicochemical and mineralogical characterisation of Musina copper mine tailings and the synthesized geopolymeric products.

Part B: Mobility, bioavailability and presence of metals and metalloid species within the copper mine tailing.

Chapter 4: Synthesis of geopolymer bricks from Musina copper mine tailings: Preliminary investigations.

Chapter 5 - Part A: Synthesis of the geopolymer material from copper mine tailings: Evaluation of optimum conditions.

Part B: Mobility, bioavailability and presence of metals and metalloid species within the synthesized geopolymeric products.

Chapter 6: Conclusion and Recommendation

Chapter 2: Literature Review

2.1 Introduction

This chapter presents a review of literature that is related to the geology of Musina copper ores, the environmental impacts of mine tailings, the management strategies that have been put in place and technology applications that may be used to reduce the tailings that occupy large spaces and the raw materials used to produce Ordinary Portland Cement (OPC).

2.2 Mining

Mining has been the heartbeat of South Africa's economy for many years and on a global scale. Mining in South Africa started in the copper rich region of Namaqualand (Springbok-Fontein farm) in the Northern Cape during 1846. However, commercial mining was discovered of diamonds in the Northern Cape in the late 1860s which struck the mineral rush (Davenport, 2010). Subsequently the Gold rushes to Pilgrim's Rest and Barberton were precursors to the biggest discovery of all, which followed the discovery on the Langlaagte farm within 1886 that expanded further within the region (Johnson, 2017 and Turrell, 1987). The gold rush in the Witwatersrand region drew many foreign expatriates to prospect the area which stimulated the increase in exploration within the region and country. Through such events it resulted in South Africa being the leading gold producers in 1898 producing 118 tons of gold (Johnson, 2017). With investors focusing on making profit and the country having no knowledge of mining implications resulted in no regulations to manage waste produced through mining. These actions are what have led to the country's environmental scare; such as chronic illnesses being caused by air pollution and disturbance of an ecosystem through industrialization. Further discussion of the environmental impacts caused by mining will be discussed in section 2.2.4 of the chapter.

2.2.1 Geology of Musina Copper (Cu) ores

The geology of this region is characterized by the Sand River Gneiss that are approximately 3790 million years old. The Gneiss forms a basement for a sequence of cover rocks such as, the Beit Bridge Complex that has been subdivided into Mount Dowe, Malala Drift and Gumbu groups based on their dominant lithology (Singo, 2013). The Musina copper mines form part of the Limpopo mobile belt that is situated in the central zone of the belt, and is subdivided into 3 zones. The northern marginal zone consists of quartz diorite, tonalite and granodiorite which

originate from magmatic rocks that crystallized under granulite-facies condition. The central marginal zone consists of rock types which includes the meta-quartzites, amphibolites, biotite-hornblende gneisses or the associated rocks of the basal Mount Dowe formation that forms part of the Beit Bridge Complex (Wilson et.al, 1998). Lastly is the Southern marginal zone that consists of a grey gneiss and granitoid intrusions. In the North- East the copper deposit strikes the Messina fault where the central zone of the Limpopo belt is situated at a length of 700 km and a width of 200 km. The Limpopo belt was formed long after the tectonic events that underwent several subsequent periods of intense deformation and a high grade metamorphism of the Sand River Gneiss and Beit Bridge Complex.

2.2.2 Minerals

Although the mines are characterised as copper mines they each have a slight variation because of difference in mineralisation, mode of formation and their local geology (Wilson et.al., 1998). This implies that the copper deposits in the area are classified based on their host rocks lithologies (Wilson et.al., 1998). According to Wilson et.al. (1998), the copper mines are composed of brecciated ore bodies that are rich in quartz, which are in some cases 1 m long, and has inclusions of shattuckite, papagoite and ajoite. The abundance of quartz which is also an attractive mineral to collectors; the quartz is present based on the habits and varieties of size, groups and numerous colours caused by secondary mineral inclusions. Most of the quartz crystals that range from a microscopic to a metre in size are present in the Messina Mine. The outer layer over the core zone that is coated by hematite, epidote, talc, sericite, chlorite, zeolites, malachite or azurite is where clear euhedral quartz is frequently found (Wilson et.al., 1998). Whereas, all larger crystals are zoned internally with over a dozen layers present in some crystals, and minute layers of hematite, kaolinite, epidote and chlorite are present within this zone (Van Graan, 1964). Copper in the area is present in primary sulphide minerals, chalcopyrite, bornite and chalcocite, and are the only metals of economic value within the ore bodies. Chalcopyrite is present in peripheries of ore bodies and is progressively being replaced by bornite, chalcocite and native copper towards the centre and downwards. Calcite was also found within the Messina mine with occasional partial or complete cover of the quartz with the calcite that is orange-yellow to white in the area (Wilson et.al., 1998).

2.2.2 Chemistry and Mineralogy of Musina Copper Tailing

Previous studies have revealed that Musina copper tailings contained unifor mLy distributed high levels of SiO_2 and Al_2O_3 (Gitari et.al., 2015; Thobakgale, 2017). Results by Thobakgale (2017) revealed that SiO_2>58.12%, which confirms the findings by Wilson et.al., (1998) who

indicated that the geology of the area is dominant of felsic rock composition. Previous studies of the tailing further indicated that the tailing are constituted by the following metals: Al, Ca, Mg, Fe, Cu, Mn, and K; and trace metals: Ni, As, Se, Ti, Co, Mo, Cr and Zn which are mainly in the non-labile phase during geochemical fractioning (Gitari et.al., 2015 and Thobakgale, 2017). XRD spectral peak analysis conducted (Thobakgale, 2017) on the tailing indicated a range of uniformity with each mineral by depth, with the main mineral phases being quartz (37.5-42.94%), epidote (21.61-23.56%) and chlorite (13.31%-16.82%). Other minerals in minor quantities are hematite, calcite, plagioclase, muscovite, actinolite and hornblende of 0.84-10.8%. Chalcopyrite has been detected to be the only primary sulphide mineral observed (Thobakgale, 2017), coupled with the high level of aluminosilicate and traces calcite (carbonates) suggests that the tailing is neutral and no harmful for use as construction material.

2.2.3 Metal Species

Metals species are simply a certain class of naturally occurring metallic elements that have high atomic weight and a density that is 5 times greater than that of water (Tchounwou et.al., 2014). The periodic table has been outlined to have 105 elements whereby 80 are considered as metals. As mentioned, heavy metals are naturally occurring elements that are present within the earth's crust however; anthropogenic activities have resulted in a wide distribution of these metals within the environment. These anthropogenic activities as indicated by Bradl (2002) and He et.al., (2005) are a result of industrial, domestic, agricultural, medical and technological application, which has led to the risen concern that these metals will have potential effects to human health and the environment. The industrialization of the world dramatically increased the overall environmental load of heavy metal (McBride, 1994). The metals toxicity on the human body is dependent upon factors such as the dose, route of exposure, chemical species, gender, age, genetics and nutritional status. The human body requires trace amounts of some heavy metals, including zinc, copper, iron, cobalt and others, but these can be dangerous at high levels (WHO/FAO/IAEA, 1996; Watts, 1989). Other metals that are known as essential nutrients include copper and chromium however; there is a narrow range between beneficial and toxic effects of these essential nutrients (Chang et.al., 1996; Wang and Shi, 2001). Other heavy metals such as mercury, lead, arsenic and cadmium (known as non-essential metals) have no established biological function and have high levels of toxicity, which ranks them as priority metals of public (Chang et.al., 1996). The prior abovementioned metals are considered systemic toxicants that have been known to cause multiple organ damage even at low exposure levels. For example, lead inhaled, ingested and through dermal contact on a regular basis

produces lung, stomach and urinary-bladder cancer (Report on carcinogens, 2004). According to the U.S Environmental Protection Agency (U.S. EPA) and the International Agency for Research on Cancer (IARC) these metals are classified as human carcinogens.

2.2.4 Mine tailings and their environmental impacts

Drechsler and Graham (2005) defined mine tailings (MT) as fine materials that are primarily ground rocks that have been left over after the extraction of valuable minerals from ore body. There are different types of tailings that are used within the mining industry namely: wet tailings in slurry form, thickened tailings and dewatered tailings. The chemical and mineralogical constituents that are present within the tailing will be dependent on the mineral composition of the ore body and the chemicals used during extraction. It is further revealed that an approximate estimation of more than seven billion tons of worldwide mine tailings are generated from the mining industry every year. The accumulation of heavy metals in the tailings tend to be that of a considerable amount and is uneconomic to extract however, these metals may be leached for years to come after mining has ceased. The effluents and dust that are emitted from tailings and waste-rock management facilities, whether controlled or uncontrolled, may be toxic to humans, animals and plants at varying degrees. These effluents may have a broad spectrum of physicochemical characteristics such as being acidic or alkaline, they may contain dissolved metals and/or soluble and entrained insoluble complex organic constituents from mineral processing, as well as possibly natural occurring organic substances such as humic and long-chain carboxylic acids from mining operations. The aforementioned substances together with the substances pH level, dissolved oxygen content, temperature and hardness thereby impact the environment.

According to Davies and Rice (2001), the geochemical reaction of tailing materials in the presence of air or water is what has led to the global problem known as AMD and the release or leaching of heavy metals that impact on human health and the environment. For over a decade mine waste has been an area of focus within South Africa and globally due to the increase in environmental impacts and human health which has been triggered mostly by old abandoned mine. The visibility period of mining impacts into the human body and environment differ based on the type of mining that has been conducted and the tolerance level of the environment and human. For instance, underground mining doesn't display environmental impacts on a short-term basis but, in the long term the environmental impacts include rising water table, groundwater contamination and AMD which shall be explained further beneath.

Whereas, surface mining technique shows environmental impacts in a short-term interval to its mining including, land degradation, habitat loss, noise pollution, etc. Mine tailings don't only consist of rock forming minerals, but also contain sulfide minerals which are the main element in AMD. AMD is defined as an acidic leachate that is produced through the exposure of sulfide minerals such as pyrite into air and water; the process that is undergone is an oxidation reaction. The basic chemical reaction for pyrite undergoing oxidation is as follows:

$$4eS_2 + 15O_2 + 14H_2O \rightarrow 8H_2SO4 + 4Fe(OH)_3$$ Equation 2. 1

In arid to semi-arid regions like Musina these metals (sulfide) are prone to wind (aeolian) dispersion and water erosion. Wind dispersion occurs when fine tailing particles such as silt or sand-like material (as that present in Musina copper tailing) and their associated contaminants are easily suspended into the atmosphere by wind and dispersed throughout the environment occurring as dust particles. There have been measurable elevated levels of intoxication in wildlife and human systems present even at a significant distance from the tailing due to the spread of metal toxicants in association with tailings particles that are dispersed through a combination of wind dispersion and water erosion (Davies and Rice, 2001). Due to lack of normal soil stabilization processes in such sites the problem can persist for decades thereby, it results in the sites not developing normal soil structure or supports the establishment of plant cover.

2.2.5 Management of tailings

Through the past two decades the management of mine tailings has been an area of study for most researchers with one aim, how to reduce or eliminate the environmental impacts that are triggered by these tailings. Below we shall discuss a few management strategies that have been implemented within the mining industry on a global scale.

- **Backfilling**

Backfilling is defined as the reinsertion of materials into the mined-out part(s) of the extraction site. The re-deposited materials are typically overburden, waste-rock and tailings, either alone or in combination with other structural products such as cement. Infilling is where other materials such as smelter slag are disposed into the mine void. However, these materials don't serve as a geotechnical requirement where the void areas structure is compressed. The purpose of backfilling within underground and open pit mining is to assure ground stability, reduce underground and surface subsidence, improve ventilation, minimise the footprint and risk of collapses, and decommissioning/ landscaping reasons. In summary backfilling has benefits

such as reduction of ground surface disturbances and reduction of 50% of the overall extracted tonnage. There are different types of backfilling methods that have been adapted to namely:

- **Cemented Paste Backfill**

CPB has acquired popularity throughout the world, particularly within the Canadian mining industry where this management strategy has in the past few years been indefinitely adopted due to the numerous operational and environmental benefits over both hydraulic and rock backfills (Hesketh et.al., 2010). CPB is described as an engineered material that is composed of a combination of three components: filtered wet tailings (75–85 wt% solids), binding agent (3–7 wt% solids) and water (Benzaazoua et.al., 2008). The minimum strength of the tailing is acquired through the addition of binders; for example, alkaline solutions such as sodium hydroxide; while water is added to reach the desired consistency (15–25 cm slump) that will provide the paste with transportation from the backfill plant to the mine stopes. Benzaazua et.al. (2004b) reported that the amount of sulphides present within the tailings had positive impacts on the uniaxial compressive strength (UCS) tests and the relationship with the sulfide content indicated that the amount of sulphides present within the tailing influences the outcome of the CPB strength (UCS). The prior statement means that the higher the sulfide contents the higher the UCS that is a beneficial effect. However, this beneficial effect has its effects where the importance of sulphate precipitation may result in sulphate attack phenomena (precipitation of expensive hydrated sulphates), leading to a deleterious effect on the strength gain (Benzaazoua *et.al*., 1999; Benzaazoua *et.al*., 2002 and Benzaazoua *et.al*., 2004b). There are various methods of backfill available which require one to understand the site based on criteria including; mineralogy, slurry pH and particle size distribution in order to decide on which system to implement (Dorricott and Grice, 2002; Ouellet et.al., 2006 and Benzaazoua et.al., 2008).

- **Dry backfill**

Dry backfill mainly contains unclassified sand, waste-rock, tailings and smelter slag, which are disposed into an underground void through a small shaft that directly enters into a stope where the deposited material may be hauled by loaders or trucks (Management of Tailings and Waste-Rock in Mining Activities, 2009). However, even though it is named dry backfill it contains some absorbed surface moisture.

- **Hydraulic backfill**

Hydraulic backfill consist of either classified slurried tailings or naturally occurring sand

deposits that are mined on the surface. The preparation of the backfill is through the dewatering of mineral processing tailings stream to a pulp density of approximately 65-70% solids and then it is passed through a hydro cyclones to remove the slimes that retain the coarse fraction for backfill (Management of Tailings and Waste-Rock in Mining Activities, 2009). Disposal of the waste is through the backfill being hydraulically pumped from the surface to the stope. In order to conduct hydraulic backfill on a mine tailing the following factors are to be considered; grain size distribution, slope of grain size distribution and particle shape (Management of Tailings and Waste-Rock in Mining Activities, 2009).

- **Desulphurisation**

Desulphurisation conducted within the environment is an attractive management alternative that is used to generate acid within tailings. The process places a primary process treatment circuit at the end of the treatment process in order to reduce a large portion of the problematic tailings through the concentration of the sulfide fraction (Benzaazoua *et.al*., 1999). Non-selective froth flotation is the most commonly adapted method used to produce desulphurised tailings where the sulfide content present within the tailing and its neutralisation potential (NP) determines the desulphurisation levels. The method is generally recommended for operating mines that are willing and able to add a flotation circuit at the end of the existing treatment process. However, this management strategy has its particular challenge, which is being able to float sulphides selectively from a pulp that is already treated and contains various chemicals, and ions that interfere with the flotation process. This floatation process contains two different fractions to manage namely; the desulphurised (non-acid generating) tailings, and a smaller quantity of sulfide enriched tailings that are acid generating (Benzaazoua *et.al.*, 1999). This method is able to substantially reduce the volume of acid generating mine tailings to manage at the surface.

2.3 Geopolymerization

Joseph Davidovits is a French chemist who pioneered a technology known as geopolymerization since 1979 and continued throughout into the 1990s. These materials were originally developed as a fire-resistant alternative to organic thermosetting polymers following a series of fires in Europe. Products based on this initial work have since found application as coatings for fire protection for cruise ships (Talling, 2002), as a resin in high-temperature carbon-fibre composites (Lyon et.al., 1997), in thermal protection of wooden structures

(Giancaspro et.al., 2006), as a heat-resistant adhesive (Bell et.al., 2005 ; Krivenko and Kovalchuk 2007), as a monolithic refractory (Comrie and Kriven 2003; Kriven et.al., 2004) and in various other niche applications. Within the past three decades, geopolymerization has emerged as a possible solution of immobilisation of toxic and radioactive wastes as well as the treatment of industrial wastes to produce value added construction materials. Davidovits (1970) defined geopolymerization as a process that transfers large amounts of alumino-silicate content from any material into value-added geopolymeric products. This process occurs through the dissolution of aluminate (Al) and silicate (Si) from aluminosilicate (Al-Si) materials using alkali solutions namely; sodium hydroxide (NaOH) or potassium hydroxide (KOH) as hydrated reaction products (catalyst) to form a [Mx $(AlO_2)_y$ $(SiO_2)_z$. nMOH.mH_2O] gel (Xu and Van Deventer, 2000; Xu, 2001). Conversion of large amounts of Al-Si waste forms value added geopolymeric products. The geopolymeric products are characterized by good chemical and physical properties such as mechanical strength, high acid and fire resistance (Xu and Van Deventer, 2002), which is what makes these products to be potentially viable for construction purposes. Theoretically, any material containing Al-Si may undergo the process of geopolymerization to form geopolymers. Some of the achievements made through the utilization of the geopolymerization technology is the higher strength and durability within 4 hours of mineral polymers (geopolymers), flexible ceramics, ceramic composites and concrete composites as compared to the best currently used concrete (Davidovits et.al., 1994a, 1988; Davidovits et.al., 1990 and 1999b).

Mobile toxins present within tailings have been predominantly induced with no or little management of the tailing. Small-scale management solutions to the tailings have been to backfill underground mine voids as mentioned in section 2.2.4; re-vegetation of surface mines, building sand dams. However, these reclamation processes don't completely solve the environmental problems faced by tailings. Problems such as occupying large hectares of lands, heavy metals leaching, dust pollution, and the potential threat from the tailing dam collapses still exist. The geopolymerization technology allows the utilization of waste materials (fly ash, mine tailings) and their reactive properties in order to create geopolymer systems that are not only mechanically durable enough to be used as construction materials, but are also potential immobilisation systems for toxic waste. The alkali activation of waste materials (especially those coming from industrial and mining activities) has become an important area of research in many laboratories because it is possible to use these materials to synthesize inexpensive and ecologically sound cement-like construction materials.

Previous research has shown an indication that the strength of geopolymers depends on the nature of the source materials (Davidovits, 2005). For example geopolymers that are synthesised from calcined source materials, such as fly ash, slag and metakaolinite demonstrates a higher compressive strength than those formed from non-calcined materials such as kaolinite, mine tailings and naturally occurring minerals (Barbosa et.al., 2000; Davidovits et.al., 1994; Davidovits, 1994; Palomo et.al., 1999a; Xu and Van Deventer, 2000;). Reports have indicated that geopolymers synthesized from non-calcined materials demonstrate high level of compressive strength during the later stage of curing (Davidovits, 1994; Palomo et.al., 1999b; Van Jaarsveld et.al., 2000; Xu et.al., 2001; Yip and Van Deventer, 2001). According to Van Jaarsveld et.al. 2000 and Xu and Van Deventer, 2000 calcined materials are introduced during geopolymerization in order to activate the inert industrial waste such as mine tailings, paper sludge's and some naturally occurring minerals. The inert industrial waste also produces mechanically strong geopolymers.

Researchers have previously mainly focused on the synthesis of geopolymers using a single component either kaolinite or metakaolinite, known as calcined kaolinite (Davidovits, 1982; Davidovits and Sawyer, 1985; Davidovits, 1994; Palomo et.al., 1992) with temperature higher than 100 °C and pressure greater than atmosphere for kaolinite and room temperature and atmospheric pressure for metakaolinite (Davidovits, 1994). Kaolinite or metakaolinite was used to produce geopolymers due to the high content of aluminate in their composition and because they are common industrial minerals which is accessible in large quantity with homogeneous properties. However, studies have diverted to the utilization of bi-component systems such as using kaolinite or metakaolinite with other minerals and industrial wastes during geopolymerization (Van Jaarsveld et.al., 1999, 2000; Xu and Van Deventer, 2000; Xu et.al., 2001). Xu and Van Deventer (2002) indicated that the focus of the geopolymerization technology on a single or bi-component system produces a narrow application of the technology. Narrow application of the technology was mentioned in the sense that the application of a single or bi-component won't be able to exploit the characteristics of the material such as its compressive strength, stability, and durability. This study will focus on utilising the copper mine tailing as a single component and in a later stage the introduction of kaolinite as an admixture will be considered. The kaolinite is used as an admixture because it is a new aspect being introduced into geopolymerization using mine tailings. Previous researcher (Zang et.al., 2013; Van Jaarsveld et.al.,2000; Roy and Gupta, 2007; Malatse and Ndlovu, 2015 and Chen et.al., 2011) focused their studies of utilising alumino-silicate rich

tailings with an admixture of fly ash, slug and/or cement as the binding mechanism. The clay material in the study is being added to determine whether the brick to be produced will attained more structural strength as compared to the single component brick.

2.3.1 Curing regimes of geopolymer material

Temperature is one of the key factors that optimizes the compressive strength attained after a geopolymer brick is produced. Temperatures that are elevated (60°C to 90°C) and longer curing time influences the rate of gain strength and the overall compressive strength of the geopolymer. There have been different curing schemes that have been investigated by numerous researchers however, these schemes all have common characteristics namely; heat curing at a constant temperature produces good compressive strength at different time intervals; based on the solid to liquid constituents and its ratio. Srinvasan and Sivakumar (2013); Goretla et.al. (2004); Bakharev (2005); Nozari et.al. (2011) and Helmy (2016) conducted their studies using a hot air oven curing method at temperatures between 75°C to 250°C which produce good results in terms of the geopolymer material compressive strength. Other researchers such as Elimbi et.al., (2011) and Natali et.al., (2011) conducted their research utilising the calcination curing method which is a thermal treatment process at temperatures ranging from 25°C to 700°C. The process produced the expected compressive strength however, it requires high levels of energy to produce the brick and emits large amounts of CO_2. Other researchers (Narayana and Shanmugasundaram, 2017) used four different curing regimes namely; ambient air, heat chamber, hot air oven and autoclave to determine the best curing method that would produce satisfactory results. These researchers used a constant temperature of 80°C throughout the different curing methods. Results indicated that the compressive strength attained through ambient air wasn't satisfactory however, the other curing methods produced a satisfactory outcome.

Diop and Grutzeck (2008) used a tarp or solar heated enclosure to cure the geopolymer brick with temperatures of 40°C, 80°C and 120°C respectively. The brick produced at 120°C with 12 M of NaOH produced better compressive strength as compared to the bricks produced at 40°C and 80°C at different alkali concentrations. This study will incorporate a greenhouse solar dryer to cure its bricks and compare its mechanical properties to a brick cured in a hot air oven dryer using the same temperature and humidity. The solar dryer will introduce a beneficial output of not utilising electricity thus saving energy resources and there will be less CO_2 emissions as compared to conventional brick production. An important aspect that will ensure

that results attained within the solar dryer are satisfactory is considering the optimizing factors such as the right temperature, alkali concentrations and material to water/ activator ratio.

2.3.2 Types of greenhouses

A greenhouse system has been defined as an enclosed structure of transparent medium (glass/polyethylene/ polycarbonate sheet) where short wavelength of solar radiations is generated into the system (Chauhana et.al., 2017). The system has been designed in a manner which traps the long wavelength radiation to create a favourable micro-climate. The medium acts an absorber which improves the trapping of the long wave radiation. It has been used worldwide for many decades as an application of crop cultivation, poultry, aquaculture, soil solarisation, and crop drying (Prakash and Kumar, 2014). The system involves heat and mass transfer phenomenon where the heat energy supplied to the product is utilized in two steps (Leon et.al., 2002).

1. The product temperature increases in the form of sensible heat.
2. The moisture present in product vaporizes through the provision of the latent heat of vaporization.

Due to the controlled environment in terms of the relative humidity and temperature provided by the system, the drying duration for crop drying becomes shortened (Prakash and Kumar, 2014). Prior to the technology being initiated crops were dried within an open sun drying however, it was realised that the duration used for drying was too long, moisture not fully removed, high time consumption and high levels of nutrients was lost during such a process. In the past 2 decades researchers have established that the greenhouse system can also be used to dry at low temperature. Thereby, the system is user friendly throughout the year. A greenhouse dryer is mainly classified into two types based on structure;

i) Dome shape which is used to maximize the utilization of the natural solar radiation.
ii) Roof even type has an advantage of being able to equally mix the air within the dryer.

There are mainly three types of solar drying systems: indirect, direct, and specialised dryer (Foster and Mackenzie, 1980). Within the direct solar dryer the material is dried within the enclosure where a transparent cover surrounds the material (Ekechukwu and Norton, 1997). The absorbed solar radiation is what generates heat inside the drying chamber. An indirect solar dryer is where the air within the solar collector becomes hot and then passes through the drying chamber to dry the material (Kreider and Kreith, 1981). Solar dryers are further classified into

two groups namely (Foster and Mackenzie, 1980);

1. Active solar dryer are scientifically designed where they contain an external fan/pump to transfer solar energy in the form of heated air from the collector area to the drying chambers. There is greater contact with the surface area of material when the heat air flows through the drying chambers.
2. Passive solar dryer use only the natural movement of warm air and can be set up with low capital cost as it is fabricated from locally available materials. The system is appropriate for small farms, where raw construction material such as wood is readily available.

Figure 2. 1:Greenhouse drying under passive mode (Jain and Tiwari, 2004)

As mentioned the dryer system is used to dry crops such as bananas, rice, tomatoes, and etc. The drying of the crops using the dryer as compared to open sun drying increases the crops quality thereby increasing its market value, it reduces contamination of crops, rainfall, space used to lay the crops and time. Within the agricultural sector the greenhouses are able to produce crops within a controlled environment and crop production of vegetation that are only suited for a specific season is possible. This study wants to introduce the concept of using a passive greenhouse solar dryer to cure the geopolymer bricks. Diop and Grutzeck (2008) conducted such study where a solar enclosure was used. Although, not all results were satisfactory due to other optimization factors success was attained at 120 ℃. The greenhouse solar dryer as mentioned is cost effective and will further increase sustainability of the geopolymerization concept.

2.3.3 Chemistry of geopolymers

Geopolymers basic building block (sialates) is a tetrahedral silicon and aluminium network

that has been bonded when the two elements share the oxygen atoms, the product is chemically known as an inorganic polysialate species. Sialate is an abbreviation of silicon-oxo-aluminate. Davidovits (1991) indicated that the chemical designation of geopolymers is polysialate with the following empirical formula:

$M_n [-(SiO_2)_z -AlO_2]_n.wH_2O$ Equation 2. 2

Where z is 1, 2 or 3; M is a monovalent cation such as potassium or sodium; and n is the degree of poly-condensation. The framework cavities of the sialates require the presence of positive ions (Na^+, K^+, Li^+, Ba^{++}, NH_4^+ and H_3O^+) in order to balance the negative charge of the Al^{3+} in IV-fold coordination. The negative charge is acquired through the substitution of Si^{4+} with Al^{3+}, which is a suitable replacement in a tetrahedral arrangement. Polysialate are chain and ring polymers that contain Si^{4+} and Al^{3+} within the IV-fold coordination that has oxygen; it ranges from an amorphous to semi-crystalline structure. However, (Davidovits 1991; 1994) synthesis of geopolymers at hydrothermal setting with hardening occurring between the ranges of 150°C -180°C will result in a crystalline structure forming. Davidovits (1999) indicated that there are three different types of monomeric polysialate structures based on the number of silicon atoms that are replaced by aluminium; Si/Al ratio. Through an increase of silicate reactants, the geopolymer structural units will range from a ratio (Fig. 2.1) of 1.0 as polysialate known as PS (-Si-O-Al-O-), a ratio of 2.0 as poly-sialate-siloxo known as PSS (-Si-O-Al-O-Si-O) and a ratio of 3.0 as poly-sialate-disiloxo known as PSD (-Si-O-Al-O-Si-O-Si-O) as shown on Table 2.1 (Xu, 2002; Sindhunata, 2006). The structures have different ranges of applications such as PS and PSS may be applied to an extent of immobilisation of toxic waste and producing construction waste through synthesis with sol-gel chemistry at room temperature. Davidovits (1991) indicated that PSD differs from PS and PSS because of its superior physical and thermal properties that are suitable for the utilization of refractory lining or tooling composite material.

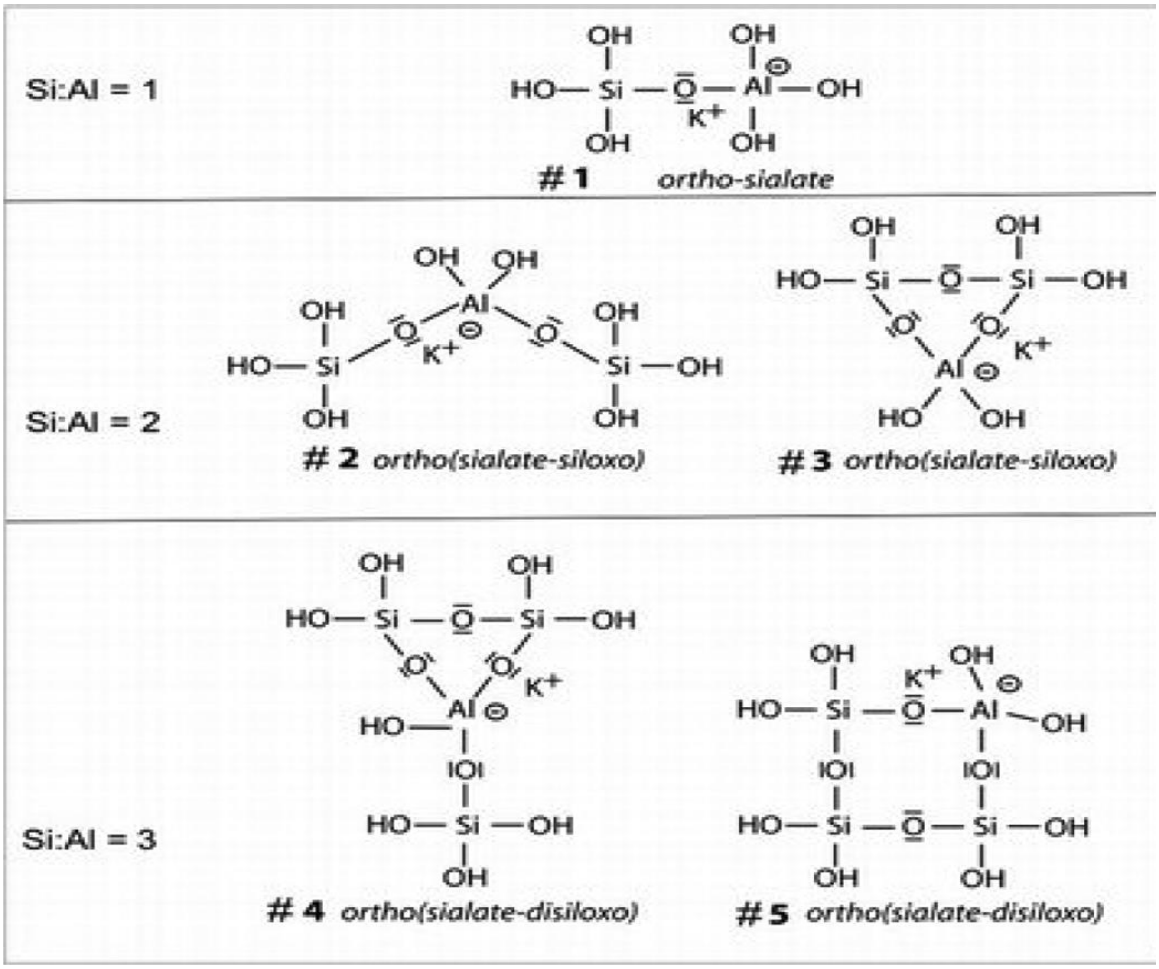

Figure 2. 2: The sialate geopolymer structure proposed by Davidovits (1982).

According to Davidovits (1988), geopolymerization may be successfully conducted if the overall molar ratio Al_2O_3: SiO_2 is between 1:5.5 and 1:6.5. However, Van Jaarsveld et.al. (1996) suggested that the ratio is not much of a critical parameter when dealing with waste materials but that the ratio allows one to know the approximate composition of the waste. Van Jaarsveld et.al. (1996) described the geopolymer reaction in three main steps:

i) Mobile polysialate species are formed through dissolution where hydration species such as alkali solutions (NaOH or KOH) are introduced.
ii) The mobile precursors undergo partially orientation and the alkali polysilicates undergo partial internal restructuring.
iii) Geopolymer system hardens into a solid monolithic inorganic polymeric structure through a process of re-precipitation.

Van Jaarsveld et.al. (1997) stated: "In order to optimise the advantages offered by geopolymers derived from waste materials, it is imperative to identify as well as quantify critical parameters

that affect the eventual structural stability of the finished product". A more comprehensive solid-state analytical technique or method is needed to provide conclusive results as far as structural analysis is concerned. Through the application of geopolymers and their cementations properties recent studies have shown it possible to use these properties for a multitude of different purposes besides the initial findings by Davidovits (1979). These properties and applications are thereof to be discussed in the following subsection.

Table 2. 1: Classification of polysialate structures with their respective applications according to Davidovits (1991).

Classification	Monomeric structure	Application
Polysialate (PS) Si:Al = 1:1	Mn-(Si-O-Al-O-) n	-thermal insulation -fire-resistant board
Poly-sialate-siloxo Si:Al = 2:1	Mn-(Si-O-Al-O-Si-O-)n	-refractory for aluminium (PSS) casting -high-performance cements -toxic wastes -fire resistant composites
Poly-sialate-disiloxo (PSDS) Si:Al = 3:1	Mn-(Si-O-Al-O-Si-O-Si-O) n	-fire resistant composites -tooling materials for use in the temperature range from 650 °C - 1000 ◦C

2.3.4 Properties of geopolymers

Geopolymers as discussed are cementitious materials that contain the following properties:

High early mechanical strength: The compressive strength of a poly (sialate) geopolymer after 1 hour of drying at 65°C is 48.1 MPa (Gokhale, 2001). Type I concrete only reaches a maximum compressive strength of 45 MPa however, Van Jaarsveld et.al. (1988) indicated that certain geopolymer matrices can achieve compressive strength values of 75 MPa.

Excellent fire resistance: The poly (sialate) geopolymer has good high temperature related properties being stable up to l300°C whereas concrete begins to degrade at 300°C.

Thermal insulation: Geopolymer matrix carbon fiber composite doesn't ignite, burn or release any smoke while glass or carbon-reinforced polyester ignites readily and releases appreciable heat and smoke when irradiation of 50 kW/m^2 levels occur (Lyon et aI., 1999).

Low density: The density of a cured geopolymer carbon fiber composite was measured at 1.85 g/cm^3 (Lyon et aI., 1999).

Acid resistance: 7% of the geopolymer matrix is destroyed in a 5% H_2S0_4 solution in

comparison to a 95% matrix breakdown for Portland cement (Van Jaarsveld et.al., 1997).

Low permeability: The hydraulic permeability of the geopolymeric cement manufactured by Davidovits (1994b) was measured at 1.0^{-9} at 28 days and 1.0^{-11} at 364 days whereas the permeability values for Portland cement are 10^{-10}**.**

Fast setting: According to Van Jaarsveld et.al. (1998) a geopolymer cured at 1 day reaches a compressive strength of 75 MPa and a type I concrete can only reach a maximum compressive strength of 45 MPa after a 90-day curing period.

Less CO_2 emission than Portland cement: Geopolymeric cement produces five times less CO_2 during manufacture than Portland cement (Davidovits, 1999b and Provis et.al., 2007).

2.3.5 Application of geopolymers

Based on the geopolymers properties the produced matrices can be applied in the following fields as mentioned by Davidovits 1999a and Duxson et.al. 2007.

1. Non-flammable composite geopolymer cement or mixed with carbon fibers are produced by mixing geopolymer with rock aggregates (fly ash). There are numerous environmental applications for the aforementioned binders such as; encapsulation of hazardous, radioactive wastes and toxic metals, capping's in waste dumps and landfill sites, as water barriers where water deflection is needed as sealants and other structures necessary for toxic waste containment sites.
2. Geopolymer cements replacement constituents of any current building component being used such as bricks and ceramic tiles. Geopolymeric pastes have a mouldability characteristic; hence, they are used in simple structures such as fences, paving materials and low-cost pipes.
3. Geopolymers concretes are ideal for structural surfaces like floors and storage due to their exhibition of other characteristics such as very high compressive strengths and early setting properties.
4. Utilising the fire-resistant properties of geopolymers, a geopolymer matrix carbon fiber composite was manufactured (Lyon et.al., 1999) and tested for use in aeroplane cabins to render the panels fireproof.

2.3.6 Geopolymerization studies in South Africa

There has been minimal research reported in South Africa on geopolymerization, most of them focus on the mechanical properties of using fly ash and raw clay materials. The focus of most researchers in the geopolymerization field directly or indirectly is to understand the

compressive strength, elastic modulus and the structural behaviour of geopolymer materials. Louw (2017) investigated the structural characteristics of alkali-activated materials (AAMs) with a thorough investigation into the mechanical properties in order to understand the most appropriate alkali solution, amount of water content, temperature and duration for curing, modulus of the activator and the coarse aggregate content and size. Louw (2017) acquired results that indicated that the mechanical properties of the AAMs were mainly influenced by calcium content, sodium hydroxide concentration and the activator modulus which gave a compressive strength of 67 MPa however, a low elastic modulus ranging between 10 GPa and 32 GPa. The main focus of researchers investigating the mechanical properties is to fill in the knowledge gap that is within the industry of whether geopolymer materials are suitable in a commercial environmental. In order for the geopolymer materials to be commercially viable, they are to have similar characteristics as OPC and there has to be a demand for the material. The SABS mainly focus on the strength of the cement which ranges from (32.5 MPa, 42.5 MPa and 52.5 MPa). Malatse and Ndlovu (2015) focused their research on the technical and economic viability of using the Witwatersrand gold tailings and cement to produce bricks with temperatures of 110 ºC. Researchers have focused in the need of utilising waste materials within the country in order to reduce unnecessary waste and acquiring the required standards. The researchers also further indicate the importance of the material being accepted commercially by providing information on the materials durability, strength, elasticity and water adsorption and weight loss.

References

Azapagic, A., 2004. Developing a framework for sustainable development indicators for the mining and minerals industry. Journal of Cleaner Production, 12(6), pp.639-662.

Babu, M.N., Sahu, K.K., and Pandey, B.D., 2002. Zinc recovery from spharelite concentrate by direct oxidative leaching with ammonium, sodium and potassium persulphates. Hydrometallurgy, 64, pp.119-129.

Bacon, J.R. Hewitt, I.J. Cooper, P. 2005. Reproducibility of the BCR Sequential Extraction Procedure in a long-term study of the association of heavy metals. Science Total Environment. Vol 337, pp. 191-205.

Bakharev, T., (2005). Resistance of geopolymer materials to acid attack. Cement and Concrete Research, 35(4), pp. 658–670.

Barbosa, V.F.F., MacKenzie, K.J.D., Thaumaturgo, C., 2000. Synthesis and characterisation of materials based on inorganic polymers of alumina and silica: sodium polysialate polymers. International Journal of Inorganic Materials. Vol 2. pp. 309–317.

Benzaazoua M, Ouellet J, Servant S, Newman P and Verburg R. (1999) Cementitious backfill with high sulfur content: physical, chemical and mineralogical characterization. Cement and Concrete Research. Vol 29, pp. 719–725

Benzaazoua, M., Belem, T., Bussiere, B., 2002. Chemical factors that influence on the performance of mine sulphidic paste backfill. Cement and Concrete Research 32 (7), 1133–1144.

Benzaazoua, M., Fall, M., Belem, T., 2003. Contribution to understanding the mechanism of cemented paste backfill hardening. Minerals Engineering 17 (2), pp. 141–152.

Blowes, D.W., Jambor, J.L., and Hantong-Fong, C.J., 1998. Geochemical, mineralogical and microbiological characterization of a sulfide-bearing carbonate-rich gold-mine tailings impoundment, Joutel, Quebec. Applied Geochemistry, 13, pp.687-705.

Bradl, H., editor. Heavy Metals in the Environment: Origin, Interaction and Remediation Volume 6. London: Academic Press; 2002.

Chang, L.W., Magos, L., Suzuki, T., editors. Toxicology of Metals. Boca Raton. FL, USA: CRC Press; 1996.

Cheng, T. W., and Chiu, J. P., 2003. Fire resistant geopolymer produced by granulated blast furnace slag. Journal of Mineral Engineering, 16(3), 205-210.

Chen, Y., Zhang, Y., Chen, T., Zhao, Y., and Bao, S., 2011. Preparation of eco-friendly construction bricks from hematite tailings. Construction and Building Materials, 25, pp. 2107–2111.

Davidovits, J., ed. 2005. Geopolymer, Green Chemistry and Sustainable Development Solutions: Proceedings of the World Congress. Geopolymer Institute.

Davidovits, C., 2003. Catchment diagnostic framework for the Klip River Catchment, Vaal barrage Oct 1998- Sept 1999. MSc dissertation submitted to University of Witswatersrand.

Davidovits, J., 1994. Geopolymers: man-made rock geosynthesis and the resulting development of very early high strength cement. Journal of Materials and Education. Vol 16 (2and3), pp. 91–137.

Davidovits, J., Davidovits, M., and Davidovits, N., 1994. Process for obtaining a geopolymeric alumino-silicate and products thus obtained. US Patent, 5342595.

Davidovits, J., 1994. Geopolymers: man-made rock geosynthesis and the resulting development of very early high strength cement. Journal of Materials and Education. Vol. 16 (2and3). pp. 91–137

Davidovits, J., 1982. Mineral polymers and methods of making them. US Patent 4349386.14.09.82.

Dimas, D., Giannopoulou, I., and Panias, D., 2009. Polymerization in sodium silicate solutions: A Fundamental process in geopolymerization technology. Journal of Materials Sciences, 44, pp.3719-3730.

Dorricott, M.G., Grice, A.G., 2002. Backfill the environmentally friendly tailings disposal system. In: Proc. Green Processing 2002, AIMM, Melbourne, pp. 265– 270.

Drechsler M, Graham A., 2005. Innovative material technologies: bringing resources

sustainability to construction and mining industries. In: 48th Institute of Quarrying Conference, Adelaide SA, Australia

Duxson, P., Provis, J. L., Lukey, G. C., Mallicoat, S. W., Kriven, W. M., and Van Deventer, J. S. J., (2005). Understanding the relationship between geopolymer composition, microstructure and mechanical properties. Colloids and Surfaces A, 269(1–3), pp. 47–58.

Duxson, P., Fernandez-Jimenez, A., Provis, J.L., Lukey, G.C., Palomo, A., and Van Deventer, J.S.J., 2007. Geopolymer technology: The current state of the art. Journal of Materials Science. Vol 42 (9), pp. 2917-2933.

Fergusson, J. E., editor. The Heavy Elements: Chemistry, Environmental Impact and Health Effects. Oxford: Pergamon Press; 1990.

Fernández-Jiménez, A., Palomo, A., and Alonso, M. M., (2005). Alkali activation of fly ashes: mechanisms of reaction Non-Traditional. Cement and Concrete Brno, Czech Republic Ed. V. Bilek and Z. Kersner, Brno University of technology, 1-12.

Fernandez-Jimenez, A., Palomo, A., and Criado, M., (2005). Microstructure development of alkali-activated fly ash cement: A descriptive model. Cement and Concrete Research, 35(6), pp. 1204–1209.

Gitari, M.W., Akinyemi, S.A., Thobakgale, R., Ngoejane P.C., Ramugondo, L., Matidza, M., Mhlongo, S.E., Dacosta, F.A and Nemapate, N., 2017. Physicochemical and Mineralogical Characterization of Musina Mine Copper and New Union Gold Mine Tailings: Implications for Fabrication of Beneficial Geopolymeric Construction Materials. Journal of African Earth Science, 137(2018), pp.218-228.

Godfrey, L., Oelofte,S., Phiri, A., Nahman, A., and Hall, J.,2007. Mineral waste: The required governance environment to enable reuse. Final report. (SIR/NRE/PW/IR/2007/0800C)

He ZL, Yang XE, Stoffella PJ. Trace elements in agroecosystems and impacts on the environment. J Trace Elem Med Biol. 2005; 19(2–3):125–140. [PubMed: 16325528]

WHO/FAO/IAEA. World Health Organization. Switzerland: Geneva; 1996. Trace Elements in Human Nutrition and Health.

Iklevay, L.M., 2000. Cardiovascular disease from Cu^{+} deficiency- A History. The Journal of

Nutrition, 130(2), pp.4895-4925.

Jones, J.M. 1993. Sequential extraction method: A review and evaluation. Environmental Geochemistry and Health. Vol 15 (2-3)

Klevay, L.M., 2000. Trace element and mineral nutrition in disease: ischemic heart disease. In: Bogden JD, Klevay LM, editors. Clinical Nutrition of the Essential Trace Elements and Minerals: The Guide for Health Professionals. Totowa, NJ: Humana Press Inc. pp. 251–271.

Lukey, C., and Van Deventer, J. S. J., (2004). Solid-particle erosion of a geopolymer containing fly ash and blast-furnace slag. Wear, 256 (7-8), pp. 714–719.

Lyon, R.E., Foden, A.J., Balaguru, P., Davidovits, J. and Davidovics, M., (1999). Properties of GEOPOLYMER-MATRIX-Carbon Fiber Composites. Proceedings of the Second International Conference on Geopolymers, France.

Malatse, M and Ndlovu, S., 2015. The viability of using the Witswatersrand gold mine tailings for brickmaking. The Journal of The Southern African Institute of Mining and Metallurgy, 115, pp.321-327.

Marsden, D.D., 1986. The current limited impact of Witswatersrand gold mine residues on water pollution in the Vaal river system. Journal of South African Institute of Mine and Metallurgy, 86, pp.481-504.

McCarthy, T.S., 2011. The impact of acid mine drainage in South Africa. South African Journal of Sciences, 107(5/6).

MINING FACTS. 2014. How are waste materials managed at mine sites. http://www.miningfacts.org/environment/How-are-waste-materialsmanaged-at-mine-sites [Accessed 6 June 2017].

Mudd, G., and Boger, D.V., 2013. The ever-growing case for paste and thickened tailings: Towards more sustainable mine waste management. Australian Institute Min. Metallurgy Bulletin, Vol. 2, pp.56-59.

Mustafa Al Bakri, A.M., Kamarudin, H., Bnhussain, M., Nizar, I.K., and Mastula, W.I.W., 2011. Mechanism and chemical reaction of fly ash geopolymer cement- A Review. Asian Journal of Scientific Research, Vol. 1(5), pp.247-253.

Olayinka, K.O. Oyeyiola, A.O, Odujebe, F.O and Oboh, B. 2001. Uptake of potentially toxic metals by vegetable plants grown on contaminated soil and their potential availability using sequential extraction. Journal of Soil Science and Environmental Management, Vol. 2 (8), pp. 220-227

Ouellet, S., Bussiere, B., Mbonimpa, M., Benzaazoua, M., Aubertin, M., 2006.Reactivity and mineralogical evolution of an underground mine sulphidic cemented paste backfill. Minerals Engineering, Vol. 19 (2006), 407–419.

Palomo, A., Blanco-Varela, M.T., Granizo, F., Vazquez, T., Grutzeck, M.W., 1999a. Chemical stability of cementitious materials based on metakaolin. Cement and Concrete Research. Vol. 29 (7). pp. 997–1004.

Palomo, A., Grutzeck, M.W., Blanco-Varela, M.T., 1999b. Alkali- activated fly ashes, a cement for the future. Cement and Concrete Research, Vol. 29 (8), 1323–1329.

Ramatsa, I.M., 2011. An investigation into the leaching behaviour of nickel-copper bearing matte. Master's thesis. University of Johannesburg

Rao, F., and Lui, Q., 2015. Geopolymerization and its potential application in mine tailing consolidation: A Review. Mineral Processing and Extractive Metallurgical Review, 56, pp.399-409.

Reeb, J and Milota, M. (1999). Moisture content by the oven-dry method for industrial testing. Oregon State University Corvallis. Available online at http://ir.library.oregonstate.edu/

Rice, K.C., and Herman, J.S., 2012. Acidification of Earth: An assessment across mechanisms and scales. Applied Geochemistry, 27, pp.1-14.

Rosenberg, E., 2016. Population growth and sustainable development. [online] Available at: www.enviropaedia.com. (Accessed 10 March 2017).

Roy, S.A.G.R., and Gupta, R.N., 2007. Use of gold mill tailings in making bricks: A feasibility study. Waste Manage Res, 25, pp. 475–82.

Salomons, W., 1995. Environmental impact of metals derived from mining activities: Processes, predictions, prevention. Journal of Geochemical Exploration, 52(1-2), pp.5-23.

Singo, N.K. 2013. An assessment of heavy metal pollution near an old copper mine dump in Musina, South Africa. University of South Africa

Stats SA, 2016. Mid-year population. [online] Available at www.statssa.gov.za. (Accessed 13 March 2017).

Tessier, A. Campbell, P.G.C. Bisson, M. 1979. Sequential Extraction Procedure for speciation of particulate trace metals. Analytical Chemistry. Vol 51, pp. 844-851

Thobakgale R., 2017. Evaluation of geochemical and mineralogical transformation at an old copper mine tailing dump. Master's thesis. University of Venda

Tokaligoglu, S. Kartal, S and Biral, G. 2001. Application of a three-stage Sequential Extraction Procedure for the Determination of Extractable metal contents in Highway soils. Turkish Journal of Chemistry. Vol 27 (2003), pp. 333-346

Tutu, H., McCarthy, T.S., and Cukrowska, E., 2008. The chemical characteristics of Acid Mine Drainage with particular reference to sources, distribution and remediation: The Witswatersrand Basin, SA as a case study. Applied Geochemistry, 23(12), pp.3666-3684.

Ure, A.M. 1996. Single extraction schemes for soil analysis and related applications. Science Total Environment. Vol 178, pp. 3-10

Van Jaarsveld, J.G.S., Van Deventer, J.S.J. and Lorenzen, L. (1996). Immobilisation of toxic metals in geopolymers. Proceedings of Chemeca 96: 24th Australian and New Zealand Chemical Engineering Conference., Sydney, Australia

Van Jaarsveld, J.G.S., Lukey, G.C., Van Deventer, J.S.J., 2000. The stabilisation of mine tailings by reactive geopolymerization. Publications of the Australasian Institute of Mining and Metallurgy, 5/ 2000, MINPREX 2000, Melbourne, Australia. pp. 363–371.

Wang S, Shi X. Molecular mechanisms of metal toxicity and carcinogenesis. Mol Cell Biochem. 2001; 222:3–9. [PubMed: 11678608].

Watts, D.L., 1989. The nutritional relationships of copper. Journal of Orthomolecular Medicine, 4(2), pp.99-108.

Wilson, M.G.C and Anhaeusser, C.R. 1998. The Mineral Resources of South Africa. 6th ed. Council of Geosciences, Pretoria, South Africa. pp. 209-207

Xu, H., and Van Deventer, J.S.J., 2002a. Geopolymerization of multiple minerals. Minerals Engineering, 15, pp.1131-1139.

Xu, H., and Van Deventer, J.S.J., 2002b. The geopolymerization of alumino-silicate minerals. International Journal of Mineral Processing, 59(3), pp.247-266.

Xu, H., Van Deventer, J.S.J., Lukey, G.C., 2001. The effect of alkali metals on the preferential geopolymerization of stilbite/kaolinite mixtures. Industrial and Engineering Chemistry Research Vol 40 (17). pp. 3749–3756.

Xu, H., Van Deventer, J.S.J., 2000. The geopolymerization of alumino-silicate minerals. International Journal of Minerals and Processing. Vol 59 (3). pp. 247–266.

Yip, C.K., Van Deventer, J.S.J. Effect of granulated blast furnace slag on geopolymerization. In: CD-ROM Proceedings of 6th World Congress of Chemical Engineering, Melbourne, Australia, 23–27 September 2001.

Zang, H. Schroder, L.J.L. Pittman, J,J. Wang, J.J and Payton, M.E. 2005. Soil salinity using saturated paste and 1:1 soil and water extracts. Soil Science Society of America Journal. Vol 69, pp. 1146-1151

Zang, L., 2013. Production of bricks from waste materials – A Review. Construction and Building Materials, 47, pp.643-655.

Zang, M., El-Korchi, T., Zang, G., Liang, J., and Tao, M., 2014. Synthesis factors affecting mechanical properties, microstructure and chemical composition of red mud-fly ash based geopolymers. Fuel, 134, pp.315-325.

Chapter 3

Part A: Physicochemical characterization and mineralogy of copper mine tailings and its implications for the production of geopolymeric materials.

Abstract

This chapter presents the macroscopic characteristics, physical, chemical and mineralogical properties of Musina copper tailings. X-ray diffraction (XRD) and X-ray fluorescence (XRF) were used to evaluate the mineralogical and elemental composition of the tailings while scanning electron microscopy (SEM) was used to evaluate the morphology of the tailings. Other physical properties such as bulk density, particle distribution, pH and EC were determined using standard laboratory techniques. The results showed that pH of the tailing ranges from near neutral pH of ±7.5 to a slightly alkaline pH of ±8.5. Furthermore, tailings paste are characterized by a very low EC, ranging from 87 µS/cm to 1204 µS/cm. Chemical composition analysis showed that Musina mine tailings (MT) mainly consist of SiO_2 and Al_2O_3 as the major oxides ranging from 52.26 to 85.15% and 11.35 to 15.97% w/w respectively, indicating that MT are alumina-silicate materials. Mineralogical analysis confirmed the dominant presence of quartz (38.3% to 55.38%); epidote (17.69 % to 29.78%) and chlorite (10.05% to 20.44%) as the major mineral phases. The morphological structure of the MT indicated sheet-like material that has large shiny crystals. Based on the physiochemical, mineralogical and gravimetric analysis conducted in this chapter it is concluded that Musina copper MT can be used in geopolymerization.

Keyword: *Mine tailings, Alumino-silicate, Acid Mine Drainage (AMD), Unified Soil Classification System (USCS), Semi-crystalline structure.*

3.1 Introduction

Mine tailings are residues containing economic minerals and uneconomic materials obtained from during mining processes. They are often characterized by fine sand to silt sized particles of quartz, alumino-silicates, carbonates, oxides, and sulfides. Tailings are hazardous waste where metal rich materials generate AMD and leachates; and a potential economic resource when there is low grade ore present within the tailing which may be easily extracted. The amount of metal species, chemical and mineralogical constituents that are present within the tailing are dependent on the mineral composition of the ore body and the chemicals used during extraction. These constituents are also further altered by the environmental and climatic conditions that are within the area. For example, tailings will result in weathering due to natural exposure to air, water, ambient air or vegetation. Such environmental factors determine the physical and geochemical stability of the material under different weathering conditions. Additionally it affects the nature, concentration of toxic, and acid generating or neutralizing chemical species that may be released (Bradl, 2002).

In this section the physical characteristics such as pH, TDS, EC, porosity, specific gravity and bulk density of the tailings were determined using standard laboratory techniques. Furthermore, the chemical composition, mineralogical composition and the morphology of the tailings were determined using X-Ray Fluorescence (XRF), X-Ray Diffraction (XRD), Scanning electron microscopy (SEM-EDS) and Transmission electron microscopy (TEM), respectively. The results attained will help us to determine whether the tailings geochemical and mineralogical assemblage is harmful in the environment and human body when the material is converted into a geopolymer material.

3.2 Materials and Methods

3.2.1 Description of study area

Musina is situated in the Northern region of the Limpopo Province in South Africa at coordinates 22° 20´17" S 30° 02´30" E / 22.33806 ° S 30.04167° E and has a maximum elevation of 560 m above mean sea level (Chinoda et.al., 2009; Bradley et.al., 2011). The region was established in 1968 and covers an area of 109.38 km^2 located near the confluence of the Limpopo River, Sand River and the Zimbabwean border (Chinoda et.al., 2009). The region is rich in diverse mineral ores such as iron ore, coal, magnetite, graphite, asbestos, diamonds, semi-precious stones and copper (Council for Geoscience, 2010). Musina is known for its beautiful Soutpansberg Mountain range and the Blouberg Massif (Limpopo DFED, 2004) that

are surrounded by gentle slopes and undulating Bushveld Complex of the Limpopo Midveld. Copper mines such as Artonvilla Messina, Spence, Harper and Western Campbell mine are present in the region (Wilson et.al., 1998).

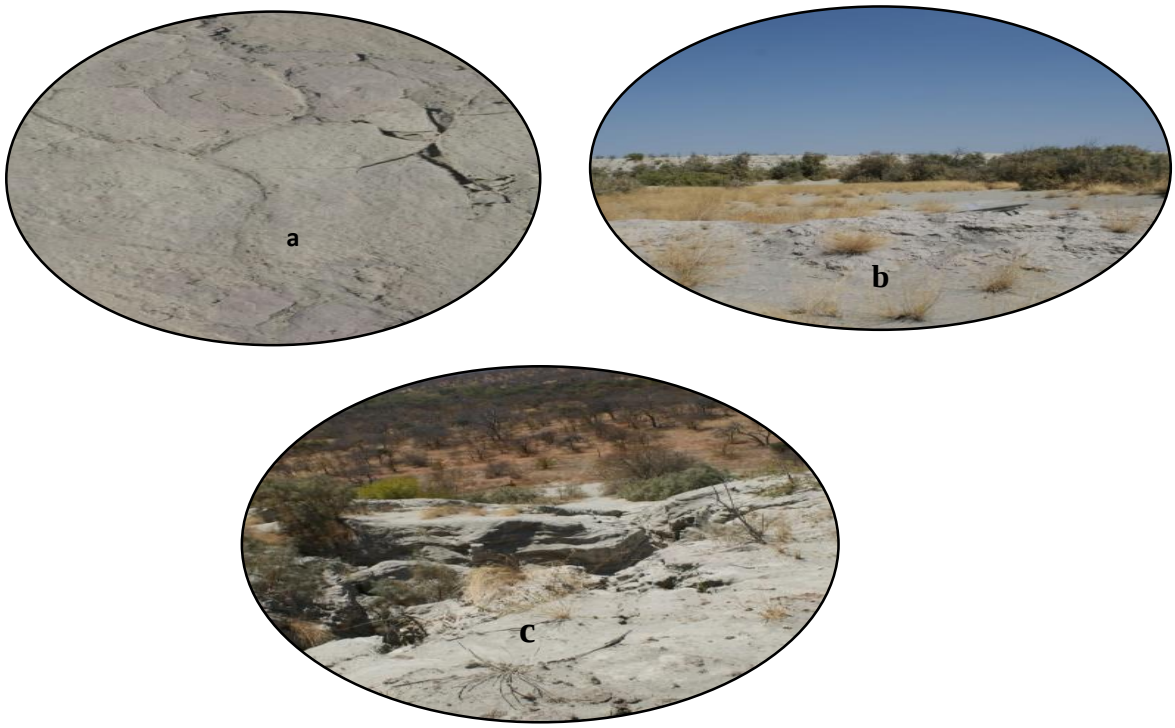

Figure 3. 1a: Surface sample of the copper mine tailing; b: Trees and shrubs surrounding sample point; c: Erosion occurring at the tailing slope.

3.2.2 Sample collection and preparation

The most important and probably the crucial aspect in the collection of samples are to identify the sampling points to be used in acquiring valid and sufficient samples for analysis. Figure 3.2 illustrates the samples points that were rando mLy selected on the tailing dam using a Geographic Positioning System (see figure 3.2).

1. Site 1 (red dot on Fig.3.1) is at a location of 22˚20.172’ S, 30˚.2.702’ E at 550 m above sea level.
2. Site 2 (blue dot on Fig.3.1) is at a location of 22˚19.845’ S, 30˚.2.926’ E at 562 m above sea level.
3. Site 3 (yellow dot on Fig.3.1) is at a location of 22˚19.887’ S, 30˚.3.061’ E at 557 m above sea level.
4. Site 4 (orange dot on Fig.3.1) is at a location of 22˚19.587’ S, 30˚.3.281’ E at 532 m above sea level.

5. Site 5 (green dot on Fig.3.1) is at a location of 22˚19.520’ S, 30˚.3.102’ E at 539 m above sea level.

Figure 3. 2: Location of the sample points (Source: Google earth).

Clearing sample points

Once the sample points were randomly chosen, the surface of the sampling point was scrapped with a spade to clear the debris and vegetation.

Auguring

Samples were collected from the above indicated points (Fig 3.2) using a handheld auger from the surface to a maximum depth of 4 m at S1; S2, S3 and S5 where augured at 1 m and S4 was augured at a depth of 1 m to 3 m. Samples were stored in a tightly tied plastic and labelled according to the depth and sample points; and then delivered to the laboratory where they were stored for further processing and analysis. Figure 3.3 illustrate the sampling procedure.

Figure 3. 3: Illustration of augering process.

3.2.3 Preparation of mine tailings

The collected samples were split using a riffle splitter in order to obtain a homogenous sample. The sample bag was weighed and recorded afterwards. Thereafter, the samples were oven dried for 24 hours at 110 °C. A fraction of the dried sample was milled in a tungsten-carbide milling pot in order to attain the samples particle size < 75 µm. A fraction of the milled sample was further dried at a 100°C and roasted at 1000 °C in order to determine the Loss On Ignition (LOI) values.

3.2.4 Physical characteristics

Moisture content

The moisture content was determined according to equation 3.1 as described by Reeb and Milota (1999).

$$\%H_2O = \frac{Wet\ wt - Dry\ wt}{wet\ wt} \times 100\% \quad \text{Equation 3. 1}$$

Where; wet (wt) = weight of the wet tailings and dry (wt) = weight of dry tailings.

pH, Total Dissolved Solids (TDS) and Electrical Conductivity (EC) analysis

The pH, TDS and EC of MT were determined according to the soil paste method (Zhang et.al., 2005). The mass of 50g of MT was weighed and placed in a beaker. This was followed by the addition of 50 mL of Milli-Q water (18.2 MΩ.cm) and the mixture was stirred to obtain soil paste. The beaker was then sealed with a watch glass and left for a minimum of 1 hour under a continuous stirring after every 15 minutes to allow the pH of the soil to stabilise. Thereafter, pH, TDS and EC were measured using a calibrated Jenway 430 multi-meter using pH4 and pH7 buffers.

Specific gravity

The specific gravity of the MT was determined according to equation 3.2 based on the Archimedes principle wherein a mass of 100 g of the dried samples were weighed and immersed into water. The displaced water weight was then determined and equation 3.2 was used to calculate the specific gravity.

$$Specific\ Gravity = \frac{Mass\ of\ dry\ solid}{Weight\ of\ displaced\ water} \quad \text{Equation 3. 2}$$

Porosity

In order to determine the porosity of the MT, a 500 mL beaker was filled with 100 g of the MT. A 100 mL measuring cylinder was filled to the 100 mL mark and water was slowly poured into the beaker until it reaches the top of the MT. The volume of water used was measured. Thereafter, equation 3.3 was used to determine the porosity (%):

$$Porosity\ (\%) = \frac{H_2O}{Vol_S} \times 100 \quad \text{Equation 3. 3}$$

Where; H_2O is the amount of water added to sample and Vol_S is the total sample volume.

Particle size distribution

The particle size distribution (PSD) of the MT was determined according to the procedure described by Whitby (1958). A mass of 1000 g of dried MT was weighed and disposed onto pre-weighed sieves with pore sizes ranging from 2 mm to 32 µm and shaken for 1hr at an

amplitude of 1.22 mm. Thereafter, sieves are weighed and the difference between the final weight and initial weight is obtained as the amount of particle size weight in each sieve.

Bulk Density

The bulk density of the MT was determined according to the procedure determined by Brady and Weil (2002). The bulk density is attained by adding the cylinder and MT mass and then subtracting the density of cylinder and MT as illustrated in equation 3.4.

$$\textbf{\textit{Bulk Density}} = \textbf{\textit{Mass of cylinder and soil}}\ (g) - \frac{\textbf{\textit{Mass of cylinder}}\ (g)}{\textbf{\textit{Volume of soil}}\ (cm^3)} \qquad \text{Equation 3. 4}$$

Mineralogical and chemical characterization

The quantitative mineralogical analysis was conducted using a PANalytical X'Pert Pro powder diffractometer in θ–θ configuration with an X'Celerator detector and variable divergence and fixed to receive slits with Fe filtered Co-Kα radiation (λ=1.789Å). The phases are to be identified using X'Pert Highscore plus software. The relative phase amounts (weight %) is to be estimated using the Rietveld method (Autoquan Program). Bulk chemical composition was determined using S1 Titan handheld Bruker XRF. The surface area and pore volume was determined by Brunauer Emmet Teller (BET) method using micrometrics TriStar II. Functional groups and surface chemistry was determined using Fourier transform infrared spectroscopy (FTIR). The surface morphology and crystallographic structure was determined using Transmission Electron Microscope (TEM) (Jeol JEM 2100) and scanning electron microscopy (SEM) (Leo1450 SEM, with a voltage of 10 Kv and working distance of 14 mm).

3.3 Results and discussion

3.3.1 Physicochemical and mineralogical characterization

Physical characterization analysis

Table 3.1 presents the physicochemical properties of the tailings collected from different points and at different elevation in Musina tailings dump.

Table 3. 1: Physical Parameters of tailing.

Sample no.	pH	TDS (mg/L)	EC(µS/cm)	Temp (°C)	Moisture content (%)
S1- surface	8,3	217	360	25,1	0,49
S1- 1m	8,4	68	113,3	24	9,98
S1- 2m	7,5	572	955	25	5,89
S1- 3m	7,8	516	864	25,3	10,09
S1- 4m	7,7	544	938	25,1	7,25
S2	7,5	733	1195	25,3	2,53
S3	8	141,9	238	25	1,84
S4- 1m	7,8	723	1204	25,5	3,27
S4-2m	7,9	638	1059	25,1	1,61
S4-3m	8,1	200	322	25	1,45
S5	8,5	52	87	25,2	3,26
Average	7,95	400,45	666,85	25,05	4,33

The pH within the MT was found to range from near neutral 7.5 to weakly alkaline 8.5 with an average of 7.95. The near neutral to alkali pH may be due to the presence of neutralising agents such as CaO, MgO, Na_2O and K_2O (Gitari et.al., 2017). Based on the mineralogy of the Bushveld complex according to Wilson et.al.,(1998) the area is rich in quartz thereby, the neutralising agents' alkali characteristics may be assumed to be due to its basic property. Furthermore, Al_2O_3 content which is an amphoteric oxide that has acidic and basic properties (Boehm, 1971). The EC was found to range from 87 µS/cm to 1204 µS/cm and an average of 666.85 µS/cm. At S4 the EC decreased by depth while at S1 there is an inconsistency in concentration by depth. The recorded EC is considered low compared to studies conducted by Rankhonondo (2006) which reported 4000 µS/cm, 1700 µS/cm and 1400 µS/cm for gold, platinum and kimberlite tailings respectively. The TDS within the MT ranges from 52 mg/L to 733 mg/L and an average of 400.45 mg/L.

The low readings are due to the low mobility of the elements present within the tailings (Reimann and de Caritat, 1998). Dissolved solids and other chemicals that ionize within water determines the ionic particles within thereby; TDS and EC are directly proportional as indicated in Table 3.1. The TDS detected throughout the MT is within the DWAF (1998) guidelines where leachable concentration is ≤ 1000 mg/L.

The moisture content of the MT influences the physical properties such as the weight, density, EC and TDS (Akinyemi et.al., 2011). The overall moisture content within the tailing is 4.33%, with a low of 0.49% at S1- surface and a high of 10.09% at S1-3 m. The moisture content in S4

decreases by depth however, S1 shows inconsistency in moisture. Based on results provided in Table 3.1, it can be said that the MT have a poor water holding capacity and will mostly be prone to wind erosion and dispersion to the surrounding areas. Due to the poor water holding capacity of the MT the absorption and retaining capabilities of the material during the process of geopolymerization might be difficult to manage thereby, leaching out of the alkali activators which will make it difficult or lead to partial dissolution process.

Gravimetric analysis

The specific surface area and particle size distribution play a vital role in the pore capacity of the tailing thereby, playing a role in the reactivity kinetics of the tailing (Amponsah-Dacosta and Reid, 2014). Table 3.2 summarizes the particle and surface properties of the MT while Fig 3.4 shows the particle size distribution curve.

Table 3. 2: The particle and surface properties of the procured copper tailings.

Unified Soil Classification System (USCS)	Copper tailing
D10 (mm)	0.09
D30 (mm)	0.2
D60 (mm)	0.28
D90 (mm)	0.5
Cu	3.05
Cz	1.18
P4 mm (%)	99.20
P 0.075 mm (%)	8.17
Specific gravity	2.5
Bulk density(g/ mL)	2.63
Pore volume (cm^3/g)	0.000607
Moisture content	3.01
Surface area (m^2/g)	0.3029
Single point surface area (m^2/g)	0.3326
Pore size (nm)	8.01
USCS	SC (clayey sands, sand-clay mixtures)

Note: D10 = diameter corresponding to 10% finer, D60 = diameter corresponding to 60% finer, D30 = diameter corresponding to 30% finer, D90= diameter corresponding to 90% finer, Cu = uniformity coefficient = $\frac{D60}{D10}$, Cz = coefficient of gradation = $\frac{D30^2}{(D10*D60)}$, P4 mm (%) = percent passing sieve no. 4 and P0.075 mm (%) = percent passing sieve no. 200.

From Table 3.2 it is noted that majority of particles in Musina copper tailings are 90 % finer, making the tailings to be classified as clayey sands. Furthermore, it is observed that MT are characterized by low pore size, pore volume, and surface area. This could be attributed with low pore size present being attributed to high levels of silt (54.6%), sand (45.3%), and minor traces of gravel (<1%) in the tailing as observed in Fig 3.4. According to the unified soil classification system (USCS) copper tailings were classified as silty clayey sand (i.e. sand with

numerous fines). The relatively low specific gravity of 2.5 has been attributed to the low Fe_2O_3 content present in the tailing. Kesimal et.al. (2005) mentioned that effectiveness of complete alumino-silicate dissolution during the geopolymerization process is determined by the materials fineness. Therefore, the copper tailings can effectively go through the process of dissolution of Al-Si material to produce geopolymer bricks based on the particle size distribution.

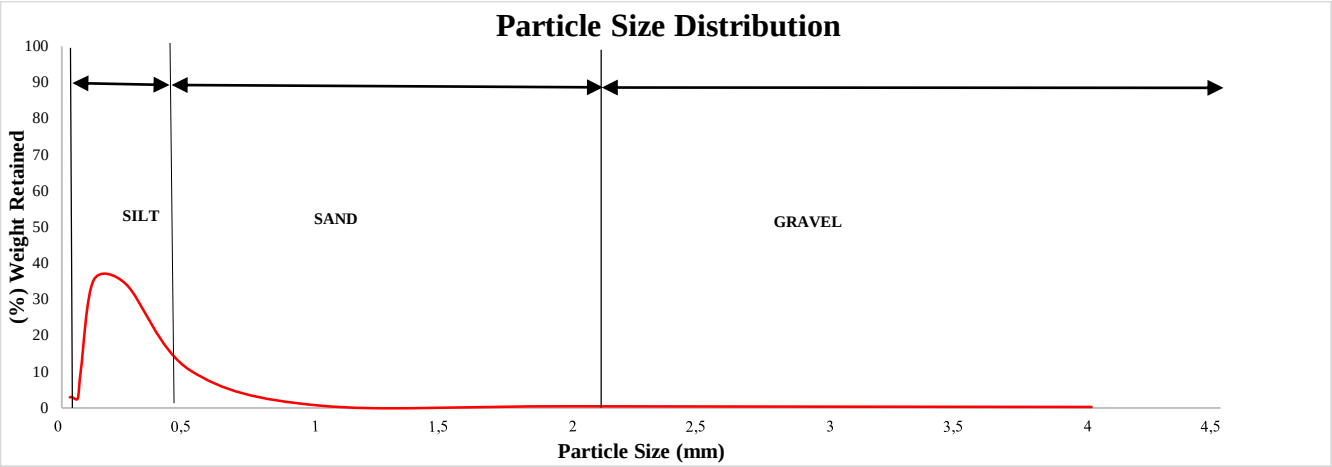

Figure 3. 4: Particle size distribution of copper tailing.

Chemical composition

The chemical composition of Musina copper tailings as determined by XRF are presented in Table 3.3. The analysis from all sampling points revealed that silica (SiO_2) is the main component within the Musina copper tailing with a percentage composition ranging from 56.24% to 85.16% with an average of 64.87%. Alumina oxides (Al_2O_3) were also found to be the main oxides ranging from 11.34% to 15.97% with an average of 12.75%. All sample points except S1 at the surface has a quartz concentration > 60%, the low quartz concentration in the surface might be due to the exposure of the sample to different harsh conditions such as rain and heat which might have triggered dissolution of the material. The similarity in Al-Si content throughout the MT indicates that the tailing is an alumino-silicate material which was extracted from the same ore body and underwent similar extraction processes. The abundance of silica coupled with alumina is a favourable combination that is used in the reactivity process of geopolymerization regarding the enhanced dissolution and the overall mechanical strength it produces. The presence of high concentration of the above-mentioned components indicates that the parent is dominated by the intermediate to felsic rock composition (Wilson et.al., 1998). These compositions are aggregated into alumino-silicates that are evenly distributed in

the parent rock because, the entire Limpopo belt and Beit bridge complex contain gneiss; known for its quartz and metaquartzite (Wilson et.al., 1998). There are significant amounts of Fe_2O_3, CaO and MgO and low amounts of TiO_2, MnO, Na_2O, K_2O, P_2O_3, Cr_2O, ZrO_2, CuO and V_2O_3 (Table 3.4). Cu is the highest trace element with a concentration average of 807.4 ppm, its presence within the minor trace elements indicates that the extraction method used to extract copper was effective. There was no Ni present in S1 at 1 m and 2 m and low concentration of Ga, Ca, As, Mo, Nb, Pb, Rb,U, Y and Th.

Table 3. 3: Major and Trace elemental composition of the Musina copper tailing.

Major Elements (%)	Certified	Analysed	S1-surface	S1-1 m	S1-2 m	S1-3 m	S1-4 m	S2	S3	S4-1 m	S4-2 m	S4-3 m	S5
SiO_2	99,6	99,7	56,24	63,19	67,16	61,41	85,16	60,68	65,48	62,39	62,99	64,84	64,03
TiO_2	0,01	0	0,76	0,62	0,61	0,67	1,02	0,86	0,88	0,71	0,81	0,75	0,75
Al_2O_3	0,05	0,01	14,8	12,9	11,88	13,09	15,97	12,37	12,06	11,36	12,05	11,45	12,34
Fe_2O_3	0,05	0,01	10,29	7,54	6,83	8,12	11,78	8,87	8,07	9,65	9,16	8,76	7,43
MnO	0,01	0	0,05	0,04	0,04	0,04	0,06	0,08	0,07	0,05	0,06	0,05	0,04
MgO	0,05	0,01	2,61	1,57	1,47	2,02	2,77	3,35	2,83	2,36	2,31	2,11	1,72
CaO	0,01	0,01	8,05	8,23	7,35	8,02	8,75	6,15	5,91	6,52	6,76	6,14	8,24
Na_2O	0,05	0,02	0,48	0,58	0,62	0,61	0,75	1,13	1,22	0,62	0,74	0,75	0,69
K_2O	0,01	0,01	1,07	0,61	0,51	0,63	0,87	0,71	0,56	0,66	0,56	0,62	0,4
P_2O_3	0	0,03	0,14	0,13	0,12	0,12	0,18	0,14	0,13	0,15	0,13	0,12	0,12
Cr_2O_3	0	0	0,04	0,02	0,02	0,02	0,04	0,03	0,02	0,05	0,02	0,02	0,03
NiO	0	0,01	0,01	0,01	0	0,01	0,01	0,01	0,01	0,01	0,01	0,01	0,01
V_2O_3	0	0	0,02	0,02	0,02	0,02	0,03	0,03	0,03	0,02	0,02	0,02	0,02
ZrO_2	0	0,01	0,02	0,03	0,03	0,03	0,05	0,03	0,03	0,03	0,03	0,05	0,03
CuO	0	0	0,17	0,07	0,06	0,07	0,1	0,08	0,08	0,13	0,12	0,13	0,04
LOI	100	0,1	4,36	3,63	3,15	4,63	-28,07	4,59	2,58	5,22	4,1	3,98	3,21
TOTAL	100	99,92	99,12	99,19	99,86	99,52	99,46	99,11	99,97	99,94	99,88	99,79	99,09

Trace Elements (ppm)	BHV01	BHV01 Analysed	S1-surface	S1-1 m	S1-2 m	S1-3 m	S1-4 m	S2	S3	S4-1 m	S4-2 m	S4-3 m	S5
As*	0,4	0	78	67	63	72	70	70	70	79	73	69	70
Cu	136	136	1472	640	417	633	645	773	669	1130	1028	1144	330
Ga	21	21	24	21	18	21	20	22	20	23	21	19	21
Mo	1,02	2	96	85	79	88	86	87	82	95	89	83	85
Nb	19	19	80	69	64	70	67	70	67	75	69	67	69
Ni	121	117	19	0	0	6	20	46	29	23	15	12	13
Pb	2,6	4	106	94	88	99	91	94	88	106	95	93	94
Rb	11	10	77	55	50	59	58	58	50	58	54	54	48
Sr	403	396	526	534	463	520	414	363	367	427	433	393	512
Th	1,08	0	84	69	67	74	70	72	66	79	70	68	69
U	0,42	0	172	150	141	157	151	152	143	166	154	146	153
W*	0,27	1	52	41	36	44	43	48	361	394	323	274	297
Y	27,6	26	89	76	72	79	75	81	80	89	83	81	76
Zn	105	102	49	27	24	32	33	49	37	60	41	41	25
Zr	179	196	225	280	235	237	263	241	275	299	273	246	247

[1]

[1] Values for elements indicated with an * should be considered semi-quantitative.

X-Ray Diffraction analysis

The XRD analysis were conducted to identify the mineral phases in the tailings and the results are presented in Figure 3.5 for S1 and S2, S3, S4 and S5 are represented in Appendix C (page70) . The minerals that have been identified are quartz, muscovite, haematite, Epidote, albite, chlorite, muscovite, calcite and plagioclase. The refractogram illustrate a uniformity in mineral composition throughout the sample points by depth. The quantitative XRD results showed that quartz (38.3% to 55.38%), epidote (17.69 % to 29.78%) and chlorite (10.05% to 20.44%) where the major mineral phases. There was no amorphous phase reported in the quantitative XRD results which means the quartz reported here existed in the crystalline form, so was epidote. Minor presence of feldspar group (0.6% to 10.8%), carbonate (0.26% to 1.99%) and iron oxide (0.23% to 1.69%) detected indicate the minor probability of AMD and other detrimental environmental impacts occurring.

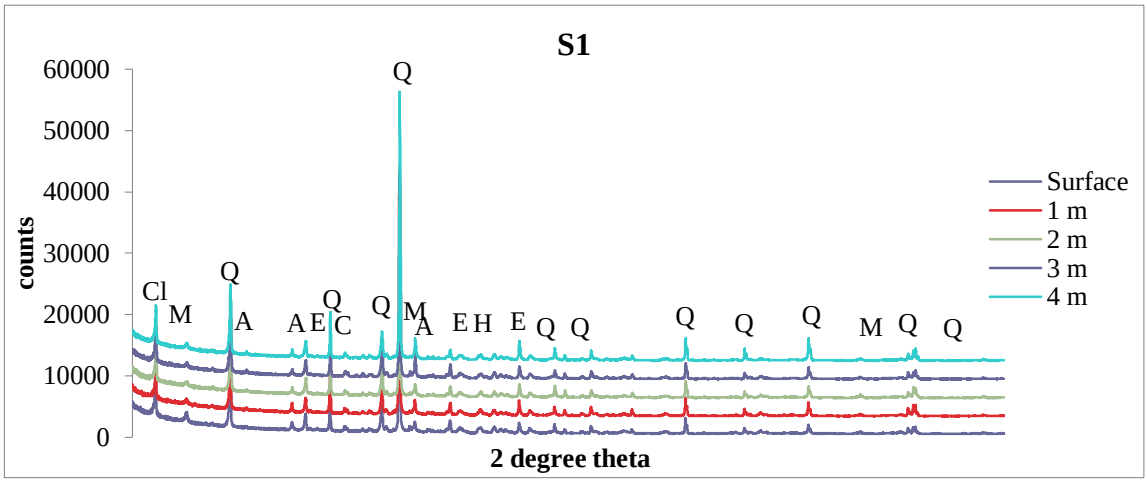

Figure 3. 5: XRD spectra of the copper tailing at sample 1 by depth. (Q- quartz, E-Epidote, Cl- clinochlorite, H-Haematite, A-Albite, M-Muscovite and C- Calcite).

FTIR

The FTIR spectra analysis of S2 was carried out in order to understand the surface chemistry and functional groups of the copper tailing. Figure 3.6 depicts FTIR spectrum obtained from Musina copper tailings. The major absorption bands were observed at wavelength range between 500 cm^{-1} to 1 250 cm^{-1}. The bands at these wavelength are mainly attributed to 509.98 cm^{-1} in the tailing sample were attributed to Si-O, Si-O-Al and Al-O bonds. This results confirms that Musina copper mine tailings are aluminosilicate material in nature. Furthermore, the results corroborate with XRF and XRD analysis which showed the dominance of SiO_2 and Al_2O_3 oxides and quartz mineral.

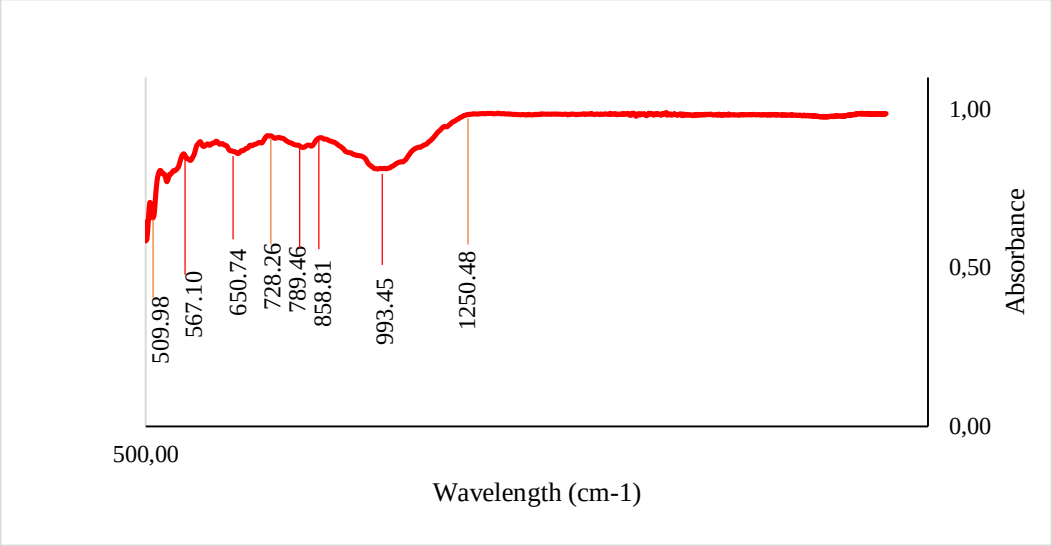

Figure 3. 6: FTIR spectra for copper mine tailing at S2.

SEM and TEM analysis

Figure 3.7 and 3.8 presents the TEM and SEM analysis of Musina copper tailings at S2. The analysis in Figure 3.7 showed that the particles of copper mine tailings are glass fibre like nature and has some angular shape. The angular shape at 200 nm could be an indication of crystalline to semi-crystalline structure (Szymanski, 1998). This structure is attributed to quartz which was found to be the dominant mineral from XRD analysis. At 10 nm particles appears to have a fibrous cleavage. This could be linked to muscovite and feldspar minerals which were also detected by XRD results.

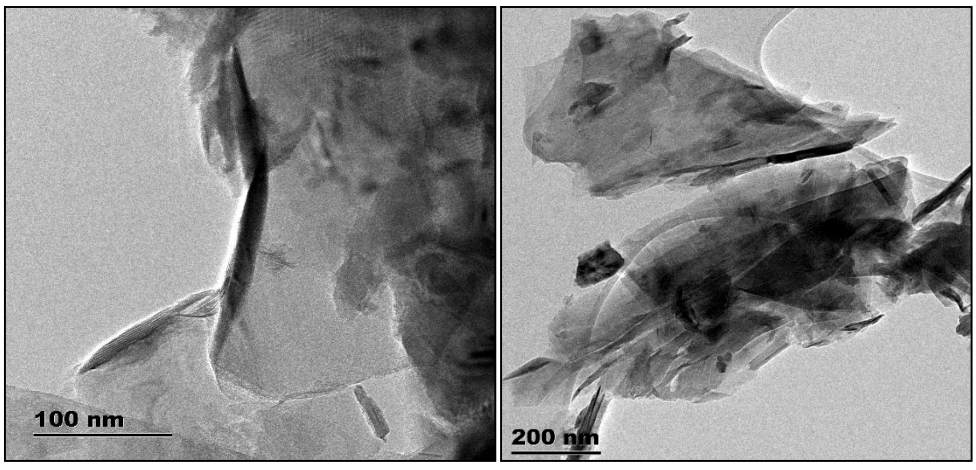

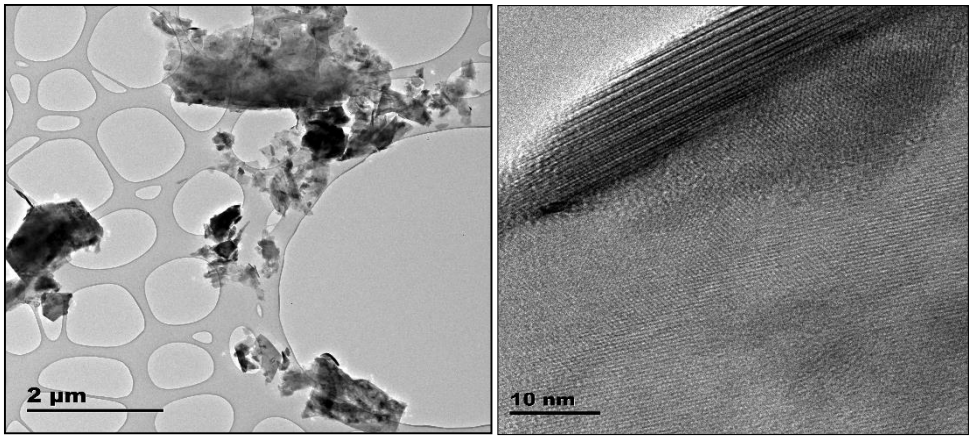

Figure 3. 7: TEM images of S2 copper tailings sample at different resolutions.

Figure 3.8 illustrates the SEM microphotograph where large silver white crystals are surrounded by dark minerals which were identified as quartz and Al-silicate minerals, respectively. The EDS quantification showed the presence of Si and Al at a concentration of 26.9% and 12%, respectively. However, the aforementioned statement doesn't necessarily mean that the Si and Al is readily available for geopolymerization when the mine tailings are reacted with alkali activators. The SEM-EDS results confirm the XRD results furthermore, the crystals within the MT confirm that the material can produce geopolymer bricks when alkali activator reacts with the material. Figure 3.8 shows that the crystals are dispersed throughout the tailing without interlocking.

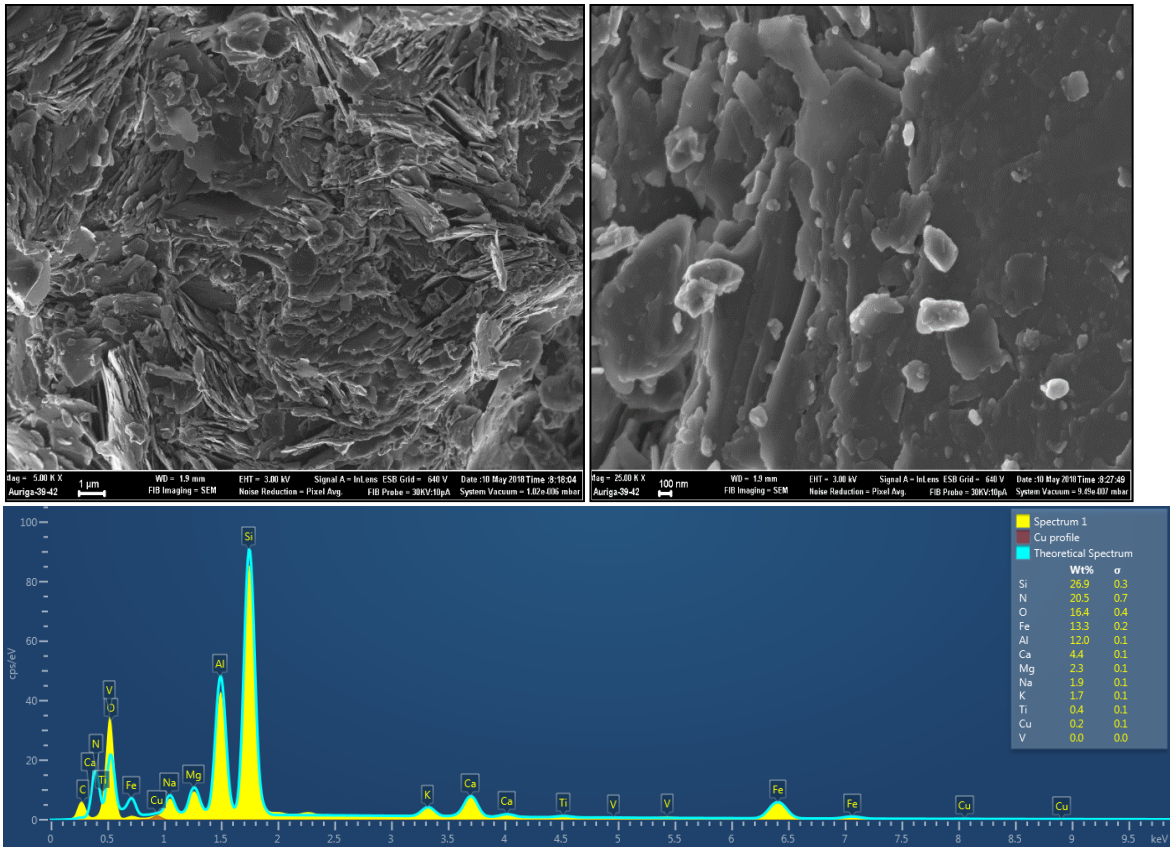

Figure 3. 8: SEM-EDS analysis of S2 copper tailings.

3.4 Conclusion

From this section the physical, chemical and mineralogical composition of Musina copper mine tailings were successfully determined. The following major conclusions were made about the composition of the tailings:

* The tailings pH ranges from nearly neutral to weakly alkaline. Whilst the EC and TDS were ranging from 87 µS/cm to 1204 µS/cm; and 52 mg/L to 733 mg/L, respectively.
* The particles according to USCS have been classified as clayey sands with fine particles > 90%.
* The oxides of SiO_2 and Al_2O_3 were found to be the major components of Musina copper tailings making them to be classified as aluminosilicate materials.
* XRD analysis showed dominance of quartz, epidote and chlorite.

Based on the aforementioned statements it can be concluded that the material has the right components to produce geopolymer bricks and the low metal concentrations present is an advantage.

Part B: Mobility, bioavailability and presence of metals and metalloid species within the copper mine tailing.

Abstract

This section presents an investigation on the geochemical partitioning of major and trace chemical species in copper mine tailings in Musina. This was an attempt to understand the mobility and bioavailability of chemical species. The chemical extraction scheme employed for the present study used four geochemical phases namely; the water soluble/ exchangeable phase, metals bound to Fe-Mn bound phase, metals bound to organic matter and sulphides phase; and residual phase. The results showed that Cu and Ca are bioavailable and highly soluble in an aqueous media. Chemical species such as; Al, Mg and Fe have a high proportion in non-labile phase > 90% which explains the reason of near neutral pH due to Fe leaching out in minimal concentrations furthermore, K and Mn have a low bioavailability. Trace species such as; As, Se, Mo and Zn have a bioavailability > 20% while Ni, Co and Cr have a high proportion in a non-labile phase > 80%, with Ti > 90%. Based on the tailings minimal toxicity the mine tailing is appropriate to produce construction material furthermore, the technology of geopolymerization will encapsulate most of the toxic elements that are highly susceptible to any liquid that will get into contact with the brick.

Keywords: *Geochemical fractioning, Leachates, Bioavailability, Water-soluble/ Exchangeable phase, Fe-Mn oxide phase, Organic and Sulphide phase, Residual phase.*

3.5 Introduction

The chemical interaction that takes place within the tailings leads to the geochemical and mineralogical transformation within the tailings which results in the mobility and transportation of these metal species (Hayes et.al., 2012 and Romero et.al., 2007). The mobility of the metal species may be affected by the physicochemical properties such as bulk density and pH. The Musina copper tailings based on the physicochemical properties in Part A are classified as carbonated silica tailings due to high levels of silica and/or calcium carbonate that acts as a neutralizing agent to any sulphide remnants. This section will determine how the minor metals present in the tailing react when in contact with an aqueous solution. As mentioned above the tailings characteristics are depicted mainly by the tailings mineralogy and understanding of the tailings action when in contact with water/atmosphere needs to be understood in order to outline the correct environmental management strategy.

Therefore, geochemical fractioning (sequential extraction) was conducted in the study to mimic a natural environment from a closed lab. The analysis enables the understanding of the chemical species reaction within the MT during different environments when in contact with an aqueous solution. Sequential extraction is an analytical process that chemically and selectively leaches metals out of the MT by mimicking the release of metals into a solution under various environmental conditions (Jones, 1993; Tessier et.al., 1979). The chemical partitioning methods used in the research was designed to understand the tailings chemistry on metal species based on their interaction with other tailing properties (e.g. clay minerals, organic matter and tailing solution) and assessing the metals bioavailability/ mobility as well as their retention (Ure, 1996; Bacon et.al., 2005). The chemical extraction scheme for the present study was adopted from the works of Tokalioglu et.al. (2003), Anju and Banerjee (2010) and Tessier et.al. (1979). This extraction scheme will be performed to better understand the mobility of the toxic metals, their retention mechanisms in different geochemical forms and bioavailability to the environment. The analysis will determine the water soluble/exchangeable phase (F1), Fe-Mn oxide phase (F2), organic and sulphide phase (F3) and residual phase (F4). Each fraction extracted represents a different form of association and mechanism of availability.

3.6 Materials and Methods

Analytical grade reagents were obtained from Rochelle Chemicals and Lab Equipment CC, South Africa Ltd. A solution containing a 0.11 mol/L of acetic acid (CH_3COOH) was prepared pipetting 6.42 mL of CH_3COOH in 1000 mL of Milli-Q water. A solution of 0.1 mol/ mL of Hydroxylammonium Chloride ($HONH_2HCL$) was prepared by dissolving 4.25 mg of $HONH_2HCL$ in 1000 mL of Milli-Q water. A solution of 1.0 mol/ mL of Ammonium Acetate ($NH_4C_2H_3O_2$) was prepared by dissolving 6.13 mg of $NH_4C_2H_3O_2$ in 1000 mL of Milli-Q.

3.6.1 Fraction 1: Water soluble/Exchangeable metals

For extraction of water soluble metals 40 mL of solution containing 0.11 mol/L acetic acid was pipetted in 250 mL polypropylene bottle. This was followed by addition of 1g of dry tailings. The mixtures were then shaken for 16 h at 22±3°C at 250 rpm in a (name +model shaker). Thereafter, mixtures were centrifuged at 5000 rpm for 7 minutes using a (name + model of centrifuge). The supernatants were acidified with 3 droplets of nitric acid and refrigerated at 4 °C until analysis by ICP-MS. The residue were then washed with 20 mL of Milli-Q water by shaking for 15 min at 250 rpm and then centrifuged at 5 000 rpm for 7 minutes. The second supernatants liquid were discarded and the residues were air dried at room temperature for 12h.

3.6.2 Fraction 2: Metals bound to iron and manganese oxides

For this test, 40 mL of 0.1 mol/ L hydroxylammonium chloride (adjusted to pH 2 with 2 mol/ L nitric acid) was added to 1g of the dried sample from fraction 1 into a polypropylene bottle in order to extract metals that are bound to the iron and manganese oxides. The mixture was shaken for 16 h at 22±3°C at 250 rpm. The liquid extract was separated from the solid phase by centrifugation at 5000 rpm for 7 minutes. The liquid was decanted into a storage container with 3 drops of nitric acid and stored in the refrigerator at 4 °C until analysis. The residues were washed with 20 mL of Milli-Q water by shaking for 15 min at 250 rpm and then centrifuged at 5000 rpm for 7 minutes. The second supernatant liquid was discarded and residues were air dried for 12 h.

3.6.3 Fraction 3: Metals bound to organic matter and sulphides

For this test, 10 mL of 8.8 mol/L hydrogen peroxide was added in small aliquots to 1g of dried residue sample from fraction 2 into a polypropylene tube and manually shaken at room temperature for 1 h. Manually shaking for an hour and then shaken at 85°C for 1h and then further heating on a hotplate until the hydrogen peroxide reaches a few millilitres. A second aliquot of 10 mL of hydrogen peroxide was added to the residue and the same procedure was

repeated until near dryness. 50 mL of 1.0 mol/ L ammonium acetate solution (adjusted to pH 2 with nitric acid) was added after the residue had cooled off order to moisten the residue and shaken for 16 h at 22±3°C at 250 rpm. The liquid extract was separated from the solid phase by centrifugation at 5000 rpm for 7 minutes. The liquid was decanted into a storage container with 3 droplets of nitric acid and stored in the refrigerator. The residue was washed with 20 mL of Milli-Q water, shaken for 15 min at 250 rpm, and then centrifuged at 5000 rpm for 7 minutes. The second supernatant liquid was discarded and the sample air dried at room temperature for 12 hours.

3.6.4 Fraction 4: Residual phase

The residual phase extraction was carried out according to the procedure described by Olayinkah et.al. (2011). Briefly, 0.5g dried sample from fraction 3 was added into a volumetric flask containing 36 mL of (3:1) HCl:HNO_3 (Olayinkah et.al., 2011) and digested on a hotplate for 90 minutes at 110°C with a glass beaker sealing the beaker. A thermometer was used to monitor and control the temperature. At near dryness, the residue was cooled off and then diluted with 10 mL of 2% (v/v with H_2O) HNO_3 and filtered using a 45 µm pore filter membrane. The liquid was transferred into a 100 mL storage container and diluted with de-ionized water until the 50 mL mark.

3.6.5 Pseudo-total digestion

The procedure was conducted to validate the above fractions results. The same aqua regia solution as in F4 was used. Next, 0.5 g dried sample from fraction 3 was added into a conical flask with 36 mL of (3:1) HCl: HNO_3 (Olayinkah et.al., 2011) and digested on a hotplate for ±90 min at 110°C with a glass beaker sealing the beaker. A thermometer was used to monitor and control the temperature. At near dryness, the residue was cooled off and then diluted with 10 mL of 2% (v/v with H_2O) HNO_3 and filtered using a 45 µm pore filter membrane. The liquid was transferred into a 100 mL storage container and diluted with de-ionized water until the 50 mL mark. The recovery was calculated using the following equation:

$$\boldsymbol{Recovery} = \frac{\boldsymbol{F1+F2+F3+F4}}{\boldsymbol{Pseudo-total\ digestion}} \times \mathbf{100} \qquad \text{Equation 3. 5}$$

Where; F1 is fraction 1, F2 is fraction 2, F3 is fraction 3 and F4 is fraction 4.

3.7 Results and discussion

Figure 3.9 and 3.10 illustrates the mobility of major and trace species, respectively as detected through analysis of geochemical fractioning. The order of relative abundance within the mobile fraction is Cu>Si>P>Na>Ca>Mn>K>Fe>Al. High levels of mobility of Cu (>88%) within the labile phase was detected which may be assumed to be due to the metal being a target species during extraction. Cu which is the mineral being extracted is dominant within the exchangeablephase (>40%) and its mobility increases by depth at S1, while within the residual phase minimal Cu is leached. The Si content is dominant within the labile phase with the main extraction present within F2 (Appendix C-C2). The order of relative abundance within the Fe-Mn oxide phase is Si>P>Cu>K>Ca>Mn>Fe>Al>Mg>Na. The Fe-Mn oxide fraction has detected a high level of Ca at >26.62 mg/kg and Al being the lowest concentration at < 10 mg/kg. The phase which according to Nieto et.al., (2007) is low due to its resistance to dissolution of the most stable secondary Fe oxide phases such as hematite under acidic condition. The order of relative abundance within the organic phase is Na>P>Si>Cu>Ca>K>Mn>Al>Fe>Mg.

The residual phase used aggressive acids to leach out metals that were strongly bound to the tailings and tailings soil-interface in the residual phase. The concentrations of potentially toxic metal species were very high in this fraction due to the silicate and secondary minerals retaining relatively high quantity of potentially toxic or heavy metal species within their crystal structures (Okoro et.al. 2012). The relatively high concentration of Na, P, and Si partitioned in this fraction indicates the inert nature of the material which makes Si difficult to disintegrate. The tailings alkali condition is confirmed by the high presence of Fe, Al and Mg (>90%) within the non-labile phase (fig 3.9).

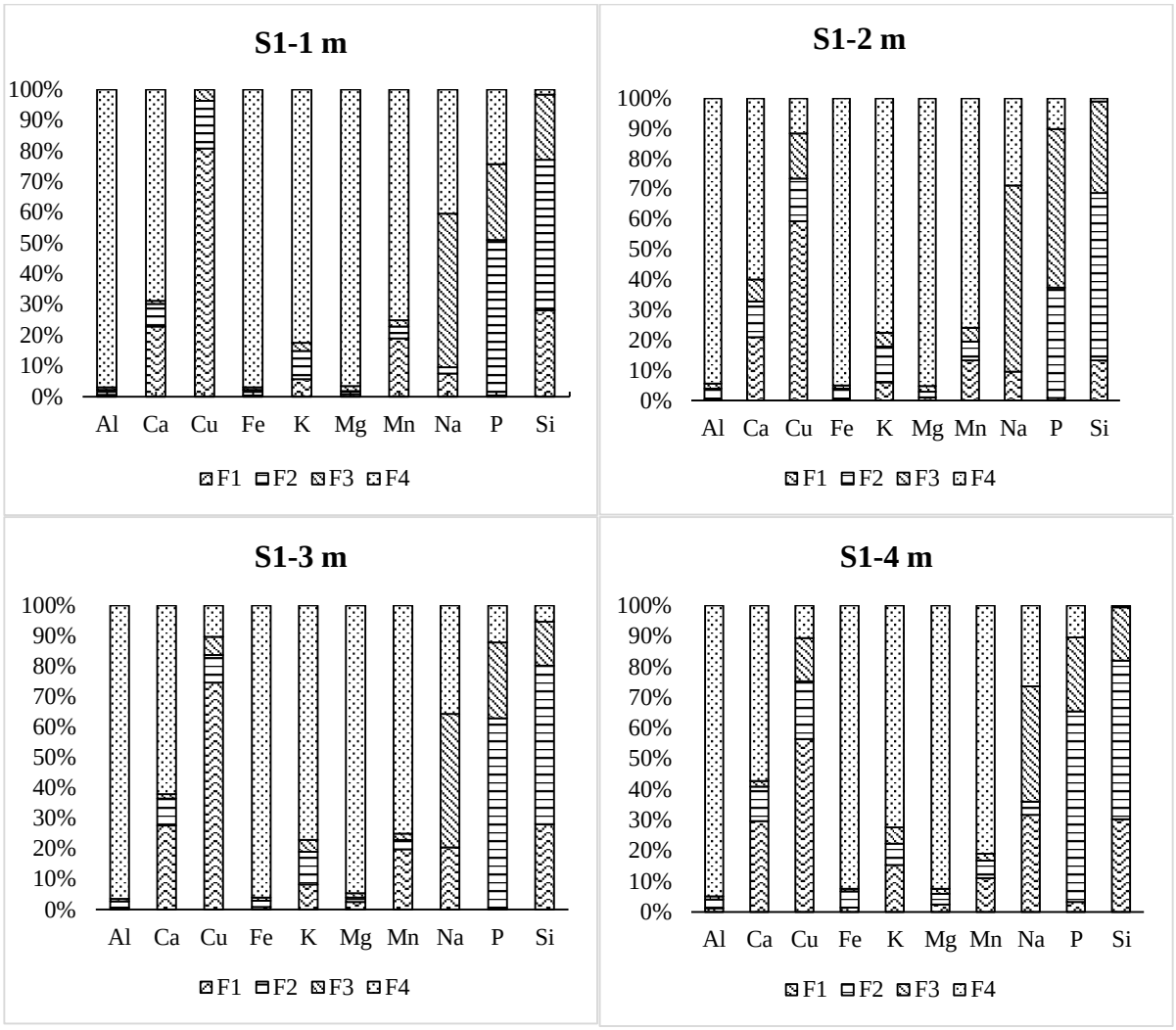

Figure 3. 9: Geochemical fractioning of sample 1 (F1 is the exchangeable fraction, F2 is the iron and manganese oxides fraction, F3 is the organic matter and sulphides fraction and F4 is the residual fraction.

Figure 3.9 and Appendix C-C2 illustrates the metal elements Al, Ca, Fe, Mg, K, Si and Mn which were detected to be relatively uniform in all samples within the residual fraction however, Ca displayed a highly significant proportion within the exchangeable fraction as compared to the other metals mentioned above. Based on the XRD and XRF results the low mobility of Al supports the high concentration of Al_2O_3 present and clay minerals detected. Further the characteristic of Al to be present mostly in the residual phase is because of the crystalline structures bound to the chemical species.

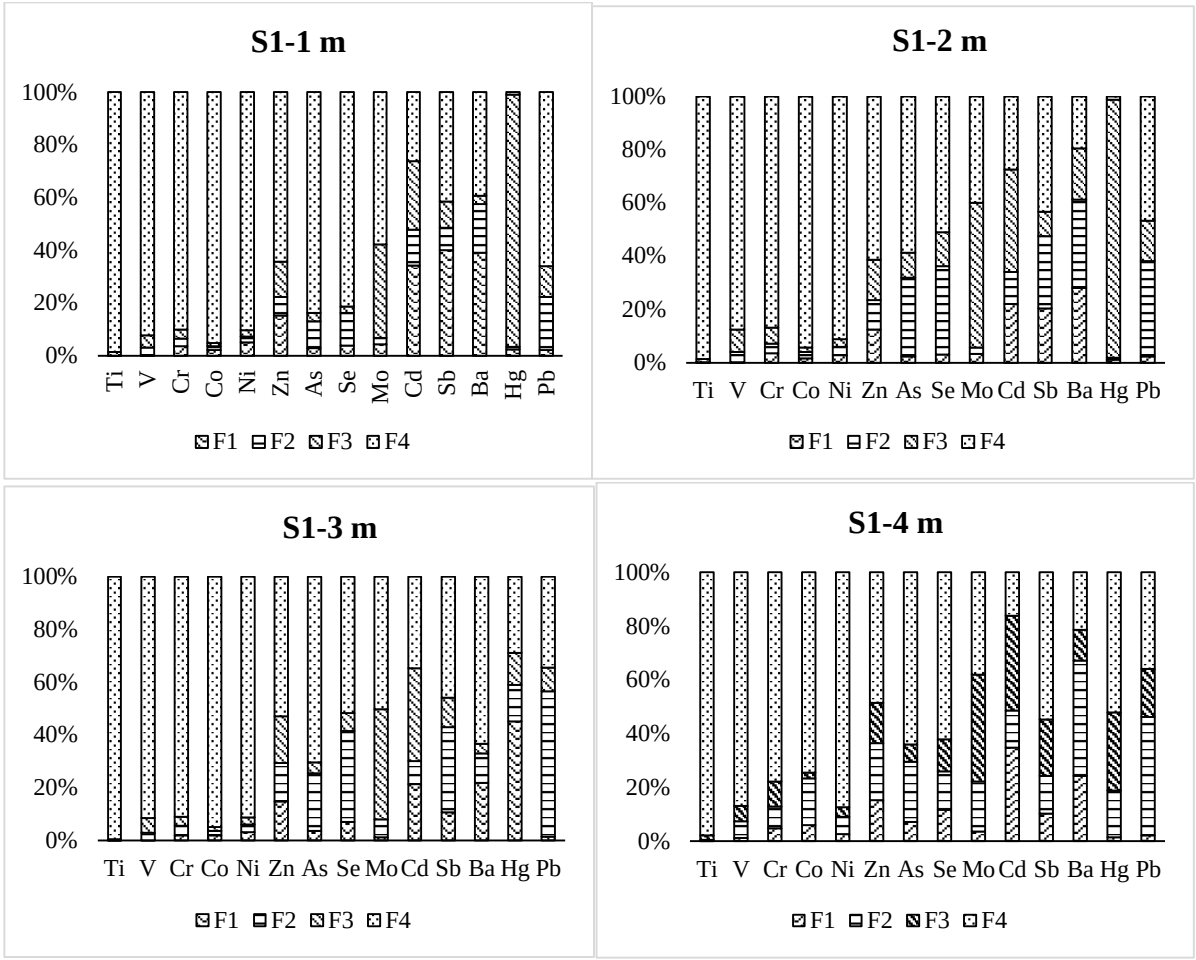

Figure 3. 10: % Minor metal species in 4 geochemical fractions of sample 1 (F1- Exchangeable fractions, F2- Iron and Manganese oxide, F3- Organic matter and Reducible, F4- Residual.

Figure 3.10 illustrates the trace metal species that are leached during the process of geochemical fraction in 4 phases. Higher level of Cd is observed within the bioavailable phase (F1) of the trace metal species. S1 pH levels decrease within the trace metals due to the mobility of Cd and Hg. The order of relative abundance within the mobile fraction is Cd> Hg> Pb> Ba> Mo> Sb> Se> Zn>As> Ni>Cr> Co> V>Ti within trace species. The bioavailable phase is very dangerous in the environment because of the high levels of metals that are released into the environment ranging from 0.59 mg/kg to 70.55 mg/kg within the labile phase. The order of relative abundance within the Fe-Mn oxide phase is Pb>Ba>As>Hg>Zn>Mo>Sb>Cd>Co> Se>Ni>Cr>V>Ti within the trace metals. Roy et.al. (2004) further indicate that the phase contains the most mobile metals, and generally those that give rise to toxicity problems, as they can be easily released as ions and therefore be in an available form. The order of relative abundance within the organic phase is Hg>Mo>Cd>Zn>Pb>Sb>V>Cr>As>Ba>Se>Ni>Co>Ti within the trace metals. The leaching concentration of Hg was >95% throughout all sample points. The metals Sb, Cd, Zn, Sb and Ba are leached out in quantities > 40 % throughout the

sample points within the labile phase which means that the metals present are most susceptible to removal when in contact with minor acids (Appendix C-C3). However, due to the low concentrations of these metals as indicated by XRF analysis the leaching of these metals will have no great impact on the environment and its surroundings as DWAF (1998) leachates guidelines indicate.

Assumptions can be made that most of the metals are locked within the non-labile phase, because they are transitional metals which are less reactive in an aqueous solution. The low reactivity of the metals in an aqueous solution indicates that the residual fraction comprises mainly of the primary minerals that locked trace metals within their crystalline structure Cuong et.al., (2006). As, Cr, Co, V, and Ni have a non-labile phase (>80%) however, Ti has the highest mobility (> 95%). According to DWAF (1998) the metals that are leached within the MT are lower than the threshold concentration indicated in Table 3.4 throughout all phases. The elements relative uniformity in concentration is assumed to be because of the ore extracted having an equal amount of minerals throughout and no secondary mineralisation occurring due to low rainfall in the area. Therefore, tailings encountered minimal transformation or leaching due to lack of reaction agent in the semi-arid area due to low rainfall.

Table 3. 4: Leachable Concentration Threshold according to the Department of Water Affairs and Forestry (1998).

Elements	Leachable concentration Threshold (LCT0) according to DWAF (1998) in mg/L.
As	0.01
Se	0.01
Ba	0.7
Cd	0.003
Co	0.5
Cu	2
Mn	0.5
Mo	0.07
Ni	0.07
Pb	0.01
Sb	0.02
Zn	5
V	0.2
Hg	0.06

3.8 Conclusion

The geochemical analysis was conducted to understand the tailings chemistry within its environment with different climatic conditions. The following major conclusions were made about the geochemical partition of the tailings:

- The bioavailable phase detected high levels of Si and Cu in the major elements and Cd within the trace metals.
- The Fe-Mn oxide phase detected Si as the dominant element leached out among the major metals and Pb in the trace metals being a highly soluble element.
- Within the organic phase Na was detected to be the highest however, compared to other phases the concentration was minor while Hg as the abundant element within the trace metals.
- In the residual phase Fe, Mg and Al is dominant in the major elements >90% while Ti is dominant trace metals with a concentration >95% in all sample points for trace elements.
- Therefore, given the tailings conditions within different environmental conditions it may be concluded that the tailing isn't harmful due to its high silicate crystalline structure which is highly insoluble. The harmful metals present don't leach in high levels and the carbonate elements neutralise the acidic conditions produced by the Fe element.

3.9 Recommendations

- Due to the low mobility of metals the material will be suitable to utilise for the production of other materials through the process of geopolymerization.
- An alternative solution is to encapsulate the waste though the process of paste backfilling to avoid environmental and health impacts.
- Further investigations should be conducted to determine whether the waste has impacts on the nearby rivers, groundwater or the health of nearby communities.

Reference

Alloway, B.J. 1995. Heavy Metals in Soils. Chapman and Hall, London.

Amponsah-Dacosta M and Reid D.L. (2014). Mineralogical Characterization of Selected South African Mine Tailings for the Purpose of Mineral Carbonation. Sui Sun, Wang (Eds.), An Interdisciplinary Response to Mine Water Challenges, China University of Mining and Technology Press, Xuzhou, China (2014), pp. 686-689

Anju, M., Banerjee, D.K. 2010.Comparison of two sequential extraction procedures for partitioning in mine tailings. Chemosphere 78, 1393-1402.

Arenas-Lago, D., Andrade, M.L., Lago-Vila, M., Rodríguez-Seijo, A., Vega, F. A., (2014). Sequential extraction of heavy metals in soils from a copper mine: Distribution in geochemical fractions.

Bacon, J.R. Hewitt, I.J. Cooper, P. 2005. Reproducibility of the BCR Sequential Extraction Procedure in a long-term study of the association of heavy metals. Science Total Environment. Vol 337, pp. 191-205.

Boehm, H.P. 1971. Acidic and basic properties of hydroxylated metal oxide surfaces. Discussions of the Faraday Society. Vol.52. pp. 264-275

Bradl, H., editor. Heavy Metals in the Environment: Origin, Interaction and 44 Remediation Volume 6. London: Academic Press; 2002.

Chen Y, Furmann A, Mastalerz, M, Schimmelmann, A. 2014. Quantitative analysis of shales by KBR-FTIR and micro-FTIR. Fuel, Vol. 116, pp. 538-549.

Chinoda, G.N. Matura, N. Moyce, W and Owen, R. 2009.Baseline Report on the Geology of the Limpopo Basin Area, a contribution to the challenge program on water and food project "Integrated Water Resource Management for Improved Rural Livelihoods: Managing risk, mitigating drought and improving water productivity in the water scarce Limpopo Basin".WaterNet working paper 7. WaterNet, Harare

Clevenger, T.E. 1990. Use of sequential extraction to evaluate the heavy metals in mining wastes. Water, Air and Soil Pollution. Vol. 50(3). pp. 241-254

Council for Geoscience 2010. Council for Geoscience: Mineral profile for the Limpopo region. Available online at http://www.geoscience.org.za//index.php

Cuong, D.T and Obbard, J.P. 2006. Metal speciation in coastal marine sediments from Singapore using a modified BCCR-sequential extraction procedure. Applied Geochemistry. Vol. 21. pp. 1335-1346

Diko, M.L and Ekosse, G.E. 2013. Characterisation of two kaolin facies from Ediki, Southwest Cameroon. Scientific Research and Essays 8. Vol. 8(18). pp. 698-704

Dold, B. (2003). Speciation of the most soluble phases in a sequential extraction procedure adapted for geochemical studies of copper sulphide mine waste. J. Geochem. Explore. Vol. 80, pp.55-68.

Dupin, J.C. Gonbeau, D. Vinatier, P. and Levasseur, A. 2000. Systematic XPS studies of metal oxides, hydroxides and peroxides. Physical Chemistry, Chemical Physics. Vol. 2(11). pp. 1319-1324.

Enkhzaya, S. Ohe,K. Shiomori, K.Oyuntsetseg,B. Bayanjargal, O and Watanabe, M. 2016. Assessment of Heavy Metals in Mining Tailing Around Boroo and Zuunkharaa Gold Mining Areas of Mongolia. Journal of Environmental Science and Technology, Vol.9, pp. 379-389.

EPA. (2012). 5.8 Total Dissolved Solids. In Water: Monitoring and Assessment. Retrieved from www.water.epa.gov

Filgueiras, A., Lavilla, I. and Bendicho, C. (2002). Chemical sequential extraction for metal partitioning in environmental solid samples. J. Environ. Monitor, 66, 823-857 pp.

Hayes, S.M., Webb, S.M, Bargar, J.R, O'Day, P.A., Maier, R.M., and Chorover, J., (2012). Geochemical weathering increases lead bio-accessibility in semi-arid mine tailings. Environmental Sciences Technology. Vol. 46, pp. 5834-5841.

Hiller, E., Petrák, M., Tóth, R., Voleková, B.L., Jurkovic, L., Kučerová, G., Radková, A., Šottník, P., and Vozár, J., (2013). Geochemical and mineralogical characterization of neutral, low-sulfide/high-carbonate tailings impoundments, Markušovce, eastern Slovakia. Environ. Sci. Pollut. Res., 20, 7627-7642 pp.

Hongbo, F. and Xie, Q. 2006. Complexes of fulvic acid on the hematite, goethite and akaganeite: FTIR observation. Chemosphere, Vol. 63, pp. 403-410.

Hua, X.U., and Van Deventer, J.S.J. 2003. The effect of alkali metals on the formation of polymeric gels from alkali feldspars. Colloids Surf A Physicochemical Engineering Asp. Vol.216, pp.27-44.

Jamieson, H.E. 2011. Geochemistry and mineralogy of solid mine waste: essential knowledge for predicting environmental impact. Elements. Vol.7. pp. 381-386

Jones, J.M. 1993. Sequential extraction method: A review and evaluation. Environmental Geochemistry and Health. Vol 15 (2-3)

Kesimal, A., Yilmaz, E., Ercikdi, B., Alp, I., and Deveci, H., (2005). Effect of properties of tailings and binder on the short and long term strength and stability of cemented paste backfilling. Materials Letters. Vol 59, pp. 3703-3709.

Limpopo DFED 2004: Limpopo State of the Environment Report (Phase 1). Limpopo Department of Finance and Economic Development. Limpopo

Masindi, V. 2016. A novel technology for neutralizing acidity and attenuating toxic chemical species from acid mine drainage using cryptocrystalline magnesite tailings. Journal for water process engineering. Vol.10, pp. 67-77.

Nieto, J.M., Sarmiento, A.M., Olías, M., Cánovas, C.R., Riba, I., Kalman, J., Delvalls, T.A., 2007. Acid mine drainage pollution in the Tinto and Odiel rivers (Iberian Pyrite Belt, SW Spain) and bioavailability of the transported metals to the Huelva Estuary. Environ. Int. 33, 445–455.

Okoro, H.K., Fatoki, O. S., Adekola, F. A., Ximba, B. J. and Snyman, R. G., (2012). A Review of Sequential Extraction Procedures for Heavy Metal Speciation in Soil and Sediments. 1, 181 pp. doi: 10.4172/scientific reports.

Olayinka, K.O. Oyeyiola, A.O, Odujebe, F.O and Oboh, B. 2011. Uptake of potentially toxic metals by vegetable plants grown on contaminated soil and their potential availability using sequential extraction. Journal of Soil Science and Environmental Management. Vol 2 (8), pp. 220-227

Onuaguluchi, O. and Eren, O., (2012). Recycling of copper tailings as an additive in cement mortars. Construction and Building Materials. Vol. 37, pp.723-727.

Perlman, H. (2014). Electrical Conductivity and Water. In The USGS Water Science School. Retrieved from www.ga.water.usgs.gov.

Reeb, J and Milota, M. (1999). Moisture content by the oven-dry method for industrial testing. Oregon State University Corvallis. Available online at http://ir.library.oregonstate.edu/

Reimann C and de Caritat P. 1998. Chemical elements in the environment- factsheet for the geochemist and environmental scientists, Berlin, Germany: Spring-Verlag

Romero, F.M., Armienta, M.A., and Gonzales-Hernandez, G. (2007). Solid-phase control on the mobility of potentially toxic elements in an abandoned lead/zinc tailings impoundment, Taxco, Mexico. Appl. Geochem., 22, 109-127 pp.

Sraeck, O. Mihaljevio, M. Kribek, B. Majer, V and Veselorsky, F. 2009. Geochemistry and mineralogy of Cu and Co in mine tailings at the Copperbelt, Zambia. Journal of African Earth Sciences. Vol. 57 (2010). pp. 14-30

Szymanski, J.T. 1988. The crystal structure of beudantite, $Pb(Fe,Al)_3[(As,S)O_4]_2(OH)_6$. Can. Mineral, Vol. 26, pp. 923-932

Tessier, A. Campbell, P.G.C. Bisson, M. 1979. Sequential Extraction Procedure for speciation of particulate trace metals. Analytical Chemistry. Vol 51, pp. 844-851.

Tokaligoglu, S. Kartal, S and Biral, G. 2003. Application of a three-stage Sequential Extraction Procedure for the Determination of Extractable metal contents in Highway soils. Turkish Journal of Chemistry. Vol 27 (2003), pp. 333-346.

Ure, A.M. 1996. Single extraction schemes for soil analysis and related applications. Science Total Environment. Vol 178, pp. 3-10

Von der Heyden, C.J and New, M.G.2005. Differentiating dilution and retention processes in mine effluent remediation within a natural wetland on the Zambian Copperbelt. Applied Geochemistry. Vol. 20. pp. 141-1257

Wanty, R.B., (1998). Eh-pH relations. Geochemistry. Vol.5, pp.182-186.

Whitby, K.T. (1958), Symp. Particle Size Measurement, ASTM Sp. Publ. No 234, 3-25, 218

Wilson et.al., 1998 Wilson, M.G.C and Anhaeusser, C.R. 1998. The Mineral Resources of South Africa. 6th ed. Council of Geosciences, Pretoria, South Africa. pp. 209-207.

Wolkersdorfer, C., and Hubert, E., (2005). Establishing a total dissolved solids: Electrical conductivity ratio for mine waters. 16th International conference of Acid Rock Drainage and IMWA Annual Conference.

Zang, H. Schroder, L.J.L. Pittman, J, J. Wang, J.J and Payton, M.E. 2005. Soil salinity using saturated paste and 1:1 soil and water extracts. Soil Science Society of America Journal. Vol 69, pp. 1146-1151.

Appendix C

Table C 1: Particle size distribution of copper mine tailings.

Total Mass of sample (g) 1000		Sieve Mass and Mass Retained (g)	Mass Retained (g)	% Weight Retained	% Cumulative Retained	% Passing
Sieve Number (mm)	Sieve Mass (g)					
0,032	258,03	285,81	27,78	2,78	2,78	97,22
0,04	250,23	279,06	28,83	2,88	5,66	94,34
0,063	252,03	276,77	24,74	2,47	8,14	91,87
0,075	263,50	367,61	104,11	10,41	18,55	81,45
0,125	236,85	590,41	353,56	35,36	53,90	46,10
0,25	240,80	582,65	341,85	34,19	88,09	11,91
0,5	291,28	393,76	102,48	10,25	98,34	1,66
1	296,02	301,26	5,24	0,52	98,86	1,14
2	326,57	329,68	3,11	0,31	99,17	0,83
4	388,74	389,99	1,25	0,13	99,30	0,70
Pan	529,6	536,33	6,73	0,67	99,97	0,03
Total			999,68	99,97		

Table C 2: The mineral composition of the copper tailing.

Minerals	**S1-surface**	**S1- 1 m**	**S1- 2 m**	**S1- 3 m**	**S1- 4 m**	**S2**	**S3**	**S4-1 m**	**S4-2 m**	**S4-3 m**	**S5**
Quartz	38,3	46,61	46,2	44,79	52,41	44,81	54,49	51,03	53,52	55,38	50,71
Plagioclase	6,33	8,63	7,9	3,37	2,91	7,54	10,8	5,78	6,27	6,03	5,29
Muscovite	9,07	5,94	7,34	7,5	5,66	7,21	2,21	5,21	4,19	3,82	3,2
Hematite	1,76	0,97	1,29		1,69	1,29					
Epidote	27,27	24,85	23,88	27,47	20,44	17,69	20,05	20,63	24,28	24,73	29,78
Calcite		1,44	1,59	1,52	1,19	2,25	0,84	1,99			
Chlorite	17,27	11,56	11,81	15,34	15,7	19,21	11,61	12,13	11,74	10,05	11,01

Table C 3: Geochemical analysis of major and trace metals

Trace metals

	Values in µg/kg	Ti	V	Cr	Co	Ni	Zn	As	Se	Mo	Cd	Sb	Ba	Hg	Pb
	F1	11,50	0,75	53,86	8,45	40,94	123,88	0,48	2,63	2,25	0,66	0,28	172,81	0,13	2,24
	F2	14,95	11,54	45,13	4,83	17,58	57,68	1,79	8,16	1,34	0,26	0,06	81,25	0,06	20,00
	F3	420,03	18,75	48,30	4,40	19,14	106,96	0,53	1,69	18,58	0,50	0,07	14,14	5,36	11,68
S1- 1 m	**F4**	30649,88	369,29	1338,18	351,82	731,00	521,74	14,38	54,22	30,26	0,50	0,29	173,25	0,05	66,04
	Sum of fractions	31096,36	400,33	1485,46	369,50	808,66	810,26	17,18	66,70	52,43	1,92	0,70	441,45	5,60	99,97
	Pseudo-Total	34072,70	348,31	1322,46	348,06	762,52	537,28	22,32	62,78	36,66	1,88	0,54	350,56	4,05	80,70
	% Recovery	91,26	114,94	112,33	106,16	106,05	150,81	76,95	106,24	143,03	102,00	129,28	125,93	138,14	123,87
	F1	7,26	0,55	48,00	4,81	19,31	105,21	0,41	2,63	1,11	0,35	0,13	68,77	0,05	2,10
	F2	20,43	12,33	52,84	7,14	20,97	96,41	5,13	29,19	0,84	0,19	0,18	81,77	0,03	33,22
	F3	313,80	26,70	86,54	5,54	20,96	129,76	1,64	11,14	18,94	0,61	0,06	47,61	4,48	14,09
S1-2 m	**F4**	24386,02	280,61	1234,84	288,18	627,10	526,20	10,28	45,02	13,90	0,44	0,29	48,20	0,06	43,37
	Sum of fractions	24727,51	320,19	1422,22	305,68	688,34	857,58	17,47	87,98	34,80	1,60	0,66	246,34	4,63	92,78
	Pseudo-Total	28155,06	395,49	2018,25	343,04	719,38	569,22	23,38	70,66	26,28	1,34	0,59	180,51	3,51	73,76
	% Recovery	87,83	80,96	70,47	89,11	95,68	150,66	74,73	124,52	132,41	119,13	112,13	136,47	131,95	125,79
S1-3 m	**F1**	5,40	0,66	32,50	7,04	27,90	105,71	0,62	5,13	0,33	0,42	0,08	109,45	0,62	1,63
	F2	38,09	9,67	58,95	5,55	24,07	102,11	3,61	24,94	1,82	0,17	0,24	56,12	0,19	62,41
	F3	123,72	19,72	55,65	4,58	21,92	124,49	0,67	4,89	11,17	0,69	0,08	18,92	0,17	10,19
	F4	27502,78	319,12	1478,80	320,78	759,02	372,92	11,62	37,58	13,46	0,68	0,34	317,32	0,40	39,24
	Sum of fractions	27669,99	349,18	1625,91	337,95	832,91	705,23	16,52	72,54	26,78	1,96	0,73	501,81	1,38	113,47
	Pseudo-Total	23121,50	356,21	1359,46	307,78	687,20	457,76	18,50	52,32	20,92	1,88	0,53	492,65	0,95	103,63
	% Recovery	119,67	98,02	119,60	109,80	121,20	154,06	89,31	138,65	128,02	104,21	139,24	101,86	145,80	109,50
	F1	11,70	4,29	80,23	25,20	25,05	112,53	1,17	8,15	1,66	0,72	0,05	79,24	0,05	2,29
S1-4 m	**F2**	82,17	22,61	141,73	74,06	63,26	155,74	3,63	9,86	8,83	0,28	0,07	140,65	0,60	47,22
	F3	341,24	20,74	159,62	9,30	33,40	110,70	1,03	8,14	18,87	0,73	0,11	37,51	1,01	19,10

	F4	19679,20	314,11	1332,52	315,46	846,94	356,32	10,38	43,06	17,94	0,33	0,27	69,80	1,79	38,23
	Sum of fractions	20114,31	361,76	1714,10	424,02	968,65	735,29	16,21	69,21	47,30	2,05	0,50	327,20	3,45	106,83
	Pseudo-Total	23987,28	364,41	1402,28	311,56	721,34	443,06	20,22	57,80	34,06	1,84	0,37	207,89	2,15	118,47
	% Recovery	83,85	99,27	122,24	136,10	134,29	165,96	80,15	119,74	138,87	111,67	135,02	157,39	160,58	90,18
S2	**F1**	32,52	2,42	52,52	14,35	85,23	70,63	1,26	3,09	0,95	0,94	0,13	83,48	0,16	2,07
	F2	13,51	27,43	72,03	6,79	58,33	85,72	3,30	13,12	0,98	0,33	0,08	113,23	0,04	21,15
	F3	299,67	49,48	91,96	6,47	39,78	130,50	1,40	11,08	15,77	0,52	0,05	23,97	0,19	12,93
	F4	13958,53	400,46	2359,72	385,78	1276,46	941,98	10,16	62,28	3,54	0,28	0,20	82,49	0,08	47,53
	Sum of fractions	14304,23	479,79	2576,23	413,39	1459,80	1228,83	16,12	89,58	21,24	2,07	0,46	303,18	0,47	83,69
	Pseudo-Total	20078,46	490,39	2656,48	358,32	1286,74	895,30	20,08	62,32	17,04	2,02	0,31	291,75	0,32	91,27
	% Recovery	71,24	97,84	96,98	115,37	113,45	137,25	80,29	143,74	124,63	102,79	150,32	103,92	150,36	91,69
S3	**F1**	13,32	1,75	36,50	10,67	60,26	50,40	0,84	1,90	0,72	0,62	0,09	50,89	0,04	2,22
	F2	20,66	25,06	98,87	12,86	49,38	84,48	3,36	10,25	1,44	0,40	0,06	91,38	0,08	21,22
	F3	425,97	39,63	125,50	6,66	31,98	128,67	1,37	7,74	25,53	0,57	0,09	39,52	0,06	14,68
	F4	24547,72	358,92	2034,66	344,48	1045,36	655,84	11,04	43,48	7,68	0,44	0,22	64,84	0,11	38,21
	Sum of fractions	25007,67	425,35	2295,54	374,67	1186,99	919,40	16,61	63,36	35,37	2,03	0,45	246,63	0,29	76,32
	Pseudo-Total	22515,10	489,31	1854,58	355,74	1105,38	697,80	22,82	62,82	26,54	1,66	0,26	228,06	0,25	87,57
	% Recovery	111,07	86,93	123,78	105,32	107,38	131,76	72,81	100,86	133,26	122,22	175,73	108,14	117,54	87,16
S4-1 m	**F1**	16,96	2,38	94,80	20,76	27,58	133,33	0,98	8,24	1,89	0,54	0,08	79,10	0,02	3,81
	F2	65,72	19,12	123,80	44,64	50,14	137,19	2,74	6,56	3,04	0,25	0,06	157,25	2,20	84,06
	F3	318,81	21,74	186,90	8,69	37,71	421,07	0,67	5,08	13,29	0,40	0,09	35,43	1,61	15,50
	F4	24832,08	363,62	1766,44	316,32	837,20	691,40	9,70	40,12	14,76	0,48	0,31	65,31	0,09	34,52
	Sum of fractions	25233,57	406,87	2171,95	390,42	952,63	1383,00	14,09	60,00	32,98	1,67	0,53	337,09	3,91	137,89
	Pseudo-Total	22101,24	552,02	935,38	225,94	580,94	1418,40	15,40	37,80	29,82	1,36	0,43	275,59	4,18	139,65
	% Recovery	114,17	73,71	232,20	172,80	163,98	97,50	91,51	158,74	110,59	122,79	123,47	122,31	93,57	98,75
S4-2 m	**F1**	8,91	1,66	8,91	8,32	20,91	43,10	4,33	11,75	1,24	0,36	0,15	44,37	0,02	3,55
	F2	38,38	17,56	53,40	7,60	28,62	61,69	2,85	9,40	3,38	0,16	0,23	72,62	0,05	28,08
	F3	144,42	20,20	37,00	5,31	20,29	137,54	0,70	6,02	18,68	0,51	0,13	24,82	0,12	18,09

	F4	15811,70	332,45	1285,30	293,66	681,22	640,08	5,90	33,50	7,28	1,42	0,23	71,38	0,05	28,74
	Sum of fractions	16003,41	371,87	1384,60	314,89	751,04	882,42	13,77	60,67	30,58	2,45	0,74	213,19	0,23	78,47
	Pseudo-Total	16862,90	264,61	1992,14	295,28	792,12	723,72	17,58	51,14	42,82	3,07	0,53	158,86	0,13	65,37
	% Recovery	94,90	140,54	69,50	106,64	94,81	121,93	78,34	118,64	71,41	79,80	139,94	134,20	176,84	120,05
S4-3 m	**F1**	4,22	1,30	7,61	7,96	17,73	46,34	4,46	10,25	0,88	0,36	0,12	51,23	0,01	2,11
	F2	43,30	18,65	32,66	7,79	15,58	90,24	2,03	8,30	2,03	0,31	0,14	67,90	0,03	19,17
	F3	194,77	12,03	34,00	3,61	15,58	145,59	7,68	1,28	5,78	1,48	0,05	22,80	0,04	12,25
	F4	15330,82	264,50	838,78	268,30	627,22	548,08	16,02	45,98	31,60	2,00	0,25	50,45	0,04	19,23
	Sum of fractions	15573,11	296,48	913,05	287,66	676,11	830,25	30,19	65,81	40,29	4,15	0,56	192,38	0,12	52,76
	Pseudo-Total	14969,10	372,36	932,82	235,72	533,08	1054,88	40,28	78,00	31,00	6,54	0,91	170,04	0,11	68,50
	% Recovery	104,04	79,62	97,88	122,03	126,83	78,71	74,95	84,37	129,97	63,46	61,54	113,14	109,09	77,02
S5	**F1**	41,22	3,60	20,70	6,44	22,00	59,76	1,38	0,95	1,06	0,36	0,11	81,25	0,13	3,63
	F2	22,70	10,57	35,77	2,89	14,70	123,78	1,65	7,94	0,66	0,29	0,09	36,36	3,69	11,53
	F3	323,35	15,81	36,30	3,30	15,66	136,67	0,61	2,49	8,18	0,52	0,07	13,89	0,10	11,74
	F4	20720,00	259,89	1376,50	258,60	693,94	507,54	5,26	15,64	5,14	0,26	0,45	42,86	0,20	18,94
	Sum of fractions	21107,28	289,86	1469,27	271,23	746,29	827,75	8,90	27,02	15,04	1,43	0,71	174,37	4,13	45,84
	Pseudo-Total	19689,20	331,56	1614,38	260,02	725,64	415,80	6,91	34,96	12,54	0,96	0,71	166,86	5,10	37,79
	% Recovery	107,20	87,43	91,01	104,31	102,85	199,07	128,76	77,28	119,94	148,93	101,08	104,50	80,84	121,31

Major elements

	Values in mg/kg	**Al**	**Ca**	**Cu**	**Fe**	**K**	**Mg**	**Mn**	**Na**	**P**	**Si**
S1-1 m	**F1**	2,40	84,57	10,61	3,11	0,82	1,52	0,72	0,62	0,07	4,40
	F2	7,04	27,19	2,04	13,52	1,33	1,79	0,14	0,18	7,78	7,70
	F3	2,91	3,80	0,49	5,48	0,39	2,58	0,08	4,12	3,79	3,32
	F4	401,00	254,40	1.67	704,00	11,96	165,84	2,83	3,34	3,75	0,25
	Sum of fractions	413,35	369,96	13,13	726,11	14,50	171,73	3,76	8,25	15,38	15,67

	Pseudo-Total	356,80	283,60	19,42	702,80	12,49	158,58	2,82	7,26	13,98	10,69
	% Recovery	115,85	130,45	67,63	103,32	116,12	108,29	133,28	113,68	110,01	146,54
	F1	1,58	55,14	6,19	2,24	0,62	1,59	0,38	0,76	0,17	2,57
	F2	9,92	31,04	1,46	19,06	1,23	3,04	0,18	< 0.5	6,52	10,74
	F3	4,41	18,54	1,56	5,43	0,46	2,87	0,13	4,83	9,39	5,90
S1-2 m	**F4**	266,80	157,12	1,20	511,40	8,02	145,16	2,20	2,27	1,84	0,19
	Sum of fractions	282,70	261,84	10,41	538,12	10,33	152,66	2,90	7,86	17,92	19,40
	Pseudo-Total	386,00	337,20	13,31	765,80	10,22	162,16	2,98	6,24	15,26	10,89
	% Recovery	73,24	77,65	78,18	70,27	101,09	94,14	97,29	125,94	117,48	178,11
	F1	2,42	80,90	9,08	5,58	0,90	4,62	0,67	1,97	0,09	3,48
	F2	6,23	25,80	1,10	11,32	1,16	2,32	0,11	< 0.5	9,22	6,50
	F3	2,88	3,83	0,74	6,18	0,42	2,80	0,07	4,23	3,68	1,78
S1-3 m	**F4**	308,60	181,26	1,24	574,60	8,32	169,04	2,54	3,43	1,80	0,67
	Sum of fractions	320,13	291,79	12,15	597,69	10,81	178,78	3,39	9,63	14,80	12,43
	Pseudo-Total	215,79	282,60	9,85	625,40	10,18	161,64	2,82	11,95	13,30	10,68
	% Recovery	148,35	103,25	123,39	95,57	106,13	110,60	120,20	80,59	111,22	116,36
	F1	3,65	76,97	10,80	9,21	1,82	4,77	0,38	4,14	0,51	8,77
	F2	7,85	29,66	3,59	32,82	0,82	6,47	0,20	0,55	9,34	15,02
	F3	2,80	4,52	2,67	5,62	0,62	2,98	0,08	4,90	3,62	5,01
S1-4 m	**F4**	261,40	148,88	2,04	581,20	8,58	172,22	2,80	3,44	1,58	0,18
	Sum of fractions	275,70	260,03	19,10	628,85	11,84	186,44	3,46	13,02	15,05	28,99
	Pseudo-Total	321,40	268,40	11,63	614,80	8,52	167,78	2,76	11,36	13,55	20,69
	% Recovery	85,78	96,88	164,19	102,28	139,04	111,12	125,25	114,65	111,08	140,13
	F1	3,34	103,60	7,74	4,62	2,75	6,40	1,69	5,15	0,13	5,25
	F2	11,81	35,68	4,63	13,32	0,79	3,84	0,24	1,45	8,31	11,45
S2	**F3**	4,12	4,29	0,71	7,33	0,53	4,83	0,12	4,72	3,36	2,63
	F4	407,80	203,00	1,97	801,20	7,74	298,80	3,24	3,28	1,58	0,13
	Sum of fractions	427,07	346,57	15,05	826,47	11,81	313,87	5,29	14,60	13,38	19,46

	Pseudo-Total	340,40	265,60	10,36	733,30	11,13	279,20	4,95	13,31	13,84	10,83
	% Recovery	125,46	130,48	145,19	112,71	106,13	112,42	106,93	109,68	96,68	179,63
	F1	2,49	92,20	8,44	3,11	1,18	3,03	0,59	1,43	0,28	3,91
	F2	9,09	28,74	3,03	14,73	0,77	3,42	0,17	0,85	8,72	9,32
	F3	3,60	3,60	1,56	6,42	0,56	4,07	0,10	4,56	3,55	5,43
S3	**F4**	331,00	159,00	2,05	647,80	5,40	240,40	3,96	3,79	1,31	0,12
	Sum of fractions	346,18	283,54	15,08	672,05	7,91	250,92	4,83	10,64	13,86	18,78
	Pseudo-Total	317,80	197,72	11,37	727,00	7,23	270,40	4,33	7,05	10,22	11,01
	% Recovery	108,93	143,41	132,59	92,44	109,43	92,80	111,32	150,83	135,56	170,48
	F1	3,58	80,71	11,13	8,55	2,15	5,46	0,42	5,76	0,41	8,65
	F2	6,11	20,89	2,93	25,22	0,66	4,93	0,16	0,50	7,37	11,38
	F3	2,71	5,71	2,77	5,59	0,61	3,07	0,17	4,76	3,65	4,61
S4-1 m	**F4**	282,40	140,31	2,52	389,80	4,47	197,38	3,17	3,70	1,54	0,18
	Sum of fractions	294,79	247,62	19,34	429,17	7,89	210,83	3,92	14,72	12,97	24,81
	Pseudo-Total	165,50	170,48	14,02	394,40	4,98	193,92	2,55	12,21	14,84	21,73
	% Recovery	178,12	145,25	137,95	108,81	158,49	108,72	153,49	120,53	87,39	114,20
	F1	1,98	37,50	12,19	3,13	1,41	3,05	0,31	4,42	0,20	3,04
	F2	4,79	23,01	1,60	10,38	0,48	2,14	0,09	1,01	8,41	5,28
	F3	2,34	3,37	3,79	4,23	0,44	2,63	0,06	4,15	3,75	3,31
S4-2 m	**F4**	257,80	117,78	2,56	551,00	6,72	184,24	2,98	3,02	0,97	0,29
	Sum of fractions	266,91	181,66	20,14	568,74	9,04	192,06	3,44	12,59	13,33	11,92
	Pseudo-Total	226,80	124,96	16,76	583,60	6,79	186,22	2,80	11,87	12,59	11,45
	% Recovery	117,69	145,37	120,14	97,45	133,12	103,13	122,90	106,09	105,84	104,11
	F1	1,86	36,86	12,75	2,73	1,43	2,19	0,31	2,00	0,20	3,02
	F2	4,20	20,01	6,62	9,57	0,65	2,07	0,08	0,15	7,73	4,74
S4-3 m	**F3**	2,38	2,80	2,74	4,31	0,30	2,14	0,05	2,60	3,62	2,08
	F4	175,80	60,44	3,90	399,00	4,56	144,76	2,40	3,14	0,96	0,79
	Sum of fractions	184,24	120,11	26,01	415,61	6,94	151,16	2,84	7,89	12,51	10,63

	Pseudo-Total	190,96	103,04	24,16	516,60	6,97	159,66	2,42	5,36	13,24	10,22
	% Recovery	96,48	116,57	107,66	80,45	99,56	94,67	117,36	147,36	94,44	103,95
	F1	2,77	57,01	1,98	3,96	0,57	2,01	0,46	0,30	0,30	4,28
	F2	4,14	24,15	0,85	7,28	0,37	1,65	0,08	0,19	9,69	3,76
	F3	2,13	3,46	2,05	3,61	0,31	2,07	0,05	3,96	3,90	2,78
S5	**F4**	215,40	90,16	1,07	427,60	3,34	143,04	2,20	0,46	0,62	0,33
	Sum of fractions	224,43	174,78	5,95	442,44	4,60	148,77	2,78	4,92	14,50	11,14
	Pseudo-Total	232,40	159,14	4,90	477,20	4,67	144,92	2,20	3,52	13,30	10,85
	% Recovery	96,57	109,83	121,48	92,72	98,49	102,66	126,29	139,61	109,01	102,73

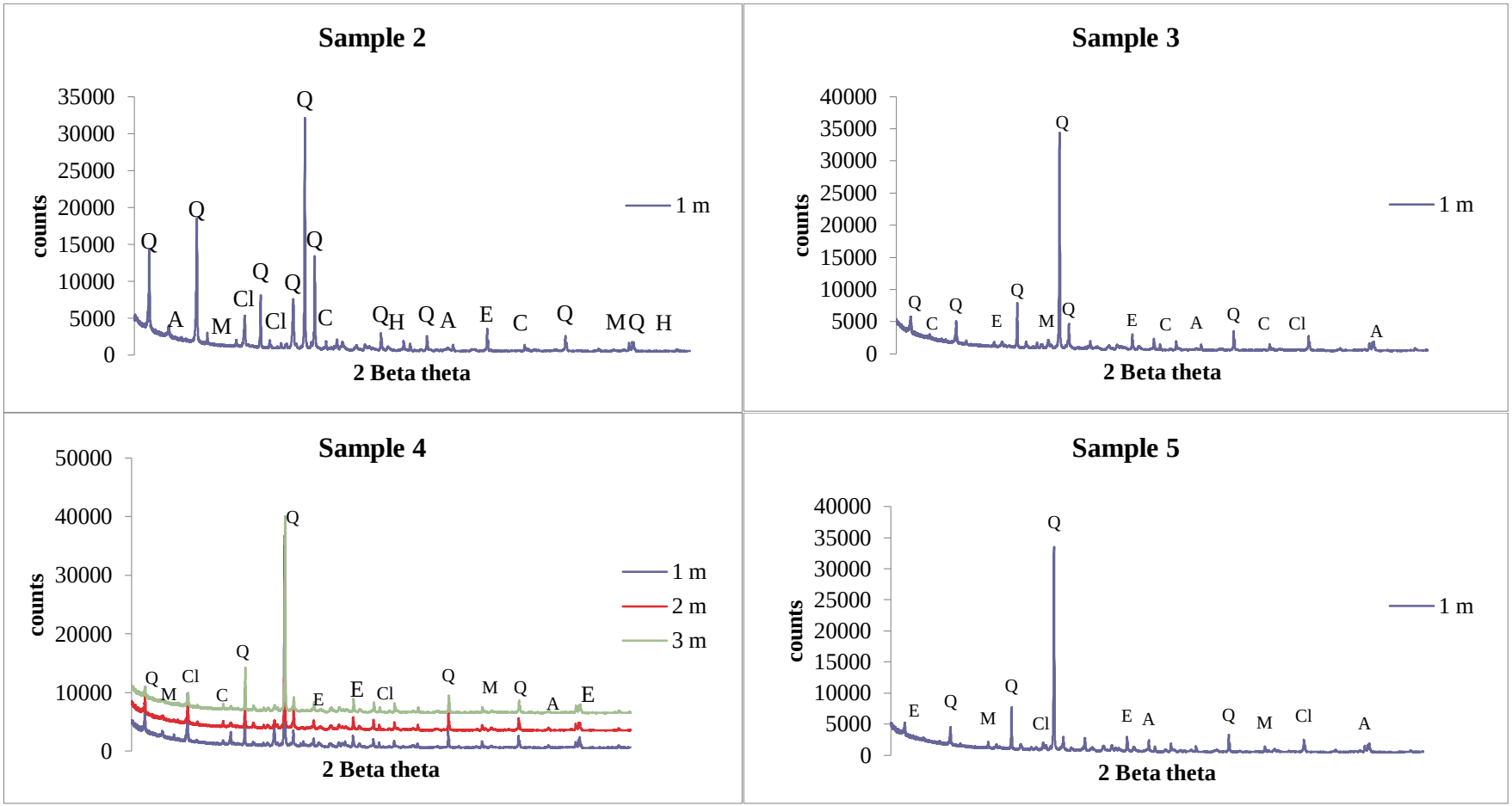

Figure C 1: X-ray powder diffractogram of copper tailings sample 2, 3, 4 and 5 (Q= Quartz, E=Epidote, C=Clinochlorite, A=Albite and M= Muscovite).

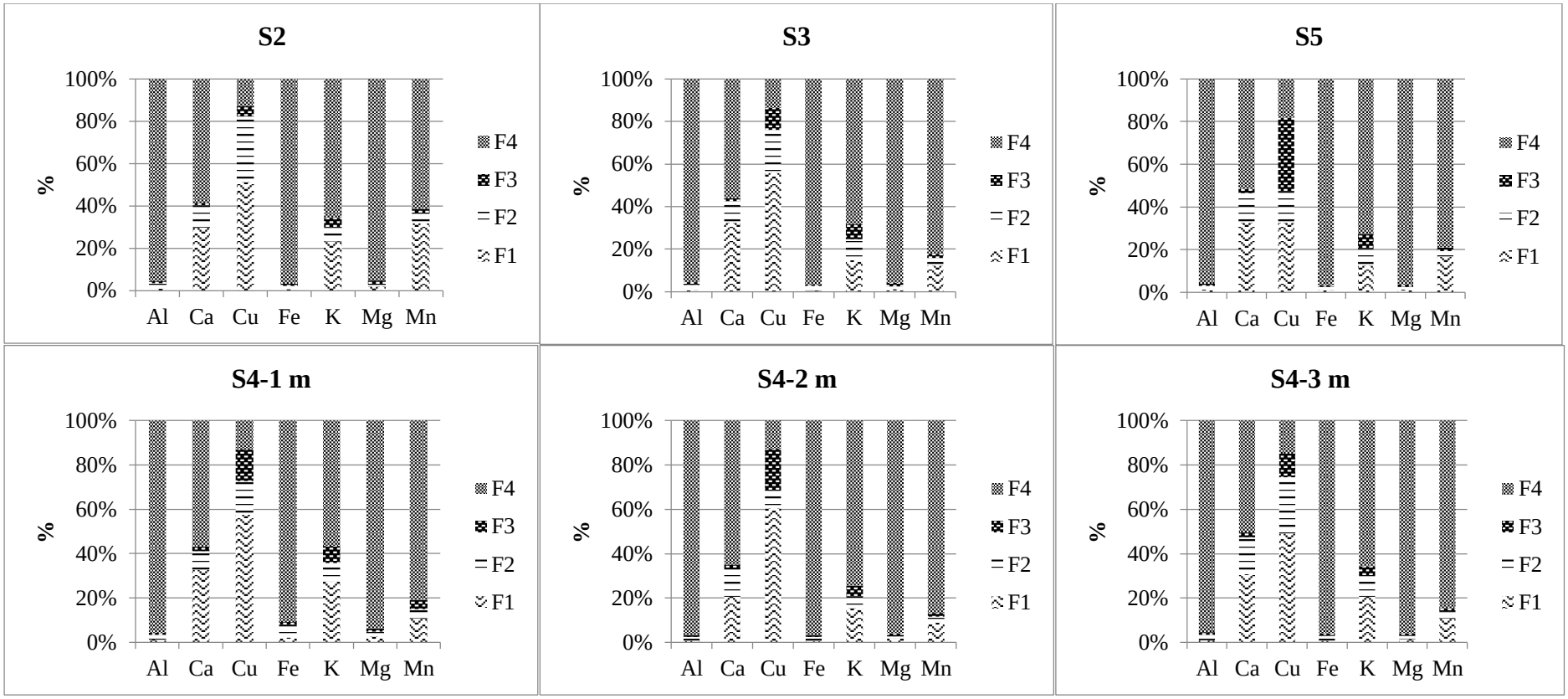

Figure C 2: % Major metal species in 4 geochemical fractions of sample 2, 3, 4 and 5 (F1- Exchangeable fractions, F2- Iron and Manganese oxide, F3- Organic matter and Reducible, F4- Residual).

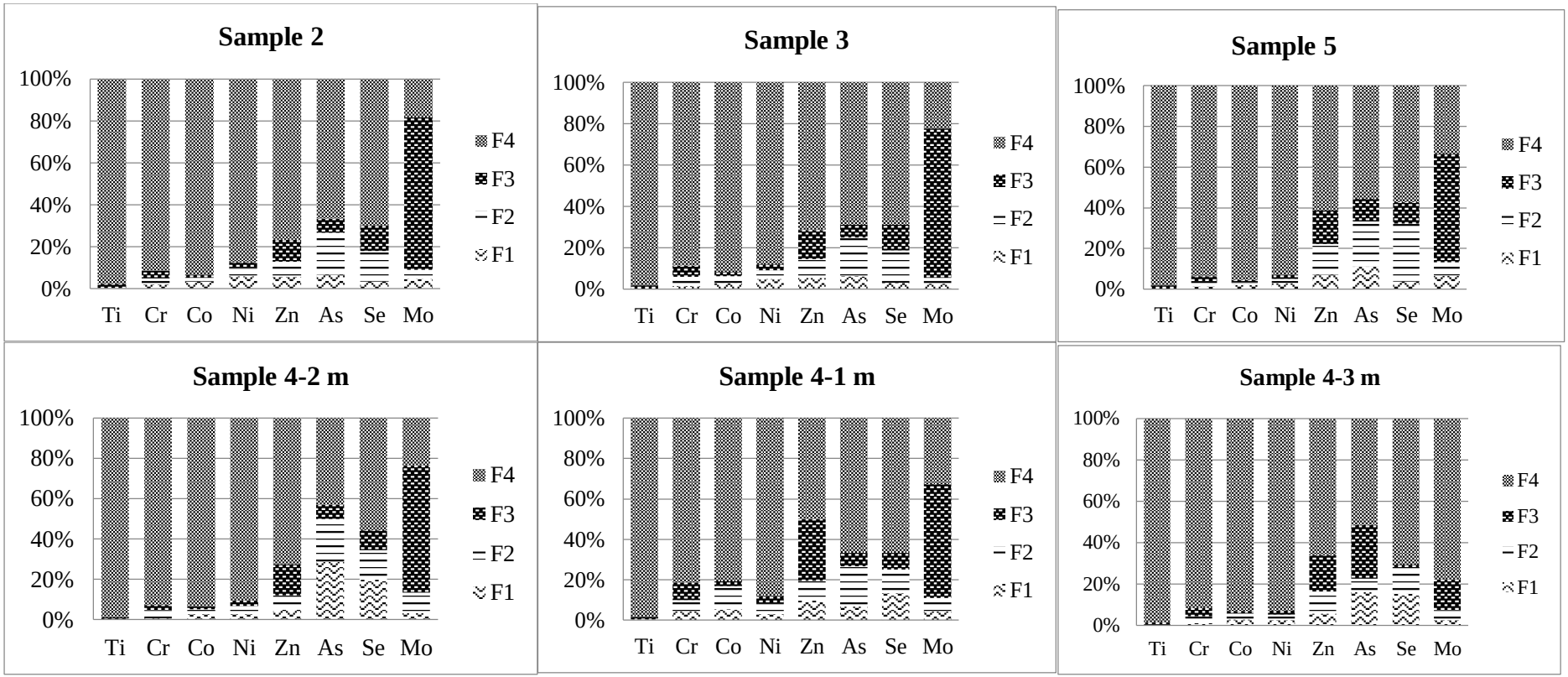

Figure C 3:% Minor metal species in 4 geochemical fractions of sample 2, 3, 4 and 5 (where; F1- Exchangeable fractions, F2- Iron and Manganese oxide, F3- Organic matter and Reducible, F4- Residual).

Chapter 4: Synthesis of geopolymer bricks from Musina copper mine tailings: Preliminary investigations

Abstract

The main aim of this chapter was to evaluate the feasibility of using the MT to produce a geopolymer bricks. The bricks were prepared using 5M NaOH, 5M $Na_2SiO_3.5H_2O$ and 5M NaOH: $Na_2SiO_3.5H_2O$ (70:30 and 80:20) with L/S ratio of 0.2; and cured using a hot air oven and greenhouse for a period of 4 and 7d respectively. Thereafter, the Unconfined Compressive Strength was measured using a Pro Ikon PGC-2002 electronic concrete compression machine (2000kN). The results showed that using 5M NaOH: $Na_2SiO_3.5H_2O$ (70:30) as an alkali activator produces a better geopolymer as compared to 5M NaOH. The Unconfined Compressive Strength (UCS) produced at 3 and 7d at 5M NaOH within a GH was 0.40 MPa and 0.42 MPa, respectively. Bricks that were cured within the hot air oven with 5M NaOH: Na2SiO3.5H2O (70:30) was 7.65 MPa. The obtained results indicate that the best curing regime was the hot air oven as compared to the GH. However, the UCS obtained with hot air oven regime was below the SANS 1215 standard. The utilization of sodium silicate to produce a geopolymer bricks was unsuccessful due to partial solidity that was influenced by the temperature thereby, the bricks couldn't be studied further because it solidified and thawed based on temperature. Studies need to focus on different parameters that are influential in the production of geopolymers and increasing the curing period.

Keywords: *Unconfined compressive strength, Partial solidification, Efflorescence, SANS 1215 and geopolymer bricks.*

4.1 Introduction

Bricks are the main material utilised for erecting buildings and within the construction industry. The Southern African Development Community (SADC) produces 5 billion bricks per annum (p.a) with South Africa being the biggest contributor of clay brick production at 70%(3.6 billion) of the overall SADC production. Clay bricks utilizes clay and shale as a source material with high kilning temperatures >900°C. Thereby, quarrying for clay and shale production is energy intensive, can release high levels of waste materials, high GHG emissions due to the kilning process and have an adverse impact/effect on the geographical landscape. Clay and cement brick production constitutes 90% of the South brick industry with both brick types requiring clay and shale in either its primary or secondary production. Unfortunately, due to the high consumption of shale and clay mostly because of brick production, there is a shortage of these resources in many parts of the world. Due to the aforementioned predicament most countries such as China have resulted in limiting bricks produced from shale and clay in order to protect the resources (Chen et.al., 2011 and China economic trade committee, 2001). Most studies have recently tried to investigate alternative construction materials with a very popular research currently being geopolymer.

The basic reaction mechanism that is undergone during the geopolymerization process is still not totally understood (Xiao et.al., 2009). For instance, parameters such as temperature required for geopolymer reaction, ratio and the dissolution rate of Si and Al differs based on the elemental concentration content and reactivity of the material. A study by Saeed and Zang (2012) indicated that an increase in water content at a constant NaOH concentration requires more NaOH for a greater Si dissolution to occur. Saeed and Zang (2012) further discovered that an increase in alkalinity in stable quartz as compared to the other minerals within the material while stimulate the dissolution of Si. The release of Al accelerates the dissolution and condensation rate of geopolymer bricks due to an increase in curing temperature within the mix design (Xu and Van Deventer, 2000; 2002a and 2002b). However, some of the various minerals used did not contain high Al quantities which made it impossible to form geopolymeric precursors.

In order for one to understand the parameters required by a feedstock material we ought to understand the chemical composition and behaviour of the material in different operational parameters. Not all materials will behave the same, it is all dependent on the type of material and reactivity rate. Thereby, preliminary studies were conducted of the mine tailing in order to understand the material behaviour and its reactivity when using 5 M NaOH, 5 M NaOH:

$Na_2SiO_3.5H_{20}$ (70:30) and 5 M $Na_2SiO_3.5H_{20}$ at a L/S ratio of 0.2 and 0.4 within an oven as compared to the greenhouse. The study is using the GH in order to further reduce CO_2 produced during the production of bricks.

4.1 Materials and Methods

4.1.1 Preparation of activation reagents

A solution containing 5M $Na_2SiO_3.5H_{20}$ was prepared prior to use by dissolving 106.07 g of $Na_2SiO_3.5H_{20}$ in a 100 mL volumetric flask using Milli-Q water. The solution was heated at a 100 °C in order to ensure the dissolution of $Na_2SiO_3.5H_{20}$. Thereafter, the solution was left to cool to room temperature. The solution containing 5 M NaOH was prepared by dissolving 20g pellets in 100 mL volumetric flask whilst being stirred in order to influence the dissolving rate.

4.1.2 Synthesis of geopolymers

To ensure that the mixes have a constant temperature during mixing, the dry constituent was weighed and placed in a temperature-controlled room approximately for 12 hours at 24°C prior to mixing. The mixing was done manually by adding 240 g binder solution to 1200g raw MT and 250 g binder solution to 1000 g raw MT simultaneously in a bowl at a ratio of 0.2 (L/S) and 0.4 (/L/S) for 3 minutes to acquire a homogeneous slurry paste. Oil is applied on the inner face of the moulds then the paste is transferred into moulds. The paste was then compacted to reduce the voids within the paste and covered by plastic to have a constant humidity for 24 hours while curing in ambient conditions. After 24 hours the moulds were de-moulded and placed into the oven and/or GH indicated in Table 4.1. Bricks cured within the hot air oven were cured at a temperature of 80 °C and within the greenhouse the curing temperature was inconsistent at a range of 14°C to 52°C. Bricks where thereafter analysed for unconfined compressive strength using a Pro Ikon PGC-2002 electronic concrete compression machine (2000kN). Figure 4.1 illustrates the greenhouse on top of a building. The greenhouse was built using planks and greenhouse UV treated polyethylene.

Table 4. 1: Preliminary mix design

Mixture Name	Copper tailings (g)	Activator/ Tailings (L/S) mixture ratio	Concentrations		Curing regime type
			5M $Na_2SiO_3.5H_{20}$ (mL)	5M NaOH (mL)	
MT0	1200	0.2	-	240	Oven
MT1	1200	0.2	-	240	Greenhouse
MT2	1000	0.4	250	-	Oven
MT3	960	0.2	72	168	Oven
MT4	960	0.2	72	168	Greenhouse

4.2 Results and discussion

4.2.1 Effects of different alkali activators on the final UCS.

Figure 4.1 present the variation of UCS of geopolymer bricks prepared using different alkali activators. In figure 4.1a the curing was done in a hot air oven while figure 4.1b illustrates curing with the GH.

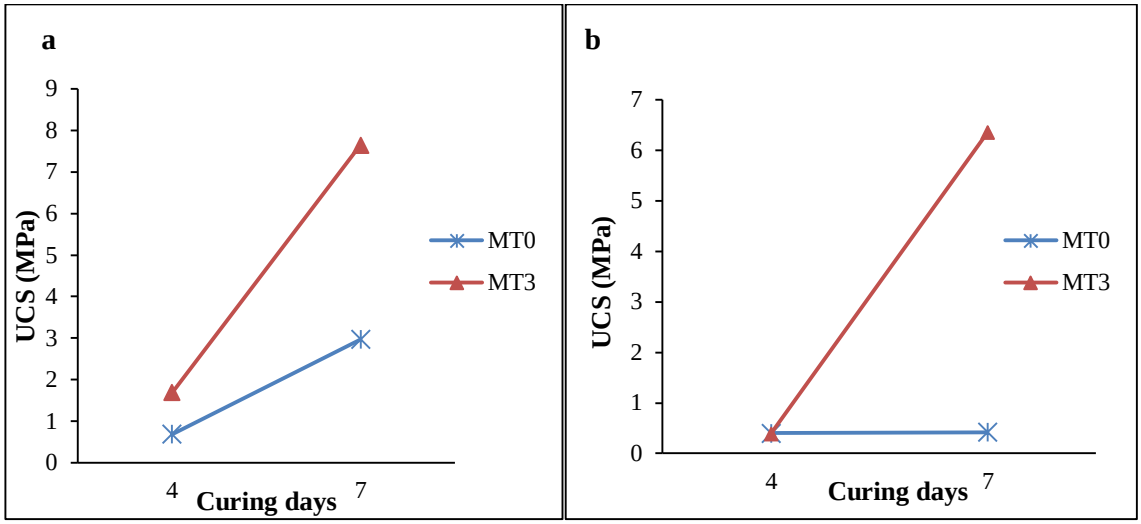

Figure 4. 1: Variation of UCS with different alkali activators at varying curing period with MT 0 is 5M NaOH and MT3 is 5M NaOH:Na2SiO3.5H2O (70:30) (where, a; is hot air oven and b; is GH).

The results in Fig. 4.1a for bricks that where cured in a hot air oven, showed that, an increase in curing days increases the UCS strength. Furthermore, bricks produced using 5 M NaOH: $Na_2SiO_3.5H_{20}$ (70:30) (MT3) showed the highest UCS of 7.65 MPa after 7d while bricks produced at 5 M NaOH (MT0) produced a UCS of 2.97 MPa after 7d as illustrated in figure 4.2. Both alkali activators at 4d produce a very low UCS due to the low alkali concentration which makes it difficult for the raw MT to initiate reactivity. (Phair and Van Deventer, 2001). For bricks cured in GH (Fig 4.1b) it is observed that geopolymer produced using 5M NaOH: $Na_2SiO_3.5H_{20}$ (MT4) has a higher UCS of 6.85 MPa after 7d while at 4d it produced a UCS of 0.39 MPa. At 5 M NaOH within the GH the UCS was low at 0.42 MPa and 0.39 MPa after 7d and 4d, respectively. The low UCS within the aforementioned samples was attributed due to the low alkali concentration, irregularity of temperatures within the GH and mainly due to the inert nature of the mine tailings. Within the hot air oven the UCS was higher than that within the GH due to a constant curing temperature that enabled reactivity of alumina and silica species. The 5M $Na_2SiO_3.5H_{20}$ produced a solid bricks within 5 minutes of mixing the bricks however, when the species was placed in the GH (fig. 4.2) it encountered partial curing during

the daytime where the temperatures where high and during the evening or cold temperatures the bricks would solidify.

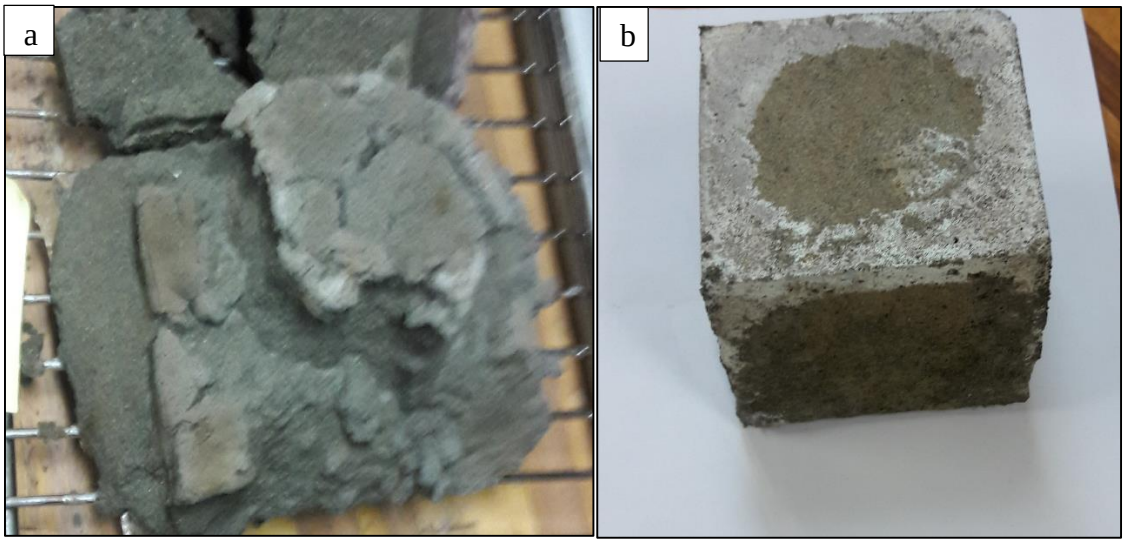

Figure 4. 2: a) collapsed brick of 5M $Na_2SiO_3.5H_{20}$ and; b) geopolymer brick of 5 M NaOH: $Na_2SiO_3.5H_{20}$ (70:30) (MT3).

Hot oven air curing regime produced a high UCS in comparison to the GH due to the constant temperature within the oven whereas, in the GH the temperatures vary based on the atmospheric temperature. High efflorescence occurs within the GH due to the rate of dissolution that is influenced by the temperature. On a rainy or cold day the temperatures within the GH are at an average of 20 °C which is below the curing temperature a geopolymer bricks can cure in (Xu and Van Deventer, 2002b). However, the GH is environmentally efficient because it uses natural energy resource to cure. The oven uses electricity which produces a by-product CO_2 into the atmosphere from the coal used to generate the electricity. Sodium silicate as a single alkali within the raw MT is unsuccessful due to the partial reactivity of the alkali, its dependence to high temperatures to solidify makes it unsuitable to use alone. Thereby, another alkali activator needs to be introduced to the mix design. Although the sodium silicate had its disadvantages it is an important key to the mix design due to the high alkalinity present with the solution which influences the UCS. Sodium hydroxide as a single alkali was not effective because it produced a low UCS due to the alkalinity within the solution.

4.3 Conclusion

This chapter presented the preliminary investigation on evaluating the potential of synthesizing geopolymer material from Musina copper MT. The following conclusions were made:

- The preliminary tests showed that the use of milled and raw tailings wasn't a success due to the high level of fineness present within the bricks. The bricks' fineness reduced the pore interconnectivity which made the activator storage minimal within the bricks thereby, forcing the binder to be leached out (bleeding).
- 5M $Na_2SiO_3.5H_{20}$ (MT2) encountered partial curing (solid) during the process of drying the bricks.
- Analysis conducted using a greenhouse for bricks 5M NaOH (MT1) and 5M NaOH: $Na_2SiO_3.5H_{20}$ (MT4) produced low UCS due to low reactivity occurring within the bricks.
- The highest UCS was observed at 5M NaOH: $Na_2SiO_3.5H_{20}$ within the hot air oven after 7d.
- The bricks produced contained a strong outer which is as a result of the bleeding activator which settles on the surface of the material dissolving various chemical components which later react/crystallize to form salts which appear as solid crusts and an unreacted inner part is due to the bleeding of the binder solution which left minimal solution within the bricks thereby, reducing reactivity of the material.
- The material showed potential for geopolymerization however, the operational parameters needs further optimization.

4.4 Recommendations

- Optimization of all parameters that influence the geopolymer bricks UCS needs to be considered.
- Further studies need to focus on the introduction of admixtures such as river sand (particle size < 2 mm) and/or cement, to increase the performance of the process.
- Sodium silicate should not be utilized without another alkali activator present within the mix design.
- Optimise the different parameters using the hot air oven and then compare the final synthesised material with the highest UCS for the GH.

References

Chen, Y., Zang, T., Chen, Y., Zhao, Y., and Bao, S. 2011. Preparation of eco-friendly construction bricks from hematite tailings. Construction Builiding Material, Vol.25, pp.2107-2111.

China economic trade committee. 2007. Tenth five-year program of building materials industry. China Building Material, Vol.7, pp.7-10.

Grahl, C. 2004. Brick market overview: Steady growth continues in the brick industry. Ceramic industry, October issue.

Xiao, Y., Zhang, Z., Zhu, H., Chen, Y. 2009. Geopolymerization process of alkali-metakaolinite characterized by isothermal calorimetry. Thermochim. Acta, Vol. 493, pp. 49-54.

Xu, H., Van Deventer, J.S.J., 2000. The geopolymerisation of aluminosilicate minerals. International Journal of Minerals and Processing 59 (3), 247–266.

Xu,H., J.S.J. Van Deventer, Geopolymerisation of multiple minerals, 2002a, Minerals Engineering 15 1131-1139.

Xu, H., Van Deventer, J.S.J., 2002b. Factors affecting the geopolymerization of alkali-feldspars. Minerals and Metallurgical Processing 19 (4), 209–214.

Hua, X.U., and Van Deventer, J.S.J. 2003. The effect of alkali metals on the formation of polymeric gels from alkali feldspars. Colloids Surf A Physicochem Eng Asp. Vol.216, pp.27-44.

Chapter 5

Part A: Synthesis of the geopolymer bricks from copper mine tailings: Evaluation of optimum conditions.

Abstract

The preliminary investigation presented in chapter 4 showed that Musina copper tailings has the potential for use in preparation of geopolymer material and recommended further investigations to evaluate the optimum conditions for synthesizing geopolymer material. Therefore, this chapter focuses on evaluating the optimum conditions for synthesizing a geopolymer bricks from Musina copper mine tailings. Optimum conditions evaluated were: curing temperature, alkali concentrations, liquid/solid (L/S) ratio, alkali activator and curing regime. The optimum conditions were determined based on the final compressive strength. Results showed that the material prepared using 5 M NaOH: Na_2SiO_3.5H2O (80:20) has the highest UCS at 3.12 MPa after 7d. However, after 28d the 5 M NaOH: $Na_2SiO_3.5H_2O$ (70:30) showed an increase in UCS (5.51 MPa) which was found to be satisfactory compared to material prepared using 5M NaOH: $Na_2SiO_3.5H_2O$ (80:20) and 5M NaOH therefore, 5M NaOH: Na_2SiO_3.5H2O (70:30) was selected to be the optimum ratio. When varying the concentration, the material prepared at 10 M alkali activator ratio showed higher UCS as compared to material prepared at 5 and 15 M alkali activator ratio. The L/S ratio of 0.2 was found to be the optimum ratio since at ratios >0.2 the material collapsed due to high liquid being present within the mixture. Bricks cured at 80 °C possess UCS required by SABS after 21d whereas the brick cured at 140 °C showed a higher UCS after 7d. The chapter will further study the utilisation of the MT using 5M NaOH; 5M NaOH: $Na_2SiO_3.5H_2O$ (80:20); and 5, 10 and 15M NaOH: $Na_2SiO_3.5H_2O$ (70:30). The 10M NaOH: $Na_2SiO_3.5H_2O$ (70:30) was then introduced to admixtures and the final mixture was then compared in the different types of curing regimes.

Keywords: *Unconfined Compressive Strength (UCS), alkali activators, alkali activator concentrations, curing regime, curing temperatures and greenhouse.*

Introduction

Geopolymerization is the production of a variety of materials such as bricks using Al-Si rich materials (Zang et.al., 2011). The process has been established to consume low amounts of energy and generate 80% less CO_2 as compared to the conventional clay brick production (Xu and Van Deventer, 2002a).There are variety of alkaline solutions that can be used as the binder activator in the geopolymer process such as sodium hydroxide (NaOH), potassium hydroxide (KOH), sodium silicate (Na_2SiO_3), potassium silicate (K_2SiO_3), sodium carbonate (Na_2CO_3) and sodium sulfate (Na_2SO_4) (Provis and Bernal., 2014). There are two important roles that are derived by alkali activators during the process of geopolymerization namely; the dissolution of silica and alumina species and secondly the charge-balancing of alumina species by providing metal cations (Stevenson and Sagoe-Crentsil, 2005).

Studies of different alkali activator concentrations have been done where it was identified that an increase in concentration increases the UCS. The increase in UCS with higher concentration is mainly due to the dissolution of more silica and alumina components and thus incorporation of larger quantities of silica and alumina components in geopolymerization. However, previous studies indicate that the process of geopolymerization occurs until it reaches a state of equilibrium due to the material withstanding a certain concentration, temperature or curing time (Guo et.al., 2010; Khale and Chaudhary, 2007 and Panagiotopoulou et.al., 2007). The point of equilibrium is possible due to high alkali activator concentration which hinders evaporation of water and formation of the polymeric structure thereby preventing the contact between the solid material and the activating solution through precipitation of Si-Al phase (Chen and Chiu, 2003; and Lee and Van Deventer, 2003).

Studies have indicated that one of the most important parameter is the curing temperature. Geopolymerization is known for its low temperature (≤100 °C) requirements to cure a geopolymer material (Mohsen and Mostafa, 2010; and Ferone et.al., 2011). However, there are some materials that require a high amount of temperature to instigate the dissolution and poly-condensation of the Al-Si material (Diop and Grutzeck, 2008). Thereby, temperature parameter needs to be investigated to determine which temperature is suitable for the MT. Another parameter that needs to be investigated is the curing regime used which will have an impact on the geopolymer materials crystallization (Nozari et. al., 2011). Srinvasan and Sivakumar (2013); Goretla et.al., (2004); Bakharev (2005); Nozari et.al., (2011) and Helmy

(2016) produced a good compressive strength within a hot air oven ranging between 75°C to 250°C. Studies by Cheng and Chiu, (2003); Fernandez-Jimenez et.al., (2005); Yip and Van Deventer, (2001) produced geopolymer materials using Al-Si rich materials with an admixture of sand, cement, raw Al-Si rich material or other Al-Si rich waste. The rate of dissolution of Al within waste or natural aluminosilicates does not produce a desirable gel composition which is mainly why researchers such as Van Jaarsveld et.al., (1997) and Rahier et.al., (1996a) used bi-components of Al-Si materials thereby; a stronger UCS is formed in a bi-component as compared to a single component. The present study evaluated the geopolymerization potential of the copper mine tailing using alkali $Na_2SiO_{3.}5H_{20}$ and NaOH as activators at different concentrations.

5.1 Materials and Methods

5.1.1 Materials

Copper mine tailings were collected from the Musina mine tailings located in the Vhembe district of South Africa. Analytical grade reagents were obtained from Rochelle Chemicals and Lab Equipment CC, South Africa Ltd and were of analytical grade. River sand and 42.5N cement was used as dry constituents in the production of bricks.

5.1.2 Preparation of activation reagents

Solutions containing 5M, 10M and 15M $Na_2SiO_{3.}5H_{20}$ were prepared prior to use by dissolving 106.07, 212.14 and 318.21 g of $Na_2SiO_{3.}5H_{20}$, respectively in 822.25 mL volumetric flask using Milli-Q water and heated at a 100 °C to dissolve the salt. Thereafter, the solution was left to cool to room temperature. Solutions containing 5M, 10M and 15M NaOH were prepared by dissolving 20, 40 and 60 g of NaOH pellets in 100 mL Milli-Q water whilst being stirred to influence the dissolving rate.

5.1.3 Optimization conditions of operation parameters for synthesizing geopolymer bricks.

To prepare a geopolymer bricks, dry constituent (MT) was weighed and placed at room temperature for approximately 12 hours prior to mixing to ensure constant temperature. A mass of 1200g of mine tailings was weighed into a bowl and this was followed by slow addition alkali activator solution under a continuous manual stirring. The measurements of alkali activator solutions are stipulated in Table E1. After mixing, the paste obtained was then transferred into well-oiled moulds (100mm x 100mm). The paste was compacted using mortar

to reduce the voids in between and then covered by plastic-what type of plastic a sheet or container to ensure a constant humidity for 24 hours while curing in ambient conditions. After 24 hours the moulds were de-moulded from the casting cubes and placed into into the hot air oven whose temperature had been set at a select value. The optimum operating parameters such as, alkali activator, alkali activator concentration, Liquid/solid ratio (L/S), curing temperature, admixture and curing regime were evaluated.

Alkali activator type/ratio

To evaluate alkali activator type/ratio5M NaOH, 5M NaOH: $Na_2SiO_35H_{20}$ at a ratio of 70: 30 and 80:20 were used and the L/S ratio of 0.2 was maintained. The bricks were cured in a hot air oven at a temperature of 80 °C at 7, 21 and 28d.

Alkali activator concentration

The effect of alkali activator concentration was evaluated by varying NaOH: $Na_2SiO_35H_{20}$ concentration from 5M, 10M and 15M (70:30) with L/S ratio of 0.2. The bricks were cured in a hot air oven at a temperature of 80 °C at 7, 21 and 28d.

Curing temperature

In order to evaluate the effect of curing temperature, bricks where prepared using alkali activator concentration of 10M NaOH: $Na_2SiO_35H_{20}$ (70:30). The L/S ratio of 0.2 was maintained and bricks were cured in a hot air oven at a temperature of 80 °C, 120 °C and 180 °C at 7, 21 and 28d.

L/S ratio

To evaluate the effect of L/S ratio, bricks where prepared using alkali concentration of 10M NaOH: $Na_2SiO_35H_{20}$ (70: 30). The L/S ratios of 0.2 and 0.3 were used. The bricks were cured in a hot air oven at a temperature of 80 °C at 7, 21 and 28d.

Admixture

To evaluate the effect of admixture, bricks where prepared using alkali concentration of 10M NaOH: $Na_2SiO_35H_{20}$ at a ratio of 70: 30 with L/S ratio of 0.2 and 5% cement or 10% river sand added respectively. The bricks were cured in a hot air oven at a temperature of 80 °C at 7, 21 and 28d.

Curing Regime

The influence of curing regime was evaluated by curing the bricks which were prepared at 10M

NaOH: $Na_2SiO_35H_{20}$ at a ratio of 70: 30 with L/S ratio of 0.2 and 5% cement. The bricks were cured in a hot air oven at a temperature of 80 °C and greenhouse with varying temperature of 14 °C to 52 °C at 7, 21 and 28d.

Table 5.1 presents the summary on optimization of optimum conditions. The UCS, water absorption and abrasion tests were used to analyse the bricks and to determine the optimum conditions.

Table 5. 1: Parameters varied during the optimization of the geopolymer bricks. .

1st parameter varied	**Constant parameters**
5M NaOH 5M NaOH: 5M $Na_2SiO_35H_{20}$ (70:30) 5M NaOH: 5M $Na_2SiO_35H_{20}$ (80:20)	Ratio of 0.2 (binder/solid) Curing at room temperature – 24 hours. Hot air Oven treatment temp 80°C. Curing time is 7, 21 and 28 days.
2nd parameter varied	**Constant parameters**
5M NaOH: 5M $Na_2SiO_35H_{20}$ (70:30) 10M NaOH: 10M $Na_2SiO_35H_{20}$ (70:30) 15M NaOH: 15M $Na_2SiO_35H_{20}$ (70:30)	Ratio of 0.2 (binder/solid) Curing at room temperature – 24 hours. Hot air Oven treatment temp 80°C. Curing time is 7, 21 and 28 days.
3rd parameter varied	**Constant parameters**
Ratio of 0.2 (binder/solid) Ratio of 0.3 (binder/solid)	10M NaOH: 10M $Na_2SiO_35H_{20}$ (70:30) Curing at room temperature – 24 hours. Hot air Oven treatment temp 80°C. Curing time is 7, 21 and 28 days.
4th parameter varied	**Constant parameters**
80°C oven dryer treatment temperature 140°C oven dryer treatment temperature 180°C oven dryer treatment temperature	10M NaOH: 10M $Na_2SiO_35H_{20}$ (70:30) Ratio of 0.2 (binder/solid) Curing at room temperature – 24 hours. Curing time is 7, 21 and 28 days.
5th parameter varied	**Constant parameters**
Admixture of 10% River sand Admixture of 5% cement (Hot air Oven vs Greenhouse)	10M NaOH: 10M $Na_2SiO_35H_{20}$ (70:30) Ratio of 0.2 (binder/solid) Oven dry treatment temp 80°C. Curing time is 7, 21 and 28 days. Curing at room temperature – 24 hours.
6th parameter varied	**Constant parameters**
Oven dryer Greenhouse	10M NaOH: 10M $Na_2SiO_35H_{20}$ (70:30) Ratio of 0.2 (binder/solid) Admixture of 5% cement Curing time is 7, 21 and 28 days. Curing at room temperature – 24 hours

5.1.4 Mechanical properties of synthesized geopolymer bricks

5.2.3.1 Unconfined Compressive Strength (UCS)

The compressive strength of the geopolymer bricks was tested after varying curing periods. The bricks were tested for UCS using a Pro Ikon PGC-2002 electronic concrete compression machine (2000kN) at a surface area of 100mmx100mm. The bricks were crushed within the machine to acquire the bricks' tension to the machine.

5.2.3.2 Water Absorption

Water absorption is conducted to determine the rate of water infiltration that occurs when the bricks get into contact with water. The bricks were left in ambient temperature to cool off after the bricks are removed from the curing regime. After cooling off the bricks were weighed to determine the bricks's initial weight. Thereafter, the bricks were immersed completely into cold water at a temperature of 27± 2 °C for 24 hours, after which they were removed and weighed again. The percentages of water absorbed by the blocks will be calculated using equation 5.1 (ASTM D789):

$$W = \frac{M_2 - M_1}{M_1} \times 100 \qquad \text{Equation 5. 1}$$

where; W= is the water absorption of the bricks

M_1 = the initial weight of the dry bricks

M_2 = is the final weight of the bricks after being immersed in water.

5.2.3.1 Durability test

Durability test was performed on the bricks through an abrasion test. After the geopolymer bricks was cured, it was weighed and recorded. The bricks was placed on a smooth and firm surface, and then all the surfaces were wire brushed in a back and forth motion 50 times, where one back and forth motion was considered a single stroke. After being brushed, the bricks mass weighed again to determine the amount of material or particles abraded. The durability of the bricks was determine using equation 5.2:

$$Abrasion = M_1 - M_2 \qquad \text{Equation 5. 2}$$

Where; M_1 is initial weight bricks

M_2 is final weight of bricks after brushing has occurred

5.2 Results and Discussions

5.2.1 Effects of alkali activators on final UCS

To evaluate the effect of alkali activator, three types of alkali activators were used namely; 5M NaOH and 5M NaOH: $Na_2SiO_3.5H_2O$ (80:20 and 70:30). The bricks were cured for 7, 21 and 28d at 80 °C with a hot air oven. Figure 5.1 shows the variation of UCS as a function of curing days for different types of alkali activators.

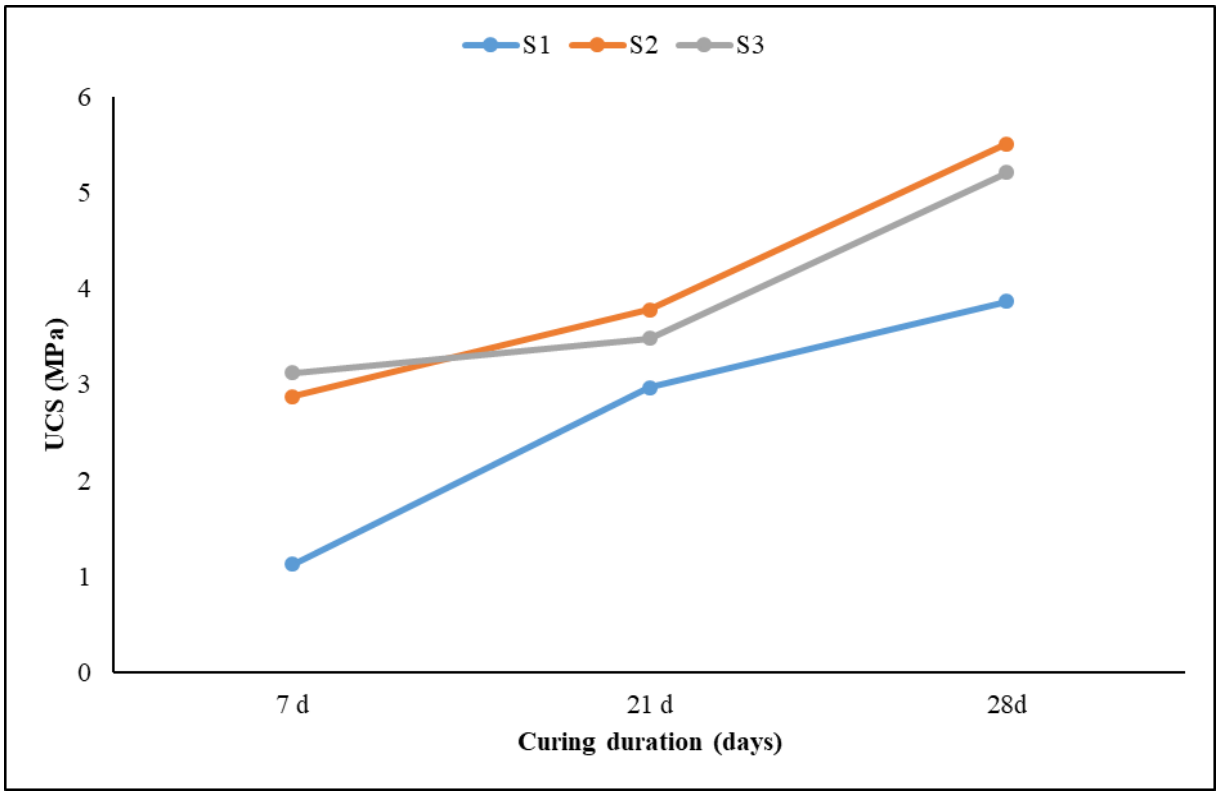

Figure 5. 1: Variation of UCS with different alkali activators at varying curing period (where; S1 is 5M NaOH, S2 is 5M NaOH: $Na_2SiO_3.5H_2O$ at a ratio 70:30 and S3 is 5M NaOH: $Na_2SiO_3.5H_2O$ at a ratio of 80:20.

From the results, it is observed that UCS increased with increasing curing period. This was observed with both alkali activators. The bricks prepared using 5M NaOH(S1) showed the lowest UCS throughout the 28d curing period as compared to the bricks prepared at $Na_2SiO_3.5H_{20}O$ at a ratio of 70:30 (S2) and 80:20 (S3). Such an outcome is due to the presence of $NaSi_2O_3$ which increases alkalinity as compared to the alkalinity present within NaOH (Phair and Van Deventer, 2001). Based on the results it is concluded that 5M NaOH is not an appropriate alkali activator to use in acquiring an optimum UCS. Thus focus remains in comparing 5M NaOH: $Na_2SiO_3.5H_2O$ (70:30 and 80:20) where S3 initially has a higher UCS as compared to S2 at 7d. However, as curing period increases S2 produces a greater UCS. The

slight variation in final UCS between S2 and S3 is due to S2 having a 10% increase in $Na_2SiO_3.5H_2$ content which directly indicates an increase in alkalinity. Furthermore, Wang et.al., (1994) confirmed that bricks produced by $NaSi_2O_3$ activator produced the best UCS thereby the greater the presence of $Na_2SiO_3.5H_2O$ the greater the UCS. Therefore, 5M NaOH: $Na_2SiO_3.5H_2O$ (70:30) was the best alkali activator solution and was applied in subsequent experiments.

5.2.2 Effects of alkali activator concentrations on final UCS

Effects of alkali activators concentration was evaluated using 5M, 10M and 15M NaOH: $Na_2SiO_3.5H_2O$ at a ratio of 70:30 as indicated in Table 5.1. Figure 5.2 illustrates the effect of alkali activator concentrations on UCS at various curing periods.

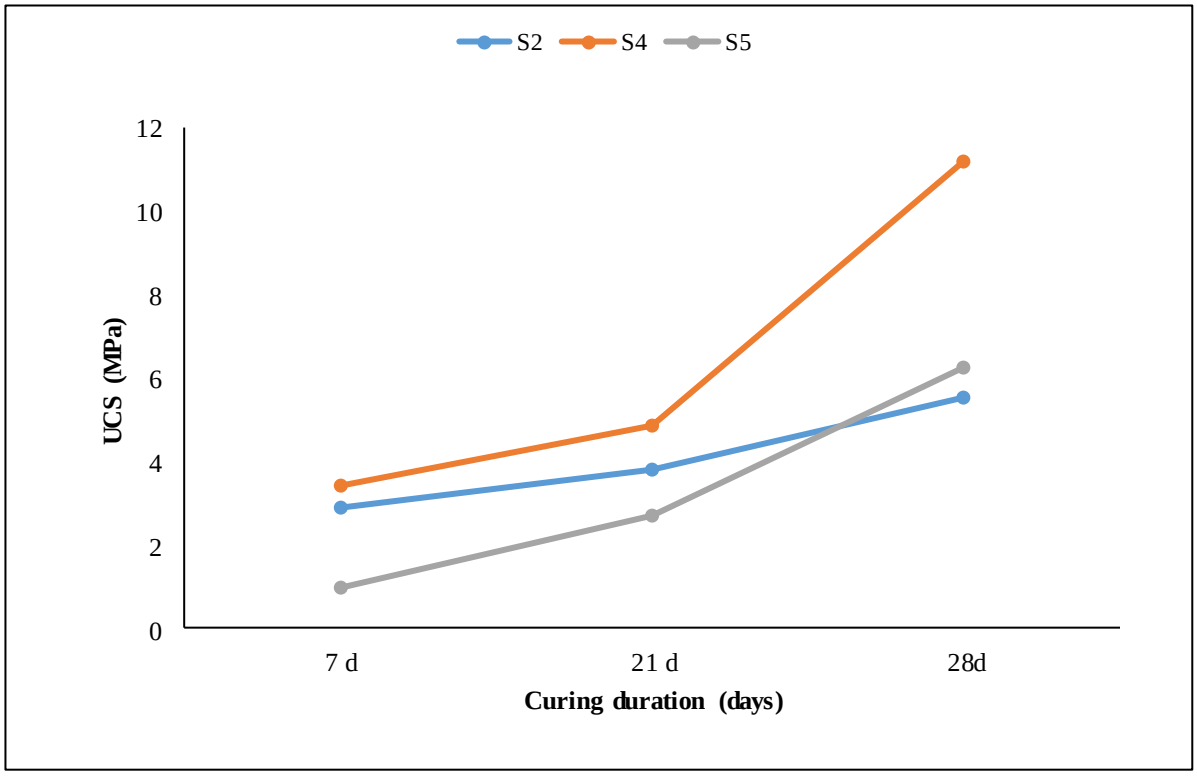

Figure 5. 2: Variation of UCS with different alkali activators concentration at varying curing period (where; S2 is 5M NaOH: Na2SiO3.5H2O at a ratio of 70:30, S4 is 10M NaOH: $Na_2SiO_3.5H_2O$ at a ratio of 70:30 and S5 is 15M NaOH: $Na_2SiO_3.5H_2O$ at a ratio of 70:30.

From the results, it is observed that UCS increased with alkali concentration from 5 to 10M then decreased at 15M. Furthermore, UCS was observed to be increasing with increasing curing time for both concentrations. Bricks S2 produced an overall final UCS of 5.51 MPa at 28d, however at 7d the UCS is higher than that of S5 due to the moist content present within the bricks. According to Kong et.al., (2007) an increase in Na_2SiO_3 resulted in inhabitation of geopolymerization reaction through the Al-Si phase precipitation which avoids contact

between reacting material and alkali activator. Thereby, excess $Na_2SiO_3.5H_{20}$ hinders water evaporation and structure formation as SEM analysis (Fig 5.14a) will indicate later. Previous studies indicated that the higher the concentration the stronger the UCS however, S5 bricks did not produce a high optimum UCS after 28d as compared to S4 and S2.

S4 produced the highest UCS at 28d with a UCS of 11.2 MPa which is approved by SANS 1215 guidelines of a concrete brick (>10 MPa). Based on the results it is concluded that 10M NaOH: $Na_2SiO_3.5H_2O$ (70:30) is the best optimized alkali activator concentration and was applied in subsequent experiments.

5.2.3 Effects of different ratios (binder/ MT) on final UCS

Effects of L/S ratios was evaluated at a ratio of 0.2 and 0.3 with an alkali concentration of 10 M NaOH: $Na_2SiO_3.5H_2O$ (70:30) and temperature of 80°C for 7, 21 and 28d. The L/S ratio of 0.2 required 1200 g of MT and 240 mL alkali solution; and the L/S ratio of 0.3 required 1200 g of MT and 380 mL of alkali solution. Figure 5.3 indicates a collapsed geopolymer bricks at an L/S ratio of 0.3 after 36 hours. Analysis was conducted to determine the appropriate ratio to use for making the bricks which would meet the SANS 1215 requirements in terms of the UCS, abrasion and adsorption rate of the bricks.

Figure 5. 3: Left side is a collapsed geopolymer bricks with 10M NaOH: $Na_2SiO_3.5H_2O$ (70:30) at a L/S ratio of 0.3 after 36 hours in an oven of 80 °C and right side is a geopolymer bricks at a L/S ratio of 0.2 with similar conditions.

Figure 5.3 depicts a bricks that was mixed at an L/S ratio of 0.3, the mix design had high content of liquid which resulted in the bricks collapsing 36 hours after being de-moulded. There were no UCS results that were recorded for the L/S ratio of 0.3 due to the extremely high liquid content present as compared to MT. This caused difficulty in compacting and moulding the paste into the mould where failure in providing good compaction can seriously depress the

compressive strength of the cement paste due to non-homogeneity. Based on the results it is concluded that 10M NaOH: $Na_2SiO_3.5H_2O$ (70:30) with L/S ratio of 0.2 was the best L/S ratio that produced an optimum UCS of 11.2 MPa after 28d and it did not collapse after a few hours due to the liquid content present.

5.2.4 Effects of different curing temperatures on final UCS

Effects of temperatures in the synthesis of geopolymer was evaluated by varying temperature from 80 to 180 °C. The alkali concentration of 10M NaOH: $Na_2SiO_3.5H_2O$ (70:30) at an L/S ratio of 0.2 was maintained. Figure 5.4 illustrates the effects of temperature on UCS at different curing periods.

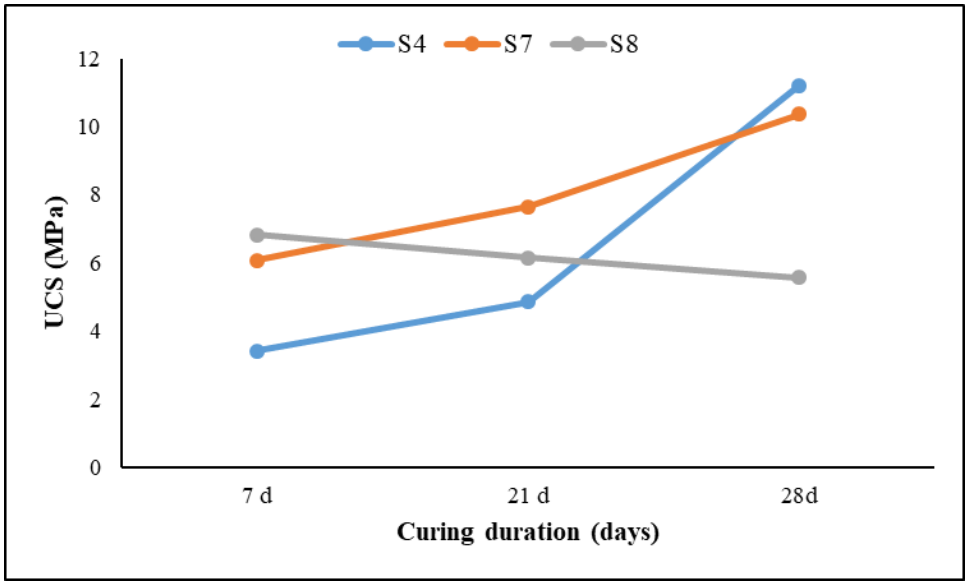

Figure 5.4: Variation of UCS with different curing temperatures at varying curing periods (where; S4 is 80 °C, S7 is 120 °C and S8 is 180 °C).

Results observed indicate that at 80 °C and 120 °C the UCS increased with an increase in curing period. At 28d the UCS produced at S4 and S7 is >10 MPa which meets the SANS requirements. The optimum UCS produced was acquired in S4 with a UCS of 11.2 MPa after 28d. At 7d the best optimum UCS was acquired at 180 °C however, as curing period increases S8 encountered a decrease in UCS. Such an outcome is due to the continuous moisture content loss within the bricks which produced voids and resulted in strength degradation which according to Guo et.al., (2010); Khale and Chaudhary, (2007) and Panagiotopoulou et.al., (2007) is a point of equilibrium within the bricks. Figure 5.5 is an image of a 7d bricks at 180 °C for which bricks showing salts crust formation on the surface of the bricks. The capillary rising of salts within the bricks leads to the disintegration or flaking of the bricks' surface which is caused by the mechanical force exerted by the salts as these crystallize just below the exposed

surface (Kishore, 2014). Based on the results it is concluded that 10M NaOH: $Na_2SiO_3.5H_2O$ (70:30) with L/S ratio of 0.2 at 80 °C is the best optimized alkali activator concentration to use in acquiring an optimum UCS. Several studies have pointed out that 80 °C is the best temperature to produce a geopolymer bricks and as identified within this section it is confirmed because the condition that produced the highest optimum UCS was at 80 °C at 11.2 MPa after 28d.The aforementioned outcome was due to the point of equilibrium at 180 °C being reached after 7d and reactivity of the material to the alkali activator became slow after 21d at 120 °C.

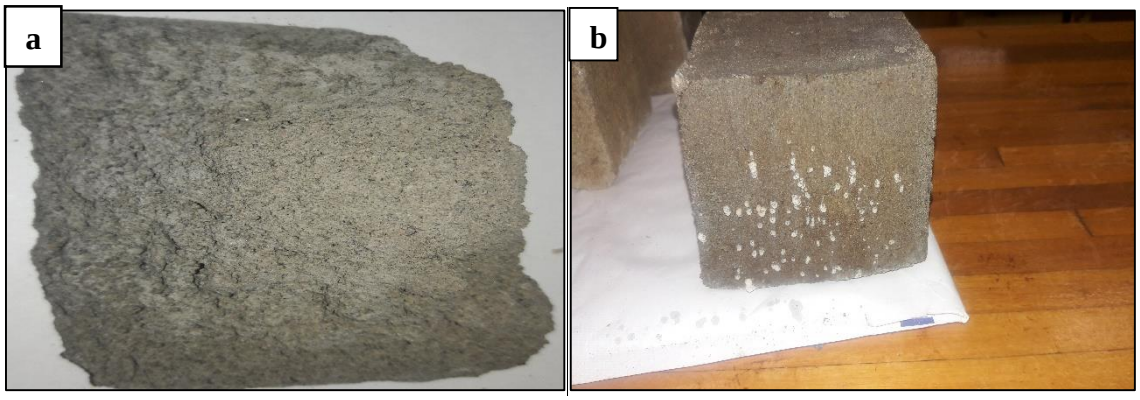

Figure 5. 5: Efflorescence of a geopolymer bricks at 10 M NaOH: $Na_2SiO_3.5H_2O$ (70:30) at 180 °C (a) 7d and (b) 28d.

5.4.5 Effects of admixture on final UCS

The river sand was sieved to particle size ≤2 mm prior to being mixed with the MT. The river sand was then mixed with the MT according to the ratios indicated in Table E1 to attain a homogeneous mixture. Figure 5.6 illustrates the effects of admixtures as compared to geopolymer bricks with MT as the dry constituent at 10M NaOH: $Na_2SiO_3.5H_2O$ at a ratio of 70:30. The analysis were conducted to determine if a greater final optimum UCS and other mechanical properties would be achieved as compared to a single material.

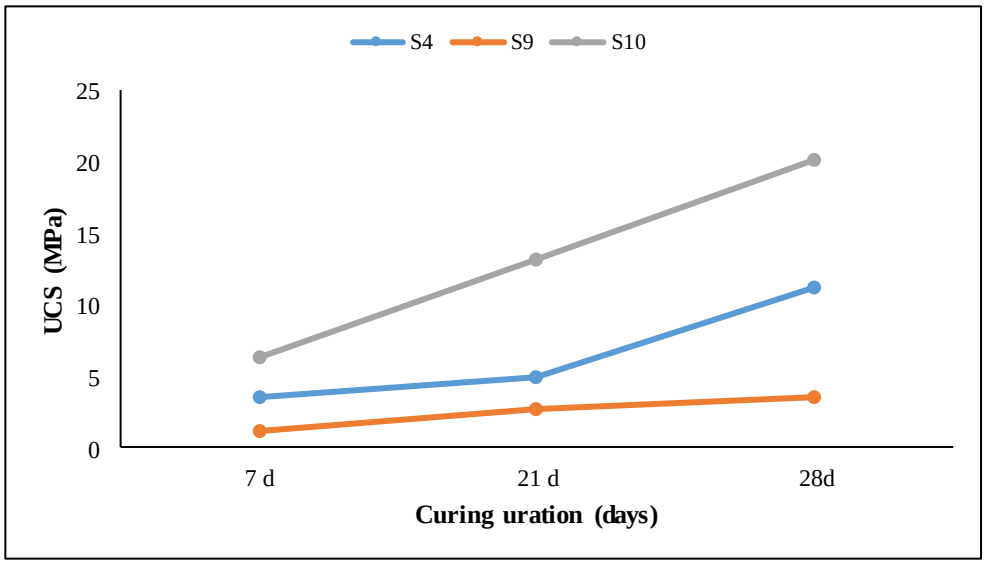

Figure 5. 6: Variation of UCS with different admixtures at varying curing periods (where; S4 is MT, S9 is river sand (10%) and S10 is cement (5%)).

From the results, it is observed that UCS increased with increasing curing period throughout the single and bi-component admixtures. However, the admixture of river sand within the MT produced a low UCS of 1.12 MPa as compared to which has thus far been the lowest at 1.13 MPa. The low UCS may be attributed to the high level of porosity present due to the particle size of the river sand as per discussed in chapter 3. The mixture of MT produced a UCS of 3.41 MPa, 4.85 MPa and 11.2 MPa after 7, 21 and 28 d curing periods, respectively. As discussed in previous parameters the UCS previously mentioned after 28d was of SANS 1215 standards however, the admixture of cement at 5% produced the best optimum final UCS as compared to MT and admixture of river sand (figure 5.7).

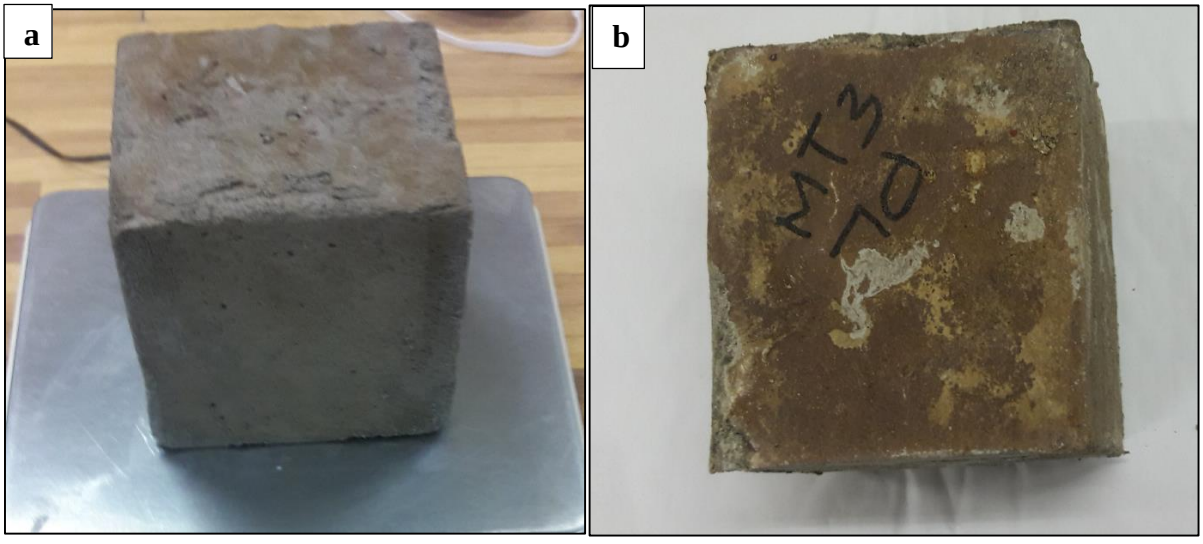

Figure 5. 7: Geopolymer bricks with admixtures; a) river sand and b) cement.

The admixture of cement produced a UCS of 6.26 MPa, 13.19 MPa and 20.16 MPa after 7, 21 and 28 d curing period, respectively. Cement is known to be a binding agent which further stimulates the MT reactivity coupled with the alkali activator thereby, influencing the interlocking of Al-Si compounds. The bricks produced at 21 and 28 d meet the SANS 1215 standards. Based on the results, it is concluded that 10M NaOH: $Na_2SiO_3.5H_2O$ with 5% cement at a ratio of 70:30 with 0.2 L/S at 80 °C is the best optimized alkali activator concentration to use in acquiring an optimum UCS.

5.4.6 Effects of curing regime on final UCS

To evaluate the effect of curing regime on the synthesis of geopolymer material, a geopolymer product was prepared using alkali concentration of 10M NaOH: $Na_2SiO_3.5H_2O$ at a ratio of 70:30 with the L/S ratio of 0.3. The synthesized product was cured in an oven and the greenhouse. The oven temperature was 80 °C and the temperature in the greenhouse ranged from 14 °C to 52 °C. The bricks were cured for 7, 21 and 28 days thereafter, the UCS was determined in order to see which of the bricks has UCS that conform to the SANS 1215 standards. Figure 5.7 compares the UCS of bricks cured in oven and in GH over a period of 7, 21 and 28 days.

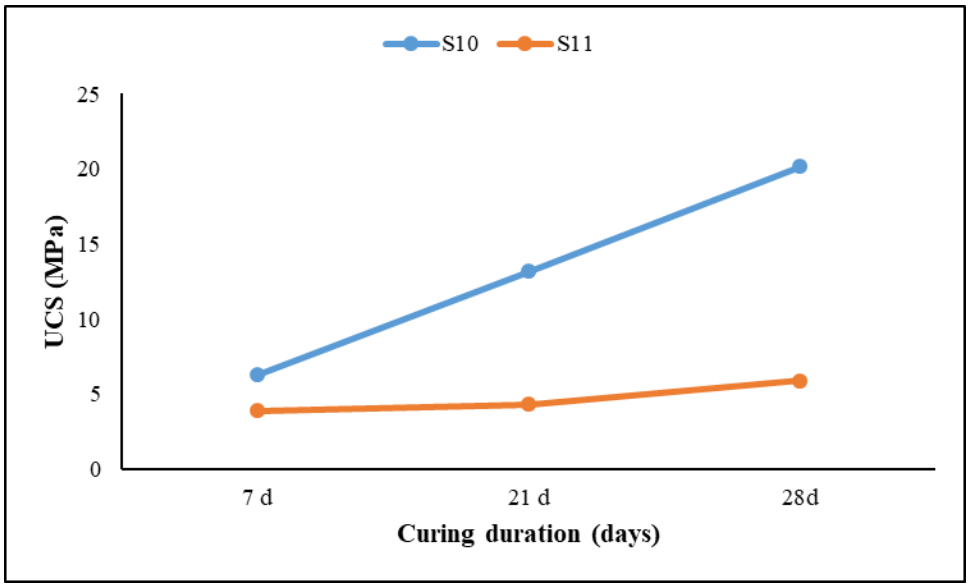

Figure 5. 8: Variation of UCS with different curing regimes at varying curing periods at 10 M NaOH: $Na_2SiO_3.5H_2O$ (70:30) at an L/S ratio of 0.2 (where; S10 is hot air oven and S11 is greenhouse (GH).

From the results, it is observed that the UCS increases as the curing period increases. This was observed in both oven and GH. After 7d both curing regimes produced a low UCS of 3.9 MPa and 6.26 MPa for GH and oven, respectively. However, as curing period increases the hot air

oven cured bricks produced a UCS of 13.19 MPa while the GH bricks only increased by 0.4 MPa from its initial output UCS at 7d. After 28 days of curing, UCS further increased to 20.16 MPa and 5. 9 MPa for hot air oven and GH, respectively. Srinvasan and Sivakumar (2013) indicated that an inconsistency in temperature results in a low UCS which verifies the reason for the low UCS produced by GH. High temperatures cause further reactivity of geopolymer bricks as it acts as a catalyst that helps stimulate the Al-Si breakdown. Furthermore, due to the inconsistency of temperature within the GH it resulted in efflorescence occurring leaching out activator salts after 21d (Fig. 5.8).

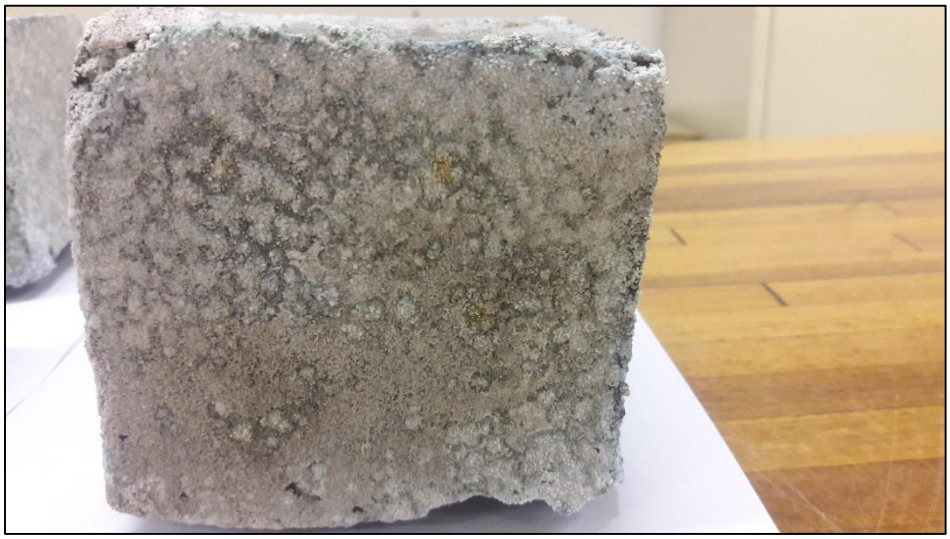

Figure 5. 9: Efflorescence of geopolymer bricks (S11) at 10 M NaOH: NaSi2O3.5H20 with L/S ratio of 0.2 at irregular temperatures after 21d.

5.4.7 Water Absorption

Water absorption test was done in order to determine the ability of the geopolymer bricks to retain water. Table 5.2 presents water absorption test of geopolymer bricks at different parameters.

Table 5. 2: Water absorption of geopolymer bricks at different parameters.

Water Absorption (%)			
Sample name	Curing period		
	7d	21d	28d
S1	Invalid		
S2	Invalid		
S3	Invalid		
S4	Invalid		
S5	Invalid		
S6	Invalid		
S7	11.25	15.68	9.83
S8	25.87	23.01	20.99
S9	Invalid		
S10	0.09	0.05	0.04
S11	0.59	0.24	0.21

Bricks S1, S2, S3, S4, S5, S6 and S9 showed poor water absorption capacity as the bricks could not maintain structural integrity after being immersed in the water for an hour (Fig. 5.8). The bricks S7 and S8 prepared using 10 M NaOH: $Na_2SiO_3.5H_2O$ at a ratio of 70:30 and cured for 120 °C and 180 °C for 7, 21 and 28 days produced an absorption capacity of 11.25, 15.68 and 9.83 % ; and 25.87, 23.01 and 20.99 %, respectively. Higher absorption capacity could be attributed to higher temperatures which increase the polymerization rate thereby reducing porosity within the bricks. From the results in UCS, materials produced at higher temperature yielded lower UCS compared to the one produced at lower temperature, which indicates poor dissolution of Al and Si at higher temperature and hence poor gel formation and poor geopolymerization, resulting in higher porosity and which will yield higher absorption capacity.

The S10 and S11 bricks were produced at 10 M NaOH: $Na_2SiO_3.5H_2O$ at a ratio of 70:30 with an admixture of cement curing in an oven and greenhouse in temperatures mentioned in section 5.4.7. Bricks S10 and S4 produced a water absorption capacity of 0.09, 0.05, 0.04%; and 0.59, 0.24, 0.21 % after 7, 21 and 28d, respectively. Bricks at 28 days showed lower water absorption capacity compared to bricks cured at 7 and 21 days. The bricks did not disintegrate as that in Fig 5.9, the bricks still retained their shape after the tests were conducted and furthermore the bricks were within the ASTM C55 guidelines of 15% water absorption capacity. Lower water

absorption capacity in these bricks could be attributed to the presence of cement that has a higher interlocking of Al-Si material and S7, 8, 10 and 11 resulting in lower porosity.

Figure 5. 10: Water absorption capacity of synthesized geopolymer bricks (5 M NaOH: $Na_2SiO_3.5H_2O$ (80:20) at a L/S ratio of 0.2 after 28d at 80 °C) after 60 minutes of being immersed in cold water

5.4.8 Durability

The abrasion tests were done in order to determine the shear stress the geopolymer bricks can adhere to. Table 5.3 depicts the shear stress of the synthesized geopolymer bricks.

Table 5. 3: Abrasion tests at different parameters.

Abrasion (mg)			
Sample name	**Curing days**		
	7 d	**21d**	**28d**
S1	4.09	2.01	1.76
S2	2.06	1.93	1.48
S3	1.45	0.96	1.24
S4	1.98	0.58	0.25
S5	11.46	9.21	0.55
S6	Invalid		
S7	0.23	0.12	0.08
S8	0.2	0.09	0.21
S9	5.43	3.25	2.48
S10	0.05	0.03	0.01
S11	0.18	0.07	0.06

Low shear stress has a link with the high UCS and low absorption rate as the section will prove. From the results, it is observed that the shear strength decreases as the curing period increases thereby influencing the water absorption. The highest shear stress was identified in S5 after 7d at 11.46 mg. The lowest shear strength was yielded by S7, 8, 10 and 11due to the low UCS furthermore, the bricks inability to withstand being immersed in water for at least an hour verifies the low shear strength present within these bricks. The low shear strength in S10 and S11 indicates that the bricks can endure high stress.

5.5 Conclusion

The chapter focused on evaluating the optimum conditions for synthesizing geopolymer material. The optimum condition evaluated were types of alkali activators, different alkali activator concentration, activator solution to MT ratio (l/s), temperature, types of curing regimes and admixture content. The following conclusions were derived from results attained:

- Overall final UCS that is within the SANS 1215 guidelines is S10 with 10M NaOH:Na_2SiO_3.$5H_{20}O$ at a ratio of 70:30 with an admixture of 5% cement at 80 °C in all curing periods and S7 after 28d which is 10M NaOH:Na_2SiO_3.$5H_{20}O$ at a ratio of 70:30 at 120 °C.
- Oven produced bricks have a higher UCS as compared to GH bricks which may be attributed mainly because of the unstable temperatures that fluctuate within a day. However, both bricks produces a shear strength that is ASTM approved.
- The water absorption test for S1, 2, 3, 4, 5, and 9 disintegrated hours within immersing the bricks however, for S7, 8, 10 and 11 the bricks were stable within their original form after 24 hours and were within the ASTM C55 guidelines.
- The shear stress of the bricks was < 0.3 mg at S 7, 8, 10 and 11 at all curing periods. At S1, 2, 3, 4, 5 and 9 the shear strength was > 0.5 mg with an exceptional high at S5 7d of 11.46 mg.
- Bricks S10 produced an overall UCS after 28d of 20.16 MPa that is 10.16 MPa greater than the guidelines by SANS 1215.
- The UCS of geopolymer bricks didn't instigate any increase in UCS when an increase in temperature, L/S ratio of 0.3 and river sand admixture where introduced as compared to S4 after 28d of curing.

5.6 Recommendations

- Future studies need to focus on curing period of 15 M NaOH: Na_2SiO_3.$5H_{20}O$ at a ratio

of 70:30, needs to be cured for a longer period than 28d to produce a UCS that is approved by the SANS 1215.

- Greenhouse curing method was found not to be suitable for synthesis of geopolymer due to high humidity and unstable temperatures as such the GH needs to be made in a way that it retains the heat it accumulates during the daytime.

Part B: Evaluation of mineralogical and chemical characteristics of geopolymer bricks and chemical species bioavailability.

Abstract

This chapter presents the macroscopic characteristics, chemical and mineralogical composition of geopolymer bricks that were presented in Chapter 5- Part A. This chapter further presents results of the leaching of geopolymer bricks within the water soluble phase using ICP-MS. The XRD analysis showed that geopolymerization leads to formation of secondary minerals such as phlogopite, diopside and actinolite; furthermore, quartz was detected as the dominant mineral although the concentration is lower than that of raw MT. The SEM images indicated needle like structures at 7d within S7 and high amorphous crystalline structures were present at 28d within S10. The EDS analysis indicated high presence of SiO_2 and Al_2O_3 although the concentration is lower than that present within the raw MT. FTIR analysis indicated formation of carbonates. The leaching test results showed that high concentration of Na was leached at 2625 mg/L which is greater than that present within the MT. Such high concentrations was attributed to the alkali activator used in the synthesis process. Si content within the geopolymer bricks was detected at 2301 mg/L compared to raw MT with an average of 15.02 mg/L was very high. The high Si content is due to the breakdown of Al-Si content however, the Si element is resistant to being soluble. Although the encapsulation of metals was identified as curing period increased, Na and Si were detected at a very high concentration due to Na not reacting completely and the disintegrated Si not interlocking with Al to produce an amorphous crystalline structure.

Keywords: *Unconfined Compressive Strength (UCS), alkali activators, alkali activator concentrations, curing regime, curing temperatures and greenhouse.*

5.7 Introduction

Through the process of geopolymerization it is understood that there has been a complete conversion of Al-Si reaction from the solid phase to an amorphous geopolymeric binder in order for the geopolymeric binder composition to be obtained from the composition of reactants and stoichiometry of the geopolymeric reaction (Davidovits 1991 and 1994). The structural and mineralogical analysis gives input into the UCS produced and understanding of the interlocking of aluminia and silica. The pores present within the microstructure of the bricks are dependent on several variables of the mix design such as the type alkali activator and alkali concentration. Studies have identified that an increase in alkali activator concentration produces a less porous microstructure thereby, influencing the final UCS of the bricks (Chareerat et.al., 2006). Through the process of geopolymerization the mineralogical content of the synthesized bricks may have undergone secondary mineralization based on the reaction of the alkali activator to the Al-Si material. XRD analysis further determines the effect of metal cations on gel phase composition. This is an important result because the gel phase composition directly influences the final compressive strength of the geopolymer.

This section presents the mineralogical, chemical bonding and morphological properties of geopolymer bricks. The analysis were done using XRD in order to determine whether the formation of new mineral species had occurred during the process of geopolymerization. FTIR was conducted to indicate the intensity of wavelengths and whether new wavelengths had formed during poly-condensation of synthesized bricks. SEM-EDS was conducted to determine the structure of the geopolymer whether an amorphous crystalline structure had been formed during synthesis. Furthermore, the leaching potential of the chemical species was also evaluated in order to determine whether the synthesized material has encapsulated all the toxic material within the MT. Leaching needs to be conducted to determine the major and minor metals released when the synthesized material has been in contact with a liquid such as H_2O or acid. Furthermore, understanding the chemistry of the bricks when in contact with a liquid will provide insight on whether the material is environmentally friendly or will cause more detrimental impacts into the environment.

5.8 Materials and Methods

5.8.1 Materials

Synthesized geopolymer bricks produced in Chapter 5 Part A were used. The MT attained from Musina mine tailings located in the Vhembe district of South Africa was used as the main dry component in the geopolymer. River sand with particle size < 2 mm and 42.5N cement were used admixtures to produce geopolymer bricks.

5.8.2 Physicochemical and mineralogical characterization

Mineralogical composition of synthesized geopolymer bricks were determined using X-ray Diffraction using a PANalytical Aeris powder diffractometer with an PIXcel detector and fixed divergence and receiving slits with Fe filtered Co-Kα radiation (λ=1.789Å). The surface morphology was determined using a Scanning electron microscopy (SEM) (Leo1450 SEM, voltage is 10Kv, working distance 14 mm). The functional groups and surface chemistry was determined using Fourier transform infrared spectroscopy (FTIR).

5.8.3 Batch leaching

Batch leaching was conducted to determine whether there are toxic metal and metalloids species leaching from the geopolymer bricks which would mainly cause environmental and health problems. Water soluble elements are implacably mobile and bioavailable thus the transfer of metals and metalloids from the geopolymer bricks to water was evaluated using standardized batch leaching test (Hiller et.al., 2013). A 10 g crushed geopolymer bricks was suspended in a 100 mL Milli-Q deionized (S/L ratio of 1:10) water in plastic bottle. Sample suspension was agitated in a shaker for 24 hours at a temperature of 22 ± 3°C, at 200 rpm. Thereafter, samples were centrifuged at 2 500 rpm for 20 minutes and filtered through a 0.45 µm membrane filter.

The clear aqueous extract was acidified to pH<2 by HNO_3 for cation analysis using Inductively Coupled Plasma-Mass Spectroscopy (ICP-MS). The obtained dissolved concentrations of cations and anions where compared to leachable concentration Threshold (LCT0) according to DWAF (SANS) 1998 in mg/L.

5.9 Results and Discussions

5.9.1 X-ray Diffraction of geopolymer bricks

The XRD spectra of geopolymer bricks at different parameters in comparison to raw MT are presented in Figure 5.9 and Appendix E-Figure E2 to E11. The spectra give details on the mineral phases present within the synthesized geopolymer bricks in comparison to the raw MT.

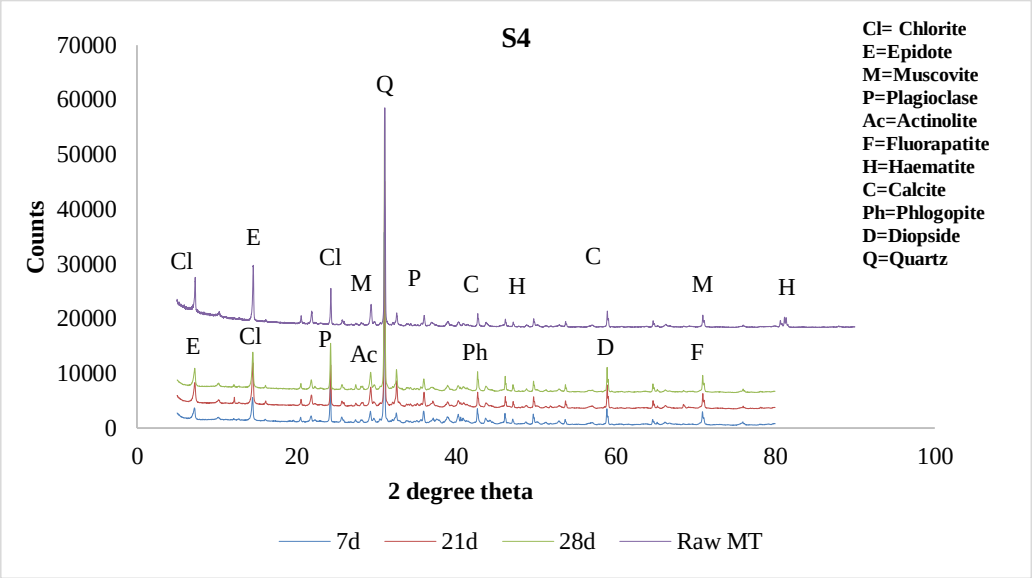

Figure 5. 11: XRD spectra of geopolymer bricks in comparison to raw MT at 10 M NaOH: Na_2SiO_3.$5H_2O$ (70:30) at varying curing periods.

The analysis in Figure 5.9 shows that the raw MT consist of quartz, epidote and chlorite as the major minerals and feldspar group, iron oxides and carbonates as minor minerals. After geopolymerization, new mineral phases were produced through secondary mineralisation namely; phlogopite which is mica mineral (muscovite), fluorapatite is a phosphate mineral (Ca minerals), diopside is a monoclinic pyroxene (Mg-Fe minerals) and actinolite is amphibole silicate. The overall mineralogy of geopolymer bricks throughout the different parameters are the same with a variation in concentration of diopside, fluorapatite, actinolite and phlogopite. The variation in the aforementioned minerals through the different parameters is concluded to be due to the reactivity rate of the raw MT material (Table E3).

5.9.2 Scanning Electron Microscopy-Energy Dispersive X-Ray Spectroscopy (SEM-EDS) analysis of geopolymer bricks

SEM-EDS was conducted to understand the morphology of the geopolymer bricks at different operational parameters. Figure 5.11 and 5.12 depicts the morphology of different geopolymer bricks in comparison to the raw MT.

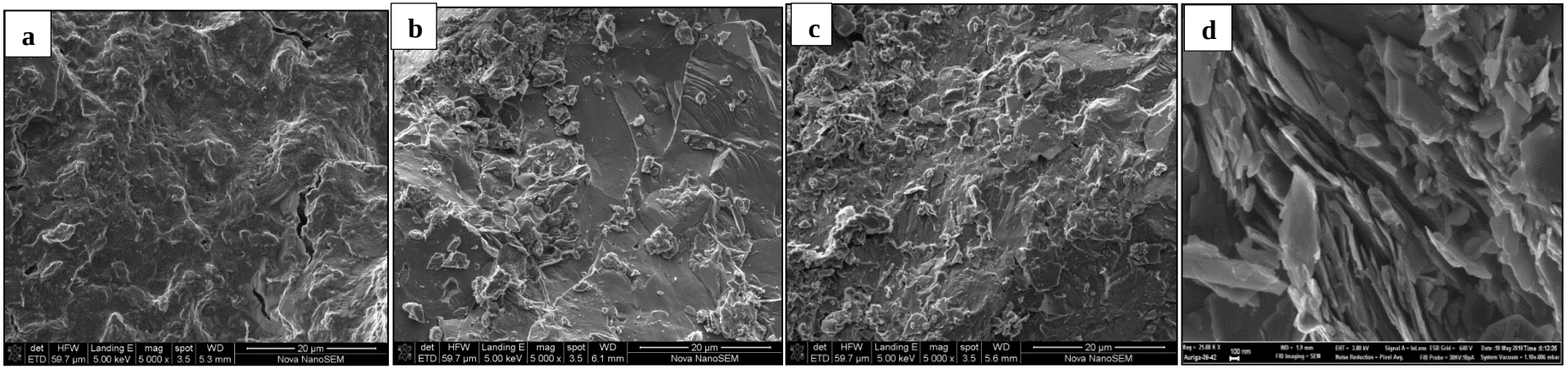

Figure 5. 12: SEM-EDS analysis of geopolymer bricks (S4) synthesised with 10M NaOH: $Na_2SiO_3.5H_2O$ (70:30) with an L/S ratio of 0.2 at 80 °C where; a) 7d, b) 21d, c) 28d and d) Raw MT.

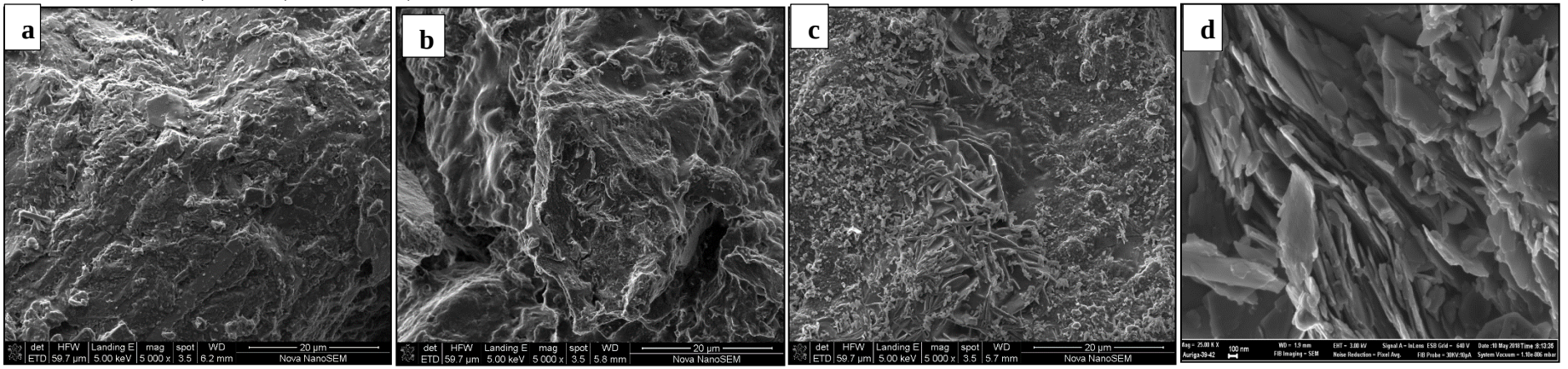

Figure 5. 13: SEM-EDS analysis of geopolymer bricks (S10) with cement admixture (5%) at 10M NaOH: $Na_2SiO_3.5H_2O$(70:30) with an L/S ratio of 0.2 at 80 °C at a ratio of 70:30 where; a) 7d, b) 21d, c) 28d and d) Raw MT.

Fig 5.11 indicates partial reactivity producing geopolymer gels and a 3D-crystalline structures. This results confirms that dissolution of alumina and silica occurred followed by condensation and formation of crystalline structures. However, although the process of dissolution and condensation produced partial reactivity and geopolymer gel the bricks only produced a UCS that meet the SANS 1215 requirements after 28d. Figure E 13 shows needle-like structures confirming the formation of crystalline phases which contribute to the UCS of the formed geopolymers. Figure 5.11a shows gelation present and as curing period increases formation of crystalline needle like structure visible after 28d (Fig. 5.11c). Table 5.4 shows the chemical microanalysis of the geopolymer bricks which were analysed using electron dispersive spectroscopy. The analysis shows the chemical concentration variances between raw MT and the geopolymer bricks at different parameter.

Table 5. 4: Chemical microanalysis of geopolymer bricks.

Samples	Curing days	C	O	Na	Mg	Al	Si	Ca	Fe	K
S4	**7d**	17,85	52,39	10,39	2,35	11,64	1,18	4,2		
	21d	15,57	51,12	4,23	0,8	5,47	13,94	6,54	5,34	
	28d	12,2	48,5	4,16	2,64	21,93	2,83	4,74		
S10	**7d**	20,6	53,3	4,89	0,32	1,91	17,33	0,57	3,69	1,39
	21d	14,65	51,72	4,9	1,24	2,2	20,86	1,04	3,39	
	28d	15,88	52,06	9,15	0,38	0,76	19,03	0,67	2,07	
Raw MT			16,4	1,9	2,3	12,0	26,9	4,4	13,3	1,7

The Fe present within the geopolymer bricks was present after 21d in S4 and decreased throughout all curing periods within S10. Fe decreased within the geopolymer bricks due to secondary mineralization. Si content decreases within the geopolymer bricks but is still the highest concentration (Table 5.4) as indicated in XRD results. Such a decrease within the element is due to the dissolution of the element to produce the geopolymer. Table E5 indicates that a high concentration of Fe was identified within S1 which is due to low reactivity of the material. From SEM-EDS images we can see that the materials are not individual particles; as an act of gelation is identified where the material is linked together through interlocking of Al-Si gels. Thereby, the images confirm that the formation of polymers (macromolecule) has taken place.

5.9.3 FTIR analysis of geopolymer bricks

FTIR spectroscopy analyses were conducted to identify the functional groups in the geopolymer bricks. The analysis revealed that both bricks have similar characteristics. Figure 5.21 shows the FTIR spectra of S4 bricks in comparison with the raw MT. Spectrums of other bricks were presented in appendices Figure E10 to E18.

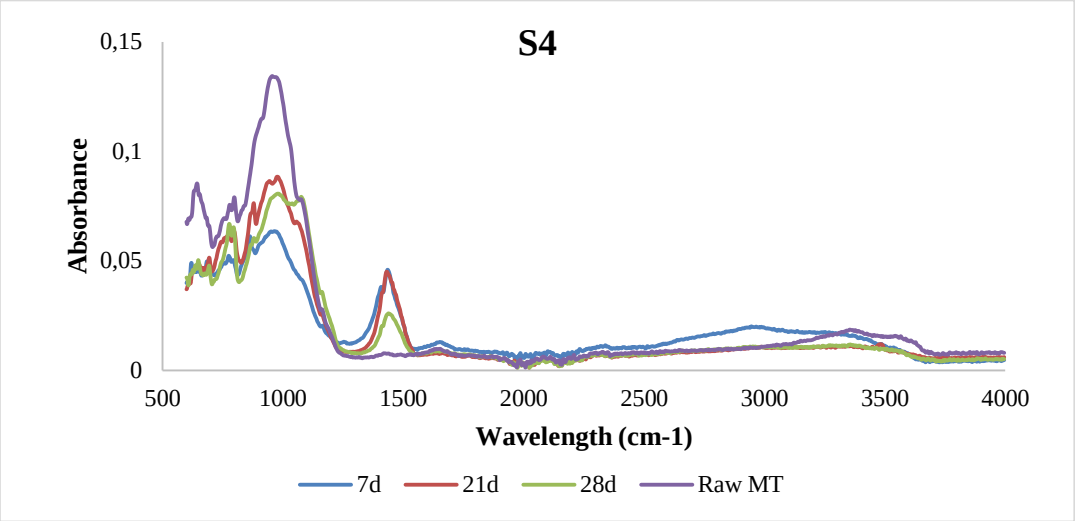

Figure 5. 14: FTIR spectroscopy of 10M NaOH: $Na_2SiO_3.5H_2O$ (70:30) with an L/S ratio of 0.2 at 80 °C at varying curing periods.

Figure 5.12 shows major absorption bands are observed at the wavelength region of 1000 cm^{-1}, 944.53 cm^{-1} and 850 cm^{-1}. These bands are attributed to the vibration of, Si–O–Si, Si-O-Al, Al-O, Al-OH, respectively. This results confirms that the material is aluminosilicate material. These results corresponds well with XRD analysis which showed the dominance of quartz and epidote. After geopolymerization, a new peak is identified at wavelength region around 1473.95 cm^{-1} which correspond to carbonates functional groups which formed through the carbonation of Ca^{2+} from raw MT. This results correspond to XRD analysis that confirmed the formation of secondary minerals.

5.9.4 Batch leaching of geopolymer bricks

Leaching tests were conducted to determine the bioavailability of the chemical species of both anions and anions within the geopolymer bricks. The analysis were conducted on both bricks that yielded highest UCS. Table 5.4 presents concentrations of chemical species leached from the geopolymer bricks. S4 and S10 leached high levels of Na (2260.83 mg/L) with a low average concentration of 0.58 mg/L P as the major species. Within the minor metal species S4 and S10 has Cd as a high concentration at an average of 129.66 µg/L and an average of 0.20 µg/L Cd being the lowest concentration. S10 and S4 major metals don't meet LCT0 according

to DWAF (1998) guidelines except for Mg and Ca that have an average concentration of 10.88 mg/L and 11.13 mg/L. Comparison of geopolymer bricks to MT in Chapter 3 indicates that there is a higher concentration of bioavailable metals within the synthesized material as compared to the raw MT. Assumptions can be made that it's due to the dissolution of Al-Si material that makes the elements easily soluble.

The high Na concentration as compared to that of raw MT is due to the alkali activator used as the activator. Si content is also present in high concentration in S10 and S4 with an average of 1008.33 mg/L which is much higher than the average concentration of 4.73 mg/L of raw MT. Furthermore, a trend was identified that as the curing period increased in S10 and S4 the leached metals concentration decreased. The trend confirms that the process of geopolymerization encapsulates the metals present within the MT.

Table 5. 5: Major and trace metals of mobile/ bioavailable geopolymer bricks.

Major metals (mg/L)	Curing period	Al	Cu	Fe	Ca	K	Mg	Na	P	Si
WHO water quality guidelines (2013)		≤0.1	≤2	≤1-3	≤150		≤70	≤200		
S4	7d	5,26	7,09	27,4	2,6	11,2	1,1	2310	0,6	1225
	21d	1,68	3,71	7,9	4,0	4,8	1,4	1889	0,6	523
	28d	4,03	2,41	11,9	4,3	8,8	2,5	2452	1,0	1019
S10	7d	4,76	0,05	0,1	8,2	28,6	0,2	2419	0,3	223
	21d	3,10	6,61	11,5	6,6	6,2	2,1	2294	0,5	1643
	28d	3,11	4,42	8,0	3,5	5,7	2,0	2201	0,5	1417

Trace metals (µg/L)	Curing period	B	V	Cr	Mn	Co	Ni	Zn	As	Se	Sr	Mo	Cd	Sb	Ba	Hg	Pb
S4	**7d**	18,02	167,93	291,73	148,14	2,21	3,14	15,05	13,60	15,00	11,56	96,35	0,19	2,44	91,14	1,66	17,85
	21d	19,00	119,12	179,43	80,69	1,77	6,30	23,26	14,13	16,75	13,54	80,92	0,23	2,05	15,33	0,54	6,64
	28d	33,83	240,44	152,35	119,31	6,30	7,65	53,35	15,43	16,47	16,42	74,29	0,24	442,48	30,06	3,38	6,39
S10	**7d**	57,44	118,53	68,18	1,89	0,06	0,63	5,44	10,22	9,21	21,28	30,28	0,02	1,19	2,94	3,48	0,32
	21d	22,25	73,08	46,83	234,99	5,58	15,67	18,00	12,30	15,28	13,22	58,22	0,36	2,13	22,08	0,43	12,86
	28d	22,19	58,96	38,67	103,65	3,82	11,79	17,09	7,54	9,80	7,32	42,47	0,17	2,21	11,46	0,46	5,84

5.10 Financial implication of geopolymer bricks

Geopolymer bricks are environmentally efficient in terms of reduction of waste material, water consumption, energy efficiency and CO_2 emission (kilning process). The process however has its own disadvantages such as the costs of alkali solution which are expensive mainly the sodium metasilicate. Thereby, the economic viability of the research outcome needs to be considered for the socio-economic beneficiation. Cost comparisons of the geopolymer bricks with traditional concrete bricks is essential thereby, the following factors need to be considered for the geopolymer bricks: Copper tailings that is available in abundance and are expected to be free of cost. Portland cement that is currently at =R84.95 per 50 kg bag (PPC cement, 2019). Sodium Hydroxide is R 79.00 per 500g and Sodium metasilicate is R 2028.00 per 3L. To produce 1 geopolymer bricks it requires R 45.21, although the production costs may be high, reductions in the costs will occur when purchasing the alkali activators on a commercial scale. Using a base figure for commercial brickmaking, the masonry cement recipe can be estimated as follows: 40 bags of cement produces 3330 concrete bricks, or 1 bag of cement produces 77 bricks with water addition being 20 litres per 50 kg of cement. The price of water for industrial companies according to the Thulamela Mayoral Committee is R20.96 per kilolitre (COT: Mayoral Committee, 2018). Thereby, for production of 3330 concrete bricks you need R 4 900.00, or 1 brick is R 1.89 (Nyambeni N.L). The production of bricks from MT is an available technology however, it requires production in a large scale and acquiring the alkali solutions in bulks in order for the opportunity to make business sense in terms of the financial implications of producing the brick and making a profit similar or greater than that of a traditional brick.

5.11 Conclusions

This chapter focused on the chemical characterization, mineralogical and water soluble phase of the geopolymer brick. The following conclusions were derived from the analysis in this chapter:

- The XRD analysis detected secondary mineralization of the geopolymer bricks where actinolite, phlogopite, diopside and fluorapatite were formed from primary minerals.
- Based on EDS analysis it is indicated that SiO2 and Al2O3 are present in high quantities but lower than that present within raw MT due to partial or complete mineralisation.

- SEM analysis indicated that S10 at 28d produced semi-amorphous crystalline structure with new interlocking shapes present within the bricks.
- A new wavelength band is detected through FTIR analysis which is due to formation of carbonates.
- Na leached out the highest concentration within the bricks and in comparison with raw MT. The high concentration is due to the alkali activator that is used for geopolymerization.
- Si element is high as compared to raw MT element due to the disintegration of the material during polymerization.

References

ASTM D570-98(2018), Standard Test Method for Water Absorption of Plastics, ASTM International, West Conshohocken, PA, 2018, www.astm.org.

Bakharev, T., 2005. Geopolymeric materials prepared using class F fly ash and elevated curing temperature. Cement and Concrete Research. Vol.35 (6), pp.1224-1232.

Cheng, T. W., and Chiu, J. P., 2003. Fire resistant geopolymer produced by granulated blast furnace slag. Journal of Mineral Engineering, Vol.16 (3), pp.205-210.

Chindaprasirt, P., Chareerat,T., and Sirivivatnanon,V., 2007. Workability and strength of coarse high calcium fly ash geopolymer. Cement and Concrete Composites, Vol.29 (3), pp. 224-229.

Davidovits, J., 1982. Mineral polymers and methods of making them. US Patent 4349386.14.09.82.

Davidovits, J., Davidovits, M., and Davidovits, N., 1988. Alkaline alumina-silicate geopolymeric matrix for composite materials with fiber reinforcement and method for obtaining same. U.S patent, 5798307.

Davidovits, J., 1994a. Geopolymers: man-made rock geosynthesis and the resulting development of very early high strength cement. Journal of Materials and Education. Vol. 16 (2 and3), pp. 91–137.

Davidovits, J., Davidovits, M., and Davidovits, N., 1994b. Process for obtaining a geopolymeric alumino-silicate and products thus obtained. US Patent, 5342595.

Duxson, P., Provis, J. L., Lukey, G. C., Mallicoat, S. W., Kriven, W. M., and Van Deventer, J. S. J., (2005). Understanding the relationship between geopolymer composition, microstructure and mechanical properties. Colloids and Surfaces A, 269(1–3), pp. 47–58.

Fernández-Jiménez, A., Palomo, A., and Alonso, M. M., (2005). Alkali activation of fly ashes: mechanisms of reaction Non-Traditional. Cement and Concrete Brno, Czech Republic Ed. V. Bilek and Z. Kersner, Brno University of technology, 1-12.

Kong, D.L.Y., Sanjayan, J.G., and Sagoe-Crentsil, K., 2007. Comparative Performance of Geopolymers Made with Metakaolin and Fly Ash After Exposure to Elevated Temperatures. Cement and Concrete Research, Vol.37, pp. 1583 - 1589.

Lee, W.K.W., and Van Deventer, J.S.J., 2003. Use of infrared spectroscopy to geopolymerization of heterogeneous amorphous aluminosilicates. Langmuir, Vol. 19, pp. 8726-8734. Doi: 10.1021/la026127e.

Malatse, M and Ndlovu, S., 2015. The viability of using the Witwatersrand gold mine tailings for brickmaking. The Journal of The Southern African Institute of Mining and Metallurgy, 115, pp.321-327.

Nyambeni, N.L., Rolling stones super sands. 064 823 6773.

Phair, J.W and Van Deventer, J.S.J., 200. Effects of silicate activator pH on leaching and material characteristics of waste-based inorganic polymers. Minerals Engineering, Vol.14 (3), pp.289-304

Provis, J. and Bernal, S.A., 2014. Geopolymers and related alkali-activated materials. Annual review of materials research. Vol.44. doi: 10.1146/annurev-matsci-070813-113515.

Rahier, H, Van Mele, B, Biesemans, M, Wastiels, J, and Wu, X., 1996. Low temperature synthesized aluminosilicates glasses.1. Low temperature reaction stoichiometry and structure of a model compound. Journal of Materials Sciences, Vol. 31, pp. 71-79.

SANS 1215, 1984, Concrete Masonry Units, South African Bureau of Standards.

Xu, H., and Van Deventer, J.S.J., 2002a. Geopolymerization of multiple minerals. Minerals Engineering, 15, pp.1131-1139.

Yip, C.K., and Van Deventer, J.S.J. Effect of granulated blast furnace slag on geopolymerization. In: CD-ROM Proceedings of 6th World Congress of Chemical Engineering, Melbourne, Australia, and 23–27 September 2001.

Appendix E

Table E 1: Mix design for producing a geopolymer bricks.

Mixture Name	Cu^{+} tailings (g)	Cement (C) / River Sand (RS)	Concentrations						Temp. (˚C)	Ratio	Curing time (days)	Curing Regime
			5 M		10 M		15 M					
			Na_2SiO_3.5H_{20} (mL)	NaOH (mL)	Na_2SiO_3.5 H_{20} (mL)	NaOH (mL)	Na_2SiO_3.5 H_{20} (mL)	NaOH (mL)				
S1	1 200		-	240					80	0.2	7, 21 and 28	Oven
S2	1 200		72	168					80	0.2	7, 21 and 28	Oven
S3	1 200		48	192					80	0.2	7, 21 and 28	Oven
S4	1 200				72	168			80	0.2	7, 21 and 28	Oven
S5	1 200						72	168	80	0.2	7, 21 and 28	Oven
S6	1 200				114	266			80	0.3	7, 21 and 28	Oven
S7	1 200				72	168			140	0.2	7, 21 and 28	Oven
S8	1 200				72	168			180	0.2	7, 21 and 28	Oven
S9	1 020	10%RS			72	168			80	0.2	7, 21 and 28	Oven
S10	1 140	5% C			72	168			80	0.2	7, 21 and 28	Oven
S11	1 140	5% C			72	168			80	0.2	7, 21 and 28	GH

Table E 2: Mechanical results attained at different parameters.

Sample name	UCS (MPa)		
	7 d	**21 d**	**28d**
S1	1,13	2,97	3,87
S2	2,88	3,78	5,51
S3	3,12	3,48	5,21
S4	3,41	4,85	11,2
S5	0,98	2,68	6,26
S6	Invalid		
S7	6,07	7,65	10,36
S8	6,83	6,15	5,56
S9	1,12	2,55	3,41
S10	6,26	13,19	20,16
S11	3,9	4,3	5,9

Table E 3: XRD qualitative results of copper MT and geopolymer bricks.

Minerals	S1 (%)			S2 (%)			S3 (%)			S4 (%)			S5(%)			S6 (%)		
	7d	21d	28d	7d	21d	28d	7d	21d	28d	7d	21d	28d	7d	21d	28d	7d	21d	28d
Actinolite	3.22	3.04	3.18	1.63	4.32	4.09	2.59	2.64	2.69	2.88	3.67	2.54		3.88	2.37	2.86	2.27	1.35
Chlorite	19.9	20.08	21.03	26.03	21.87	20.53	20.12	21.01	21.41	22.36	18.06	16.65	22.94	20.13	23.69	20.07	23.51	20.13
Diopside	2.38	2.42	2.44	2.95	4.02	3.49	2.44	2.53	2.58	2.86	2.75	2.41		2.79	4.47	2.78	2.94	3.15
Epidote	13.16	14.25	14.84	14.62	13.28	15.78	7.76	7.05	7.58	17.4	18.67	17.14	18.9	17.99	18.43	17.28	14.89	14.93
Fluorapatite	1.28	1.40	1.49	0.67	0.71	0.78	1.04	1.22	1.61	5.9	0.77	0.56	3.66	0.49	0.56	0.99	0.33	0.73
Phlogopite	3.46	2.01	3.51	3.81	3.88	3.89	10.95	11.15	11.68	0.93	2.47	1.4	0.43	3.95	2.39	8.75	4.65	2.96
Plagioclase	14.88	15.03	10.92	5.56	6.28	6.42	11.97	12.01	9.54	7.32	12.78	10.58	10.02	2.09	4.89	5.44	6.91	10.75
Quartz	41.72	41.77	42.59	44.73	45.64	45.02	43.13	42.39	42.91	40.35	40.83	48.72	44.05	48.68	43.2	41.83	44.5	46
	S7 (%)			S8 (%)			Ss9 (%)			S10(%)			S11(%)					
	7d	21d	28d	7d	21d	28d	7d	21d	28d	7d	21d	28d	7d	21d	28d			
Actinolite	0.77	1.24	1.35	1.3	1.8	2.37	2.23	1.8	1.53	2.02	2.68	2.31	3.04	3.67	4.09			
Chlorite	14.05	20.4	20.13	21.7	19.91	23.69	21.2	21.52	21.88	23.19	19.81	18.21	20.08	18.06	20.53			
Diopside	2.38	2.63	3.15	3.37	4.82	4.47	9.18	5.57	2.88	5.55	2.94	2.96	2.42	2.75	3.49			
Epidote	9.58	17.07	14.93	7	15.42	18.43	10.4	12.35	18.17	12.99	15.61	14.03	14.25	18.67	15.78			
Fluorapatite	0.35	0.36	0.73	1.11	7.59	0.56	7.66	8.24	0.48	4.31	0.87	0.58	1.40	0.77	0.78			
Phlogopite	3.17	4.5	2.96	7.73	4.2	2.39	3.16	4.24	3.75	2.33	2.32	6.17	2.01	2.47	3.89			
Plagioclase	35	7.35	10.75	9.76	5.06	4.89	6.69	3.73	4.29	9.29	10.14	10.47	15.03	12.78	6.42			
Quartz	34.7	46.45	46	48.02	41.2	43.2	39.5	42.55	47.02	40.38	45.63	45.27	41.77	40.83	45.02			

Table E 4: Chemical microanalysis of geopolymer bricks

Samples	Curing days	C	O	Na	Mg	Al	Si	Ca	Fe	K
S1	**7d**	17,58	45,94	1,32	1,65	4,84	15,53	4,77	8,35	
	21d	28,21	47,32	5,4	0,66	2,74	15,87	4,03	0,97	
	28d	16,4	48,01	8,29	2,46	18	1,58	5,26	0,18	
S2	**7d**	25,21	49,42	3,5	0,56	2,01	14,34	2,19	2,77	
	21d	18,03	52,59	5,1	0,56	2,38	18,2	1,13	2,03	
	28d	10,07	52,76	3,48	0,22	7,35	13,63	11,64	0,85	
S3	**7d**	17,64	51,19	6,38	1,68	2,92	13,01	2,02	5,18	
	21d	19,15	47,79	8,29	0,66	2,74	13,52	4,77		
	28d	28,21	51,5	12,54	0,87	2,04	9,76	0,21	2,27	
S5	**7d**	14,94	50,99	8,83	0,72	2,97	16,43	2,19	2,93	
	21d	11,35	52,69	4,1	0,87	10,25	14,01	6,3		
	28d	18,46	49,88	4,71	1,49	2,69	16,69	1,22	4,86	
S7	**7d**	20,19	50,49	3,86	1,47	3,89	13,52	2,22	4,35	
	21d	19,15	47,79	2,1	2,16	4,15	12,29	3,27	1,65	7,44
	28d	17,84	50,94	9,67	0,81	1,87	14,84	0,21	1,08	2,73
S8	**7d**	21,96	49,12	7,33	1,06	3,52	10,39	0,6	2,27	3,75
	21d	16,31	50,86	12,54	0,31	1,94	13,44	0,32	2,54	1,73
	28d	13,22	48,66	8,36	0,45	2,04	11,68	1,02	3,41	2,58
S9	**7d**	14,43	46,5	11,51	13,2	4,61	9,76			
	21d	21,54	47,02	3,33	2,95	15,63	5,82	3,71		
	28d	13,11	53,99	2,52	1,63	25,89	2,87			
S11	**7d**	15,11	48,95	8,03	0,93	3,52	13,61	3,41	6,45	
	21d	19,06	49,53	4,52	0,95	2,99	15,02	2,43	5,5	
	28d	10,07	52,76	3,48	0,22	7,35	13,63	11,64	0,85	

Table E 5: Major and trace metals of mobile/ bioavailable geopolymer bricks

Major metals (mg/L)	Curing period	Al	Cu	Fe	Ca	K	Mg	Na	P	Si
WHO water quality guidelines (2013)		≤0.1	≤2	≤1-3	≤150		≤70	≤200		
S1	7d	9,60	4,09	15,7	12,6	6,7	2,9	1278	0,7	387
	21d	0,76	0,85	1,5	3,2	3,9	0,6	1479	0,7	247
	28d	10,47	13,70	24,0	8,6	7,8	4,0	3019	0,7	1122
S2	7d	0,66	0,55	1,3	4,0	4,0	0,6	1357	0,6	223
	21d	1,68	3,71	7,9	4,0	4,8	1,4	1889	0,6	523
	28d	2,12	2,16	6,7	4,4	2,9	1,5	1398	0,5	417
S3	7d	10,48	4,67	23,3	8,4	6,5	4,2	2240	0,6	1009
	21d	6,81	11,32	17,6	33,0	9,1	2,2	2138	0,9	2227
	28d	0,06	0,66	0,1	32,9	6,9	1,4	1925	0,5	63
S5	7d	7,68	4,98	23,3	10,8	10,5	4,3	2593	1,2	1160
	21d	8,75	3,28	16,7	6,7	6,7	3,4	2001	0,5	772
	28d	6,03	15,38	20,4	22,5	10,1	2,9	2625	0,9	2301
S7	7d	12,96	8,27	43,1	13,0	13,9	4,2	2847	1,2	1285
	21d	2,09	1,69	4,6	2,7	2,8	1,2	1274	0,4	381
	28d	6,23	1,87	11,5	4,0	10,5	2,2	2798	1,2	1104
S8	7d	1,65	2,07	5,3	3,4	3,1	1,6	1442	0,4	530
	21d	6,37	0,07	0,1	10,6	29,8	0,1	2497	0,4	266
	28d	4,03	2,41	11,9	4,3	8,8	2,5	2452	1,0	1019
S9	7d	8,12	0,05	0,1	8,9	28,7	0,2	2426	0,3	266
	21d	5,35	0,11	0,2	9,0	25,9	0,6	2125	0,5	237
	28d	10,47	13,70	24,0	8,6	7,8	4,0	3019	0,7	1122
S11	7d	0,76	0,85	1,5	3,2	3,9	0,6	1479	0,7	247
	21d	6,81	11,32	17,6	33,0	9,1	2,2	2138	0,9	2227
	28d	2,12	2,16	6,7	4,4	2,9	1,5	1398	0,5	417

Trace metals (µg/L)	Curing period	B	V	Cr	Mn	Co	Ni	Zn	As	Se	Sr	Mo	Cd	Sb	Ba	Hg	Pb
S1	**7d**	20,11	174,64	303,94	190,39	5,75	13,69	12,62	16,44	17,83	36,83	95,61	0,19	1,73	65,75	0,48	12,98
	21d	7,97	120,03	129,90	19,51	0,50	2,57	6,10	18,15	24,36	11,24	110,09	0,03	1,61	7,60	2,34	2,12
	28d	43,98	146,37	214,71	255,42	6,11	19,68	24,69	19,79	24,16	23,13	96,82	0,32	2,48	50,78	2,60	23,88
S2	**7d**	3,18	110,50	128,23	10,65	0,32	2,25	3,91	14,08	16,42	10,86	86,01	0,03	1,22	6,91	69,91	1,38
	21d	19,00	119,12	179,43	80,69	1,77	6,30	23,26	14,13	16,75	13,54	80,92	0,23	2,05	15,33	0,54	6,64
	28d	4,89	76,43	30,66	76,98	2,20	6,46	20,04	7,80	10,08	9,47	40,11	0,19	1,13	12,12	56,56	5,58
S3	**7d**	22,53	166,08	99,82	216,41	8,18	13,25	33,80	11,84	11,85	26,20	60,29	0,44	2,28	75,19	9,49	18,40
	21d	25,54	61,93	35,61	276,86	3,22	19,50	22,34	12,48	13,79	38,37	61,73	0,48	2,19	29,68	1,66	17,05
	28d	23,07	11,12	2,34	81,67	0,98	8,96	0,50	12,19	14,81	39,18	65,77	0,07	0,93	32,91	0,20	0,22
S5	**7d**	37,16	256,47	177,52	223,18	9,79	11,98	34,47	16,71	15,90	24,86	81,84	0,38	3,81	59,94	0,78	16,55
	21d	16,18	171,79	104,10	198,85	8,23	12,12	30,54	8,19	7,66	24,61	50,97	0,31	2,45	66,18	1,47	9,24
	28d	48,83	74,40	68,83	428,85	5,88	29,60	34,40	14,26	17,46	42,74	72,82	0,93	2,38	51,43	1,16	26,05
S7	**7d**	10,70	193,85	214,12	281,27	9,23	10,14	52,30	15,79	10,08	38,87	101,86	0,61	3,28	158,57	30,90	20,49
	21d	1,56	89,62	33,71	53,17	1,87	5,43	19,55	7,29	9,15	7,58	36,40	0,16	0,89	10,01	0,47	4,77
	28d	41,42	273,23	132,87	113,18	5,99	8,60	45,05	15,52	16,89	16,00	67,30	0,19	83,42	33,38	0,54	7,99
S8	**7d**	11,96	107,51	38,96	73,39	2,56	6,07	18,46	10,80	12,02	12,63	50,35	0,14	1,46	17,08	0,06	4,65
	21d	77,97	119,91	84,91	4,57	1,31	1,85	6,18	9,17	5,92	18,46	21,58	0,83	0,44	2,27	2,52	0,92
	28d	33,83	240,44	152,35	119,31	6,30	7,65	53,35	15,43	16,47	16,42	74,29	0,24	442,48	30,06	3,38	6,39
S9	**7d**	81,10	116,11	76,50	4,57	0,06	0,56	3,49	8,67	7,32	20,27	18,93	0,01	0,40	2,75	0,45	0,33
	21d	74,90	112,15	67,23	4,76	0,58	0,60	7,60	7,77	5,99	22,31	16,86	0,02	0,42	5,12	2,26	0,50
	28d	43,98	146,37	214,71	255,42	6,11	19,68	24,69	19,79	24,16	23,13	96,82	0,32	2,48	50,78	2,60	23,88
S5	**7d**	37,16	256,47	177,52	223,18	9,79	11,98	34,47	16,71	15,90	24,86	81,84	0,38	3,81	59,94	0,78	16,55
	21d	16,18	171,79	104,10	198,85	8,23	12,12	30,54	8,19	7,66	24,61	50,97	0,31	2,45	66,18	1,47	9,24
	28d	48,83	74,40	68,83	428,85	5,88	29,60	34,40	14,26	17,46	42,74	72,82	0,93	2,38	51,43	1,16	26,05
S7	**7d**	10,70	193,85	214,12	281,27	9,23	10,14	52,30	15,79	10,08	38,87	101,86	0,61	3,28	158,57	30,90	20,49
	21d	1,56	89,62	33,71	53,17	1,87	5,43	19,55	7,29	9,15	7,58	36,40	0,16	0,89	10,01	0,47	4,77
	28d	41,42	273,23	132,87	113,18	5,99	8,60	45,05	15,52	16,89	16,00	67,30	0,19	83,42	33,38	0,54	7,99
S8	**7d**	11,96	107,51	38,96	73,39	2,56	6,07	18,46	10,80	12,02	12,63	50,35	0,14	1,46	17,08	0,06	4,65
	21d	77,97	119,91	84,91	4,57	1,31	1,85	6,18	9,17	5,92	18,46	21,58	0,83	0,44	2,27	2,52	0,92
	28d	33,83	240,44	152,35	119,31	6,30	7,65	53,35	15,43	16,47	16,42	74,29	0,24	442,48	30,06	3,38	6,39
S9	**7d**	81,10	116,11	76,50	4,57	0,06	0,56	3,49	8,67	7,32	20,27	18,93	0,01	0,40	2,75	0,45	0,33
	21d	74,90	112,15	67,23	4,76	0,58	0,60	7,60	7,77	5,99	22,31	16,86	0,02	0,42	5,12	2,26	0,50
	28d	43,98	146,37	214,71	255,42	6,11	19,68	24,69	19,79	24,16	23,13	96,82	0,32	2,48	50,78	2,60	23,88

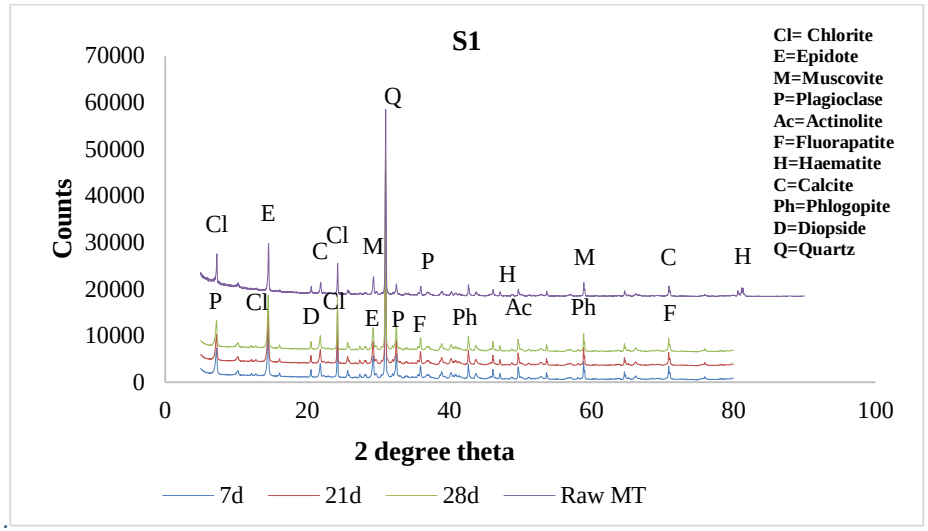

Figure E 1: XRD spectra of geopolymer bricks with 5 M NaOH at varying curing periods.

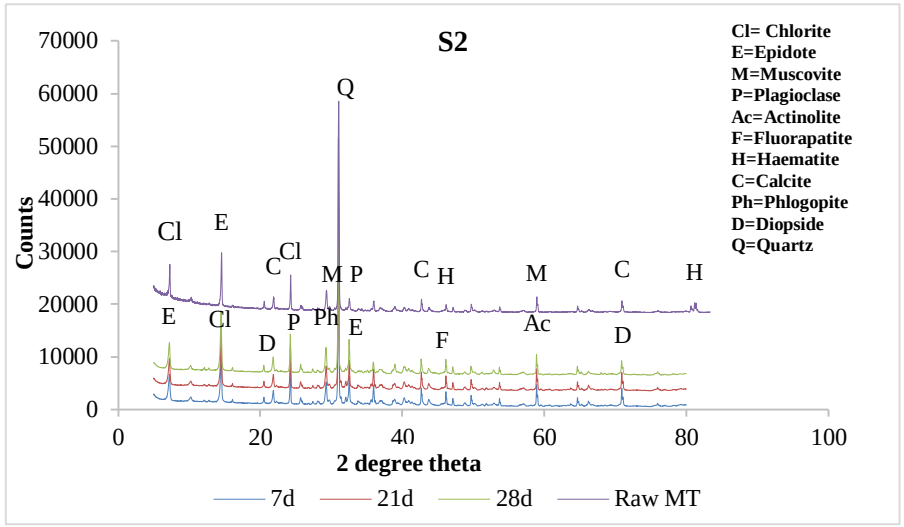

Figure E 2: XRD spectra of geopolymer bricks with 5 M NaOH: $Na_2SiO_3.5H_2O$ (70:30) at varying curing periods

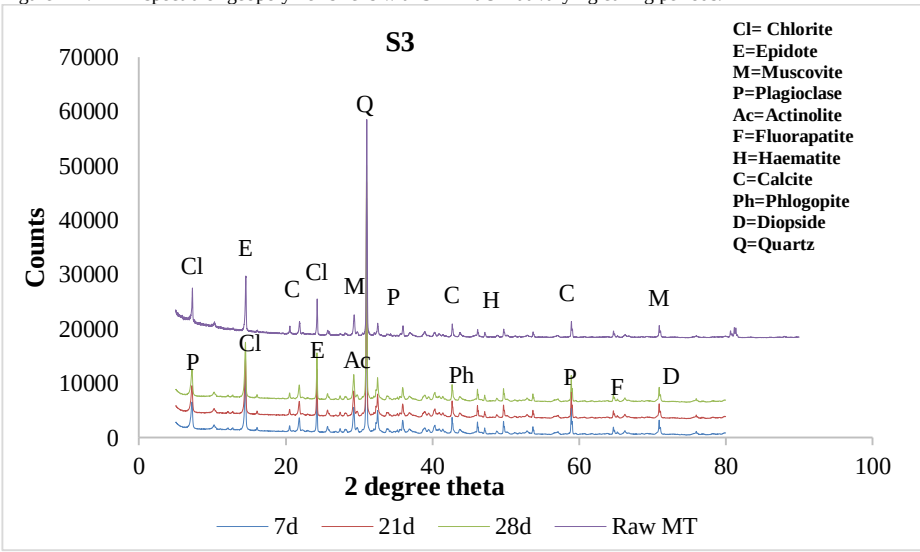

Figure E: XRD spectra of geopolymer bricks with 5 M NaOH: $Na_2SiO_3.5H_2O$ (80:20) at varying curing periods.

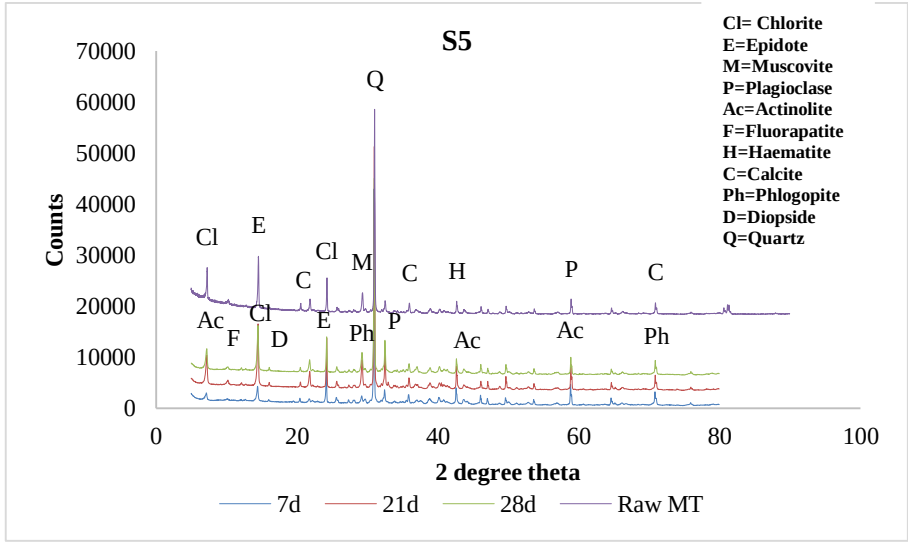

Figure E 3: XRD spectra of geopolymer bricks with 15 M NaOH: $Na_2SiO_3.5H_2O$ (70:30) at varying curing periods

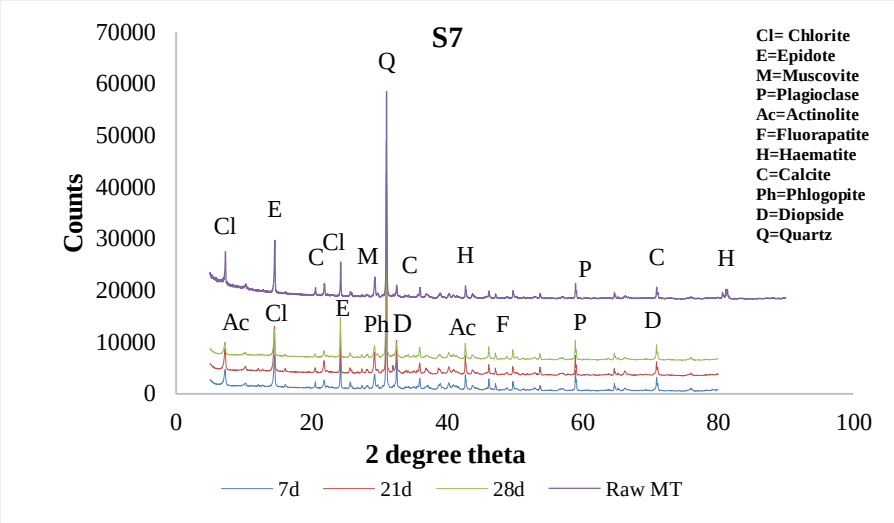

Figure E 4: XRD spectra of geopolymer bricks with 15 M NaOH: Na_2SiO_3.$5H_2O$ (70:30) at 120 °C.

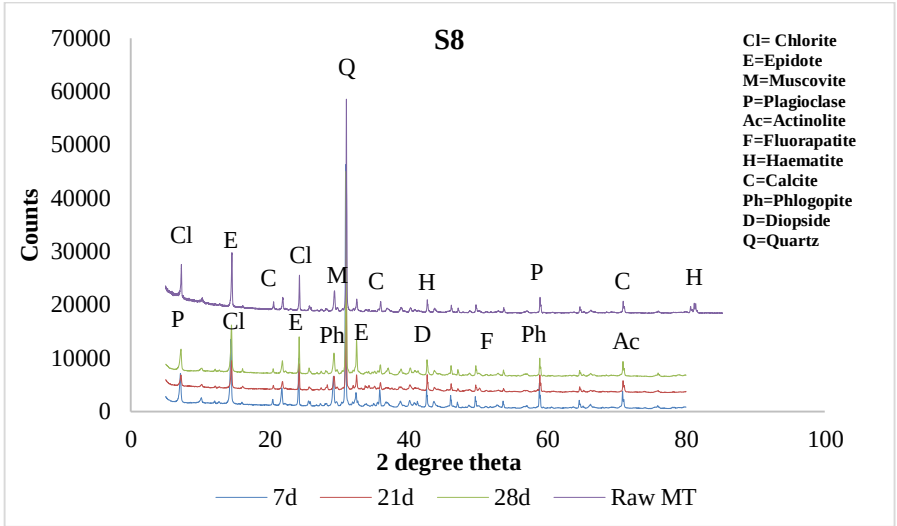

Figure E 5: XRD spectra of geopolymer bricks with 10 M NaOH: Na_2SiO_3.$5H_2O$ (70:30) at 180 °C.

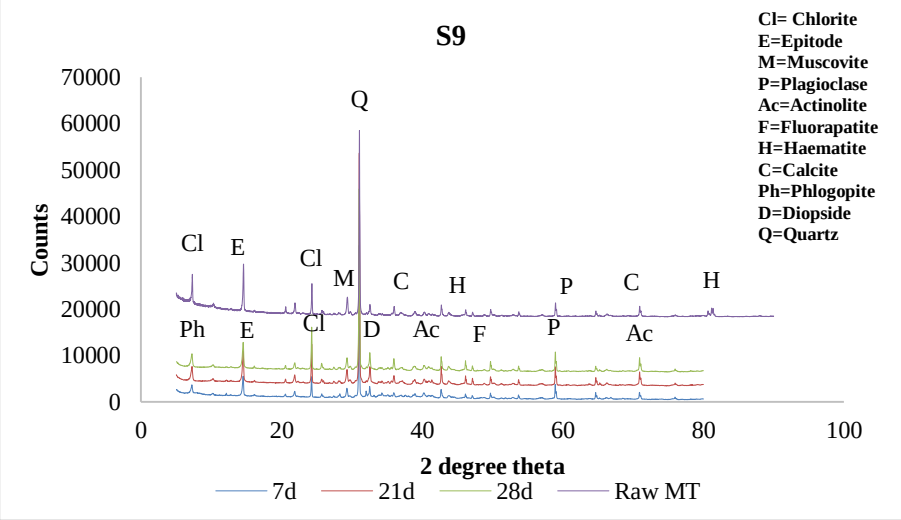

Figure E 6: XRD spectra of geopolymer bricks with 10 M NaOH: Na_2SiO_3.$5H_2O$ (70:30) and river sand (10%).

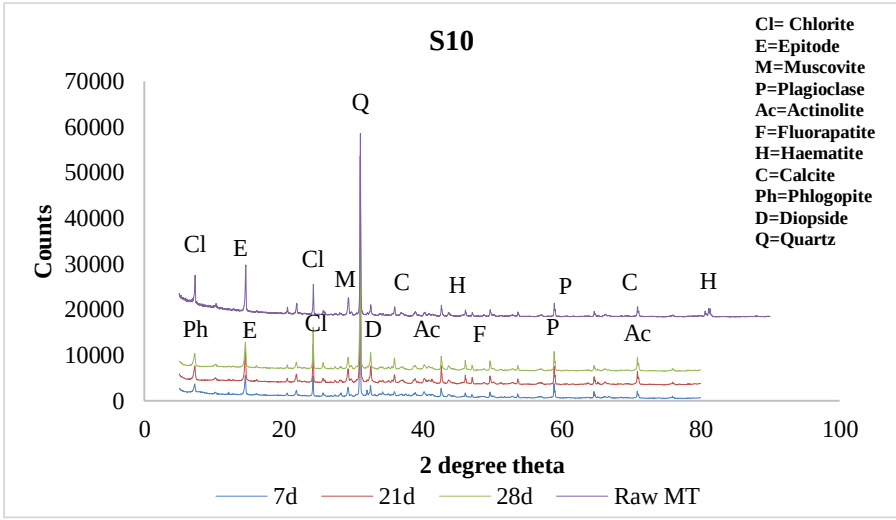

Figure E 7: XRD spectra of geopolymer bricks with 10 M NaOH: Na_2SiO_3.$5H_2O$ (70:30) and cement (5%).

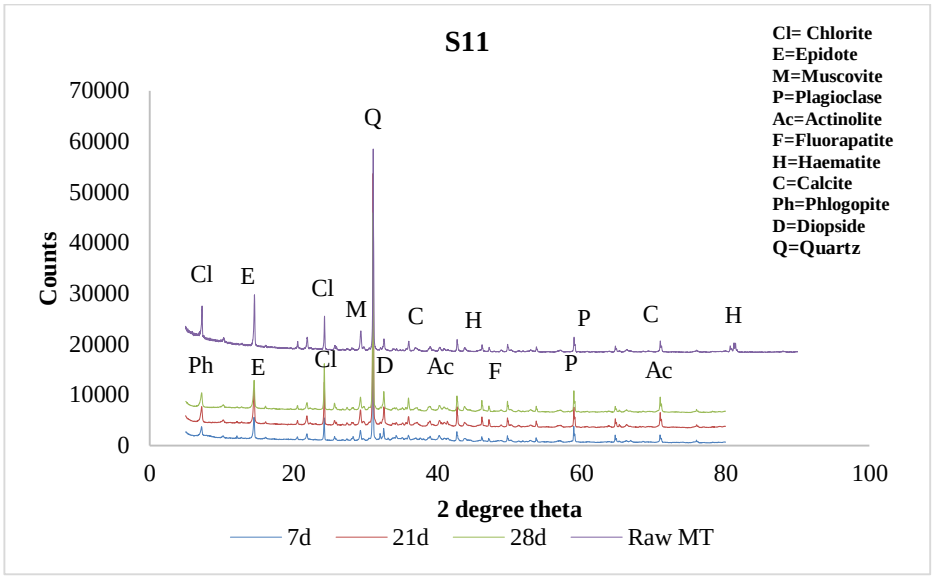

Figure E 8: XRD spectra of geopolymer bricks with cement, 10 M NaOH: Na_2SiO_3.$5H_2O$ (70:30) at varying curing periods in a GH.

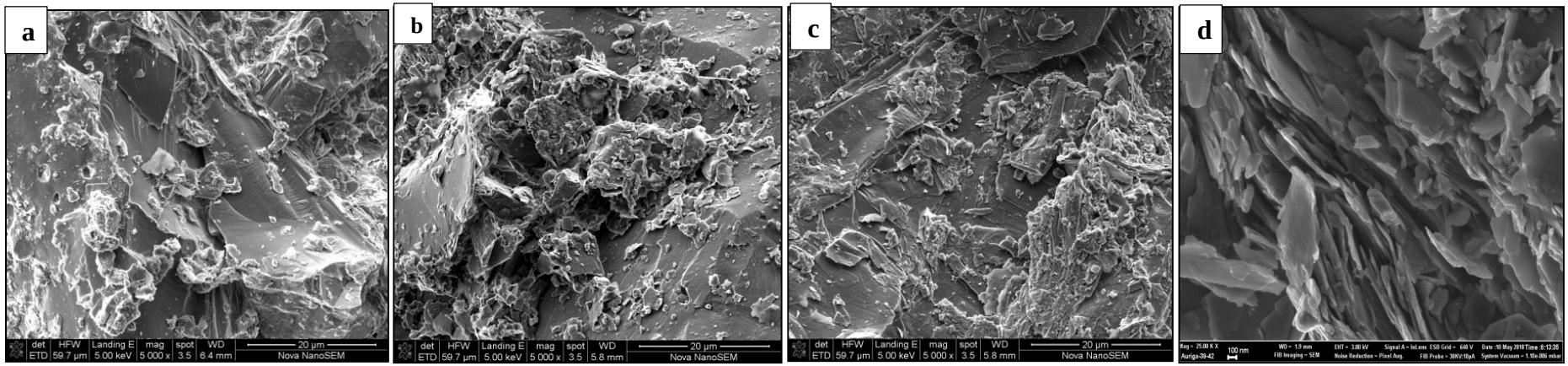

Figure E 9: SEM analysis of geopolymer bricks (S1) at 5M NaOH with an L/S ratio of 0.2 at 80 °C where; a) 7d, b) 21d, c) 28d and d) Raw MT.

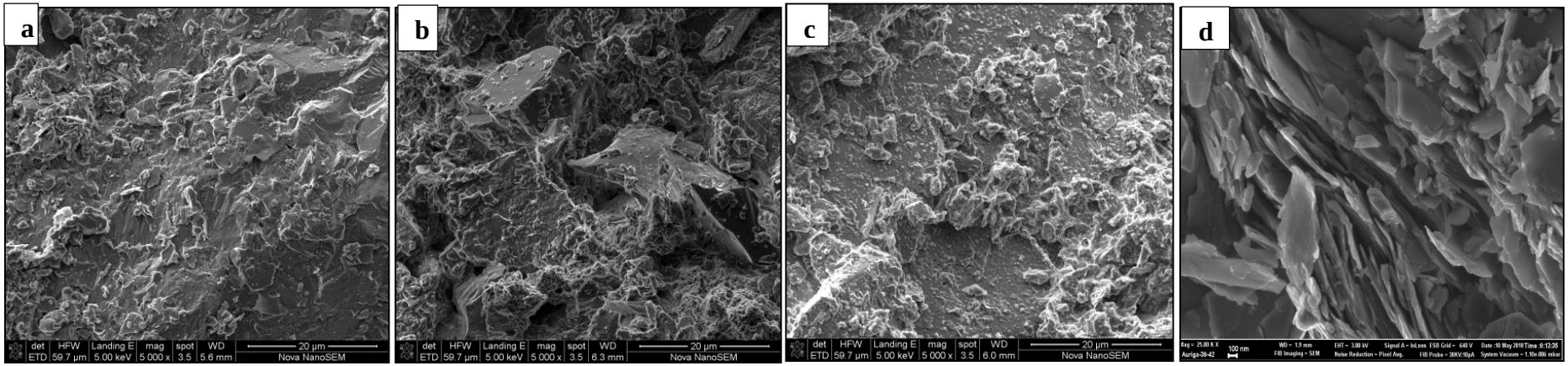

Figure E 10: SEM analysis of geopolymer bricks (S2) with 5M NaOH: $Na_2SiO_3.5H_2O$ (80:20) with an L/S ratio of 0.2 at 80 °C where; a) 7d, b) 21d, c) 28d and d) Raw MT.

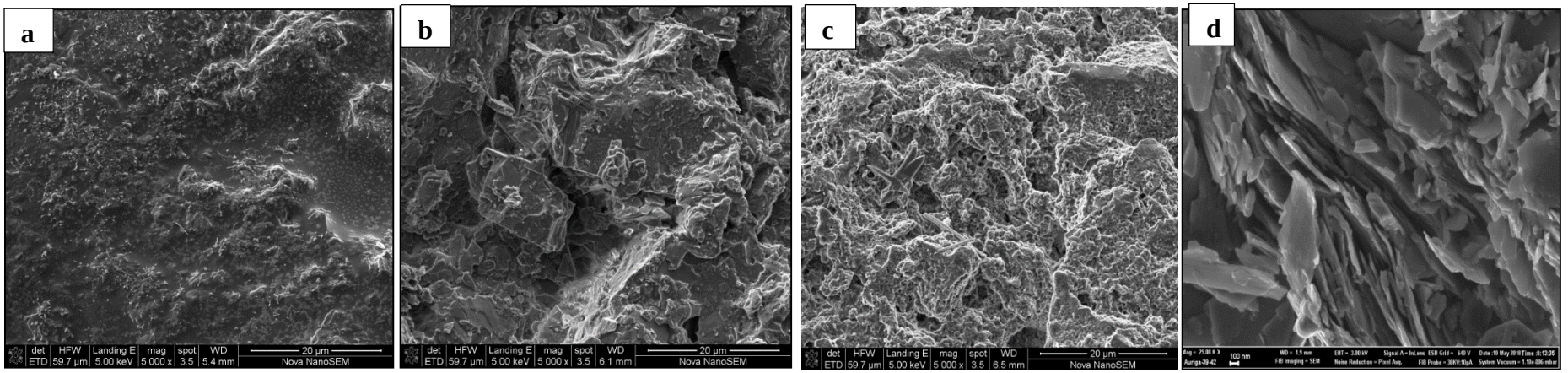

Figure E 11: SEM analysis of geopolymer bricks (S5) at 15M NaOH: $Na_2SiO_3.5H_2O$ (70:30) with an L/S ratio of 0.2 at 80 °C where; a) 7d, b) 21d, c) 28d and d) Raw MT.

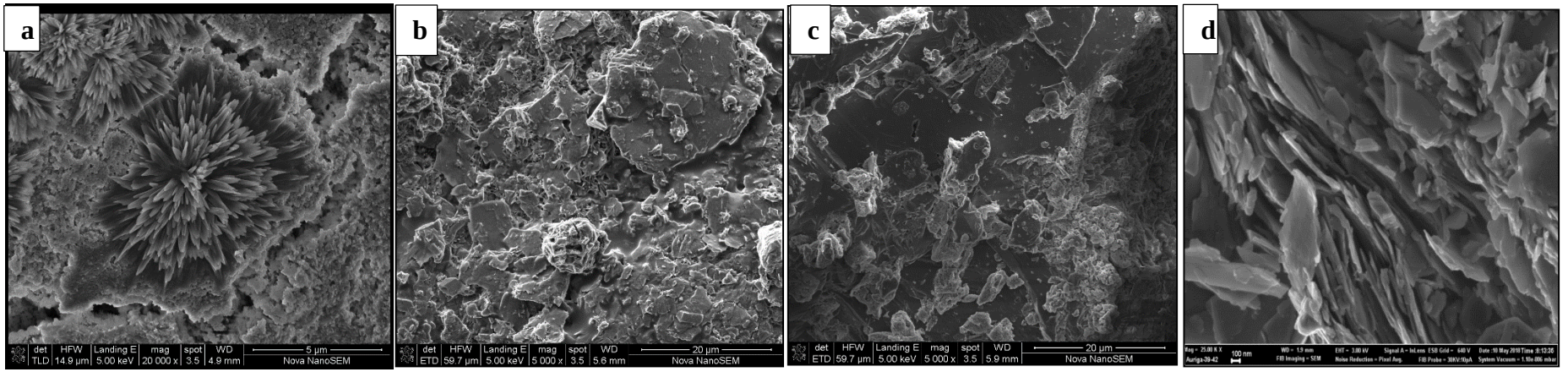

Figure E 12: SEM analysis of geopolymer bricks (S7)at 10M NaOH: $Na_2SiO_3.5H_2O$ (70:30) with an L/S ratio of 0.2 at 120 °C where; a) 7d, b) 21d, c) 28d and d) Raw MT.

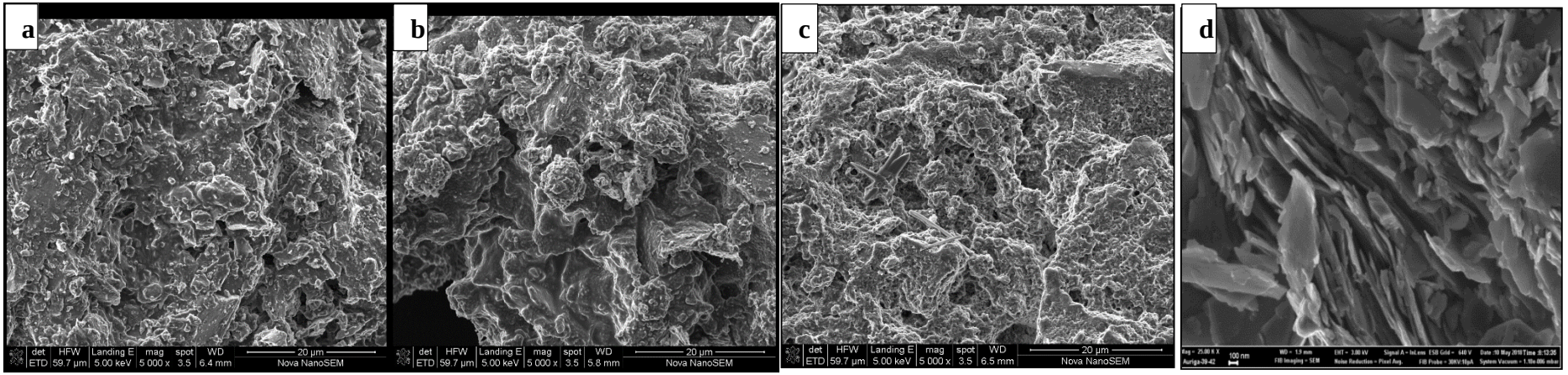

Figure E 13: SEM analysis of geopolymer bricks(S8) at 10M NaOH: $Na_2SiO_3.5H_2O$ (70:30) with an L/S ratio of 0.2 at 180 °C where; a) 7d, b) 21d, c) 28d and d) Raw MT.

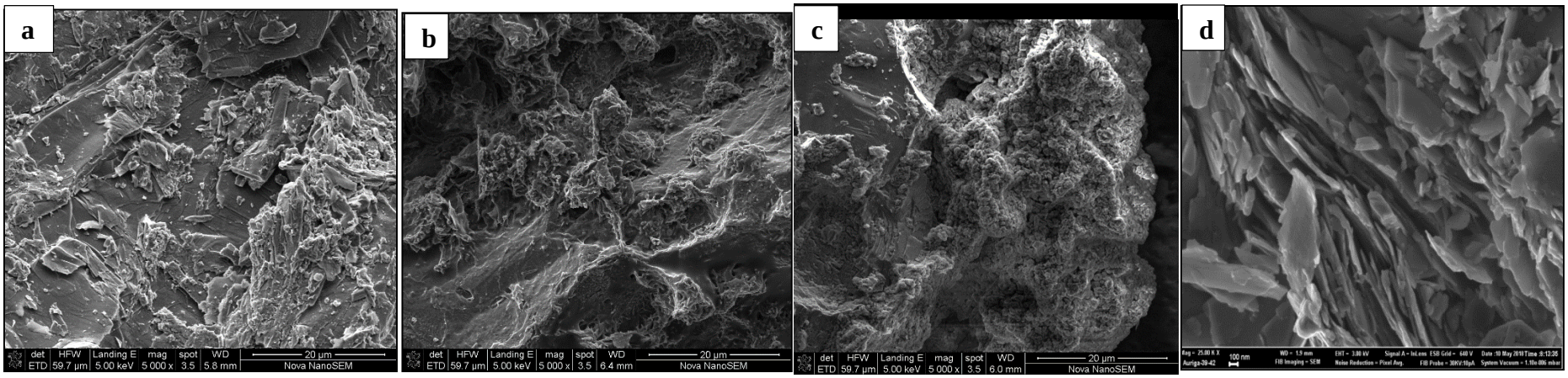

Figure E 14: SEM analysis of geopolymer bricks (S9) with river sand admixture (10%) at 10M NaOH: $Na_2SiO_3.5H_2O$ (70:30) with an L/S ratio of 0.2 at 80 °C where; a) 7d, b) 21d, c) 28d and d) Raw MT.

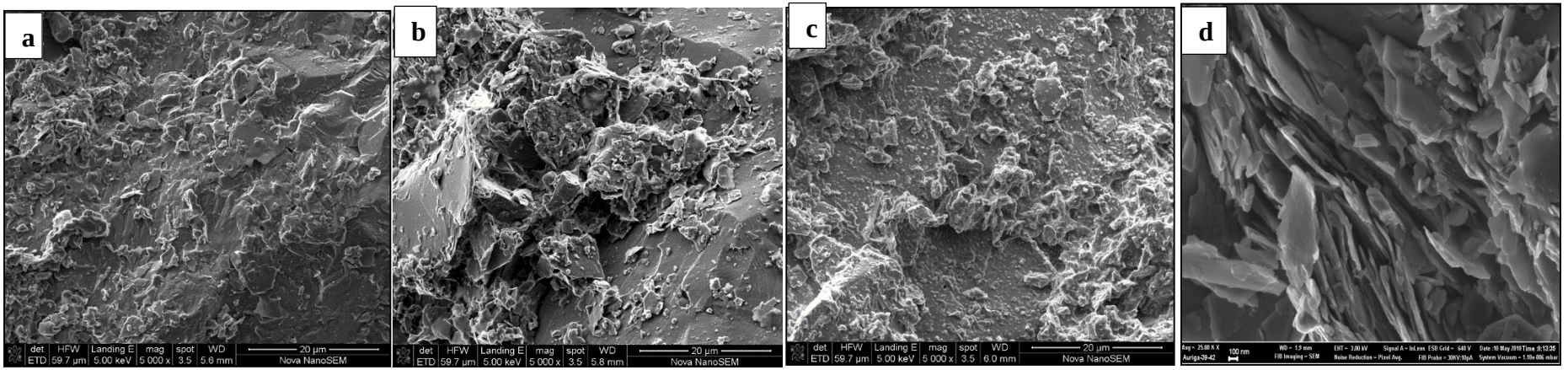

Figure E 15: SEM analysis of geopolymer bricks (S11) with cement admixture (5%) at 10M NaOH: $Na_2SiO_3.5H_2O$ (70:30) with an L/S ratio of 0.2 at 80 °C in a GH where; a) 7d, b) 21d, c) 28d and d) Raw MT.

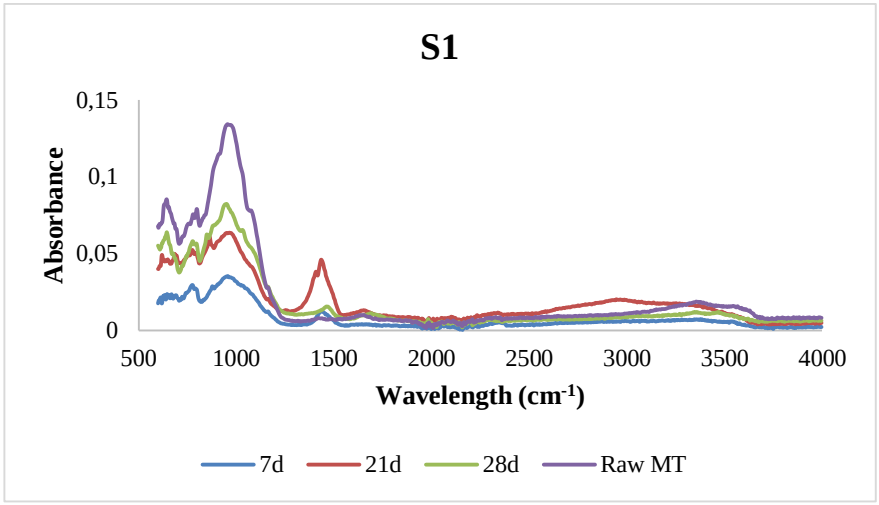

Figure E 16: FTIR spectroscopy of 5M NaOH at varying curing periods.

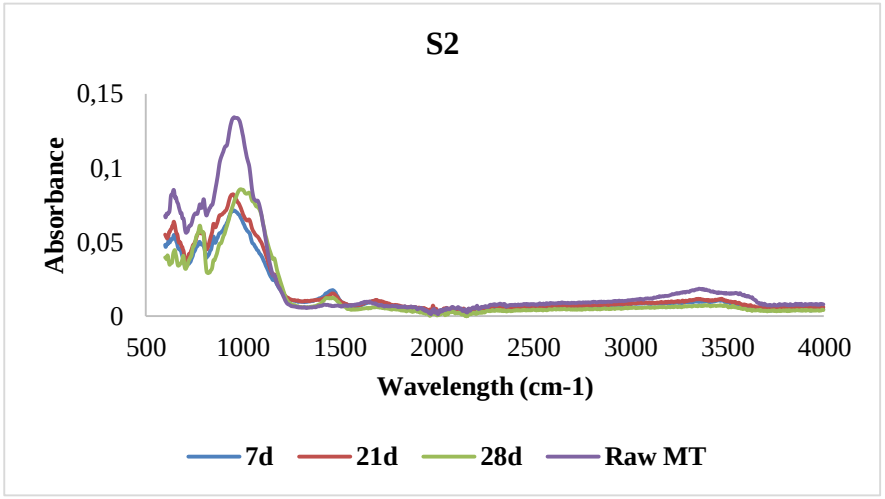

Figure E 17: FTIR spectroscopy of 5M NaOH: $Na_2SiO_3.5H_2O$ (70:30) at varying curing periods

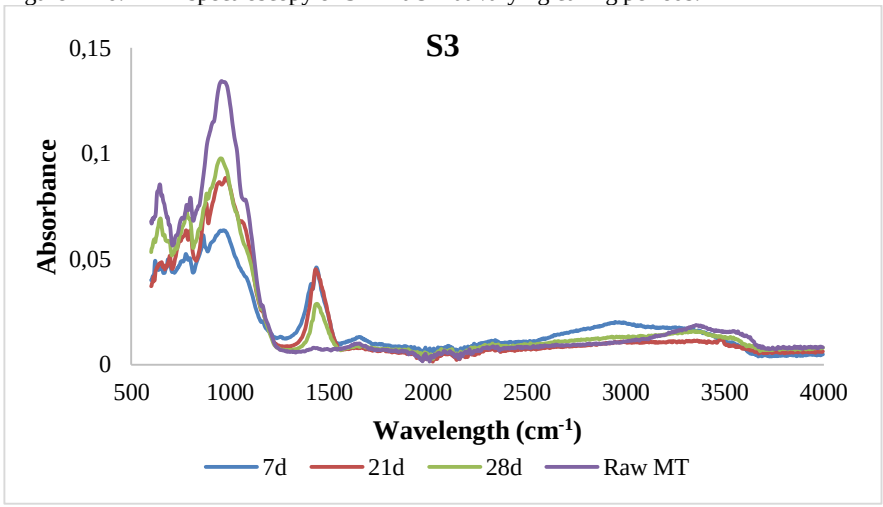

Figure E 18: FTIR spectroscopy of 5M NaOH: $Na_2SiO_3.5H_2O$ (80:20) at varying curing periods.

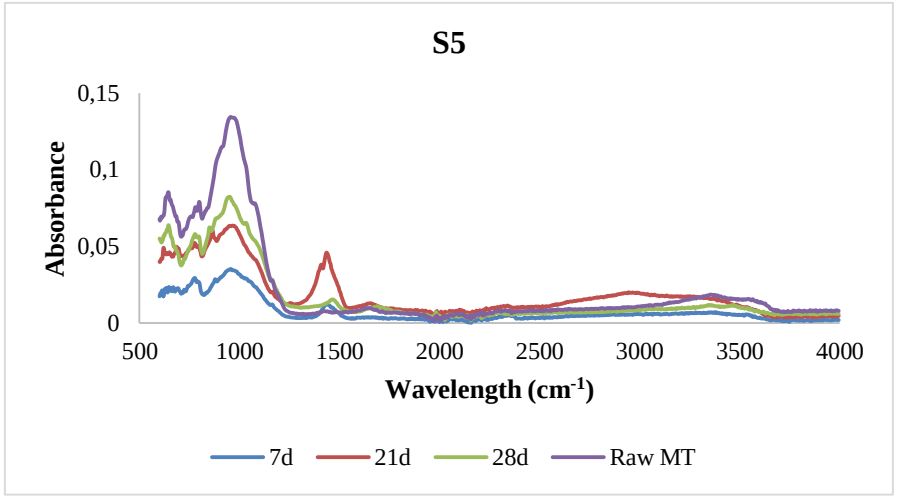

Figure E 19: FTIR spectroscopy of 15 M NaOH: $Na_2SiO_3.5H_2O$ (70:30) at varying curing periods.

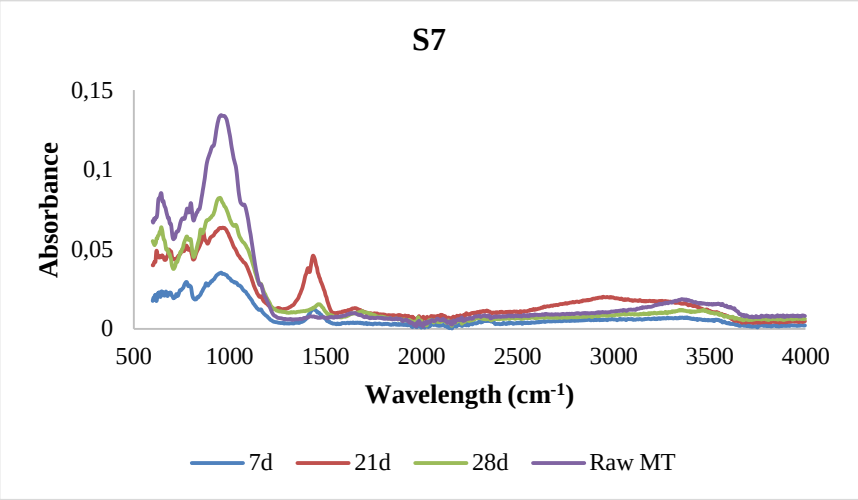

Figure E 20: FTIR spectroscopy of 10M NaOH: $Na_2SiO_3.5H_2O$ (70:30) at 120°C.

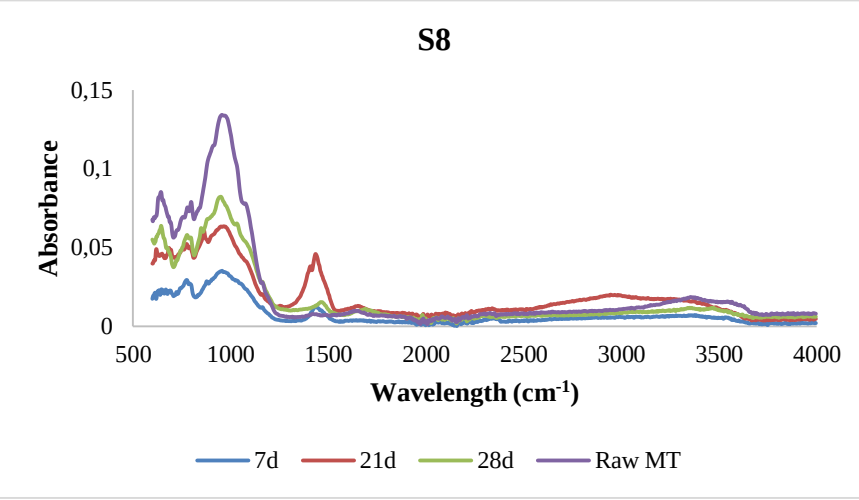

Figure E 21: FTIR spectroscopy of 10M NaOH: $Na_2SiO_3.5H_2O$ (70:30) at 180°C.

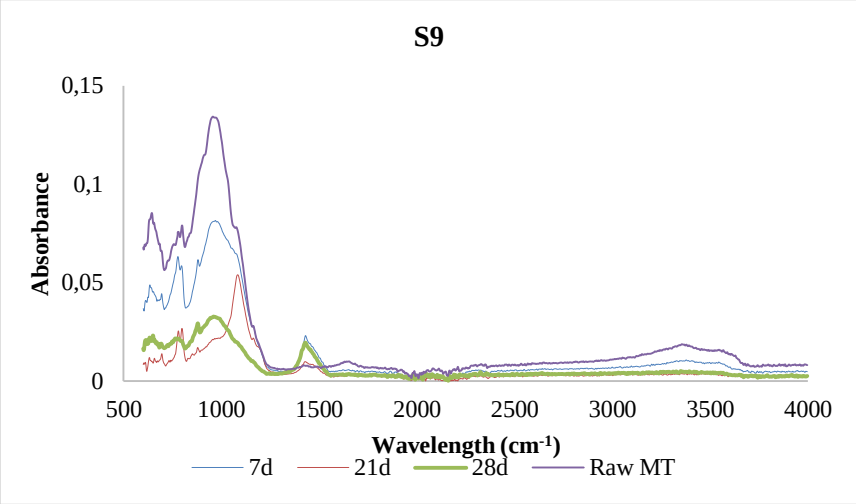

Figure E 22: FTIR spectroscopy of 10M NaOH: $Na_2SiO_3.5H_2O$ (70:30) with river sand.

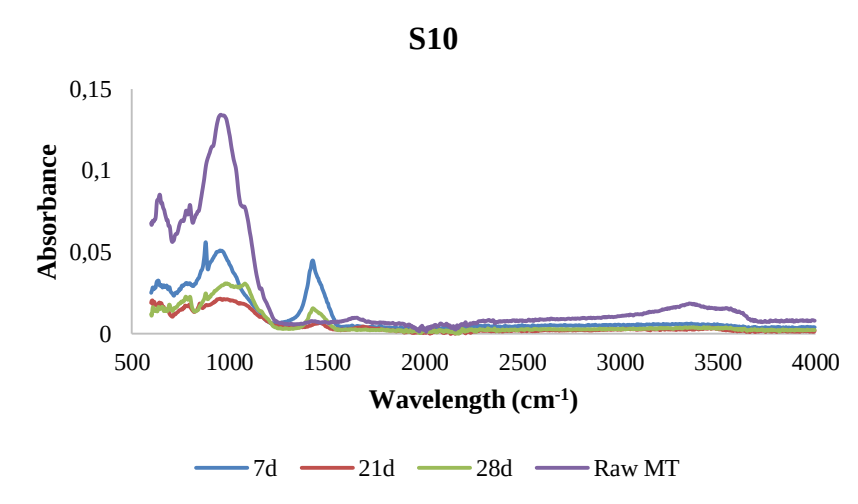

Figure E 23: FTIR spectroscopy of 10M NaOH: $Na_2SiO_3.5H_2O$ with cement admixture.

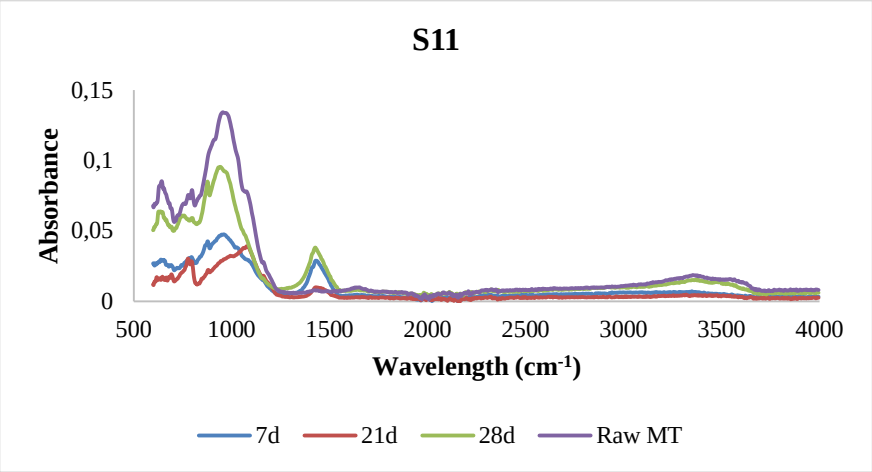

Figure E 25: FTIR spectroscopy of 10M NaOH: $Na_2SiO_3.5H_2O$ with cement admixture, at varying curing periods in a GH.